

PRECURSOR STATES
FOR THE
GRAPHITIZATION OF BENZENE

by

Syeda Tasmin Jahan
B.Sc(Hons), M.Sc.

A thesis presented to the Department
of Physics in partial fulfilment for
the degree of M.Phil.



BANGLADESH UNIVERSITY OF ENGINEERING AND TECHNOLOGY
DHAKA, BANGLADESH
MARCH, 1985

Acknowledgement

The author expresses her deep sense of gratitude to her Supervisor Dr. Tafazzal Hossain, Associate Professor, Department of Physics, Bangladesh University of Engineering and Technology, Dhaka, without whose constant guidance and encouragement, untiring help and invaluable suggestions this work would not have been completed.

The author is grateful to Dr. Giasuddin Ahmad, Professor and Head, Department of Physics, BUET for providing her with the necessary facilities in connection with her work and also for constant encouragement. The author would also like to offer her thanks to Professor Md. Ali Asgar, Dr. Nazma Zaman, Mrs. Dil Afroza Ahmed and Mr. Abu Hashan Bhuiyan for their keen interest in her work. The author also acknowledges with thanks many valuable help received from M/s. Kazi Ahmed Reza, Jiban Podder and Md. Abdur Rashid.

The author would like to thank the DAERS, Bangladesh University of Engineering and Technology, Dhaka for allowing her to use the facilities of various workshops of the University. In this connection, sincere thanks are also due to Mr. Ahmed Ali Mollah, Mr. Julfiqur Ali Bhuiyan and Mr. Rabiul Islam for their kind co-operation in setting the experiments.

Thanks are also due to Dr. Shahidul Alam, Mr. M.A. Beg and Mr. Shafiul Haque for their help in developing and printing of the photo-micrographs obtained in connection with her works.

The author also wish to extend her heartfelt gratitude to the Library staff of BUET, AEC, BCSIR for their sincere co-operation.

The author also expresses her gratitude to Dr. Abdur Rob Mollah, Director, Health Physics Division, Atomic Energy Centre, Dhaka for allowing the author to seal the samples in the glass-blowing workshop. The glass blower Mr. Abdur Rouf deserves thanks specially for sealing the samples on her behalf.

The author is also thankful to Mr. Md. Asadullah Khan, Controller of Examinations, BUET for providing many useful assistance in connection with her work. The author would also like to thank Mr. Md. Aminul Haque for typing the manuscript of this thesis and Mr. Shafiuddin Khan for drawing some diagrams of the thesis.

The author would like to thank Bangladesh University of Engineering and Technology for all the financial support.

ABSTRACT

Pyrolysis of benzene has been carried out to examine whether it is possible for it to be fused together so as to produce planer sheets of aromatic rings to form graphite. In the initial stages of nucleation and growth a liquid-state mesophase of optical anisotropy appears as spherules as in all graphitizable organic materials. With the progress of carbonisation, the growing mesophase spherules coalesce and change in shape in forming relatively complex bulk mesophase. Reflected polarized-light micrography using cross polarizers has been employed to investigate the microstructure of carbonaceous mesophase. A thermal analysis of the sample has been undertaken to locate the temperature intervals of mesophase formation. A particle size analysis has been carried out using polarized-light microscopy in order to find out the size of the spherules at different heat-treatment temperatures.

CONTENTS

	<i>Page</i>
CHAPTER I	
INTRODUCTION	1
References	9
CHAPTER II	
CARBONISATION AND GRAPHITIZATION	
2.1. Introduction	11
2.2. Different forms of Carbon	12
2.3. Structure of Carbons as determined by X-rays.	15
2.4. The carbonisation process	17
2.4.1 Pressure effects on mesophase microstructure	23
2.4.2 Different types of mesophase spherules	24
References	30
CHAPTER III	
THE POLARISING MICROSCOPE AND OPTICS OF CRYSTALS	
3.1. Introduction	33
3.2. The Polarizing Microscope	34
3.2.1 Modes of observation in a polarizing microscope	37
3.2.1.1 Orthoscopic arrangement	37
3.2.1.2 Conoscopic arrangement	42
3.2.2. Types of illumination used in Polarizing microscope	44
3.3. Optics of Crystals	46

	<i>Page</i>	
6.2.4	<i>Thermal analysis</i>	95
6.2.5	<i>Micrographic preparation of samples for mesophase observation</i>	97
6.2.6	<i>Polarized light microscopy</i>	99
6.3.	<i>Results and discussions</i>	100
6.3.1	<i>Different types of carbons obtained by sealed tube pyrolysis of benzene</i>	100
6.3.2	<i>Thermal analysis</i>	101
6.3.3	<i>Heat-treatment temperature, duration and also pressure together promote the growth of mesophase formation</i>	102
6.3.4	<i>Polarized-light photomicrograph</i>	104
6.4	<i>CONCLUSIONS</i>	105
	<i>Reference</i>	137

	<i>Page</i>
3.4. <i>Basic principle of a tint plate</i>	50
3.5. <i>Optical studies of the carbonaceous mesophase spheres</i>	52
<i>References</i>	66
 <i>CHAPTER IV</i>	
<i>THERMAL ANALYSIS</i>	
4.1. <i>Introduction</i>	67
4.2. <i>DTA apparatus</i>	68
4.3. <i>Thermal behavior of carbonising and graphitizing materials</i>	70
<i>References</i>	78
 <i>CHAPTER V</i>	
<i>PYROLYSIS CHEMISTRY OF BENZENE</i>	
5.1. <i>Introduction</i>	80
5.2. <i>Aromatic hydrocarbons</i>	82
5.2.1 <i>Benzene</i>	85
5.3. <i>Pyrolysis of benzene</i>	86
<i>References</i>	91
 <i>CHAPTER VI</i>	
<i>EXPERIMENTAL RESULTS, DISCUSSIONS AND CONCLUSIONS</i>	
6.1. <i>Introduction</i>	92
6.2. <i>Experimental</i>	93
6.2.1 <i>Sample</i>	93
6.2.2 <i>The safety device for opening sealed tubes containing heat-treated organic samples</i>	93
6.2.3 <i>Increasing pressure developed inside pyrolysed sealed tube accelerates carbonisation process</i>	95

CHAPTER - 1

INTRODUCTION



Many workers¹⁻¹⁷ have recognised that the early stages of carbonisation process are important in deciding whether the final product of carbonisation is graphitic or not. Those materials which ultimately produce graphitizing carbons pass through a fusion stage during carbonisation which usually occurs in the temperature range 350^oC-600^oC. This is a necessary but not sufficient condition for graphitizable organic materials. Recent studies by several groups⁵⁻¹⁷ and most notably the work by Brooks and Taylor^{5,6} on the structural conditions for graphitizability have demonstrated the significance of mesophase transformation which takes place as a precursor state in all graphitizable organic materials during carbonisation. This transformation is a liquid-state structural transition in which the large planar molecules formed by the reactions of thermal cracking and aromatic polymerisation become aligned in a parallel array to form an optically anisotropic liquid crystal. Although the life-time of the mesophase is limited by its hardening to a semi-coke, the alignment of the lamellar molecules achieved in the mesophase transformation is essential for thermal graphitizability of the pyrolysis product.

In the initial stages of nucleation and growth, the carbonaceous mesophase appears as small spherules which are suspended in the optically isotropic matrix with a simple structure^{5,6} as illustrated in three-dimensions in fig.1.1.

As observed with cross polarizers, the extinction contours are rather simple and define the loci of points where the layers are parallel or perpendicular to the plane of polarization of the incident light. The layer planes of the simple spherules are stacked perpendicularly to the polar diameter and curve to meet the interface of the isotropic phase normally.

Formation of the anisotropic mesophase is a function of heat-treatment temperature and heat-treatment duration. As carbonisation proceeds with increasing temperature and heat-treatment duration, the growing mesophase spherules, which are denser than the isotropic parent phase, sink to the bottom of the container. When spherules meet coalescence occurs to produce larger droplets, leading eventually to a bulk mesophase as shown in fig. 1.2. When observed microscopically with cross polarizers, the bulk mesophase displays a complex ensemble of extinction contours. The polarized-light extinction contours show nodes and crosses. When the specimen is rotated, the extinction contours sweep over the polished surface, but the nodes and many of the crosses remain fixed in position while the contours rotate about them either with or against the rotation of the incident light^{16,17}.

A parallel plate of quartz or gypsum sometimes called the 'first order red plate', the thickness of which is adjusted to give a path difference between the two transmitted components equal to one wavelength of yellow light, is inserted at 45° between crossed polars. Between crossed polars it gives the violet-red interference colour at the end of the first order

and if it suffers a very small subtractive effect, there is a very marked change to orange or yellow, while if it suffers a very small additive effect, the red colour is raised to indigo or blue. By the use of this so-called sensitive tint method, changes in pleochroism and in extinction contours for condensed and for deformed mesophases are observed. This method permits distinction between crosses and nodes and so enables four types of linear defects in the stacking of the aromatic layer planes to be identified. They are now termed as O-type co-rotating crosses, X-type counter-rotating crosses, U-type co-rotating nodes and Y-type counter-rotating nodes. The four types of linear defects are represented schematically in Fig. 1.3. The O-type co-rotating cross is seen to correspond to a simple circular or, more generally, helical arrangement of layer planes. The X-type counter-rotating cross is due to a more complicated structure, which possesses four-fold symmetry in the idealised case and in which the curvature of the layer planes is convex to the centre of the cross. The U-type co-rotating node corresponds to a simple arc structure, with the layer planes lying concave or radial relative to the centre of the node. The Y-type counter-rotating node possesses a delta structure with three-fold symmetry in the idealised case, and the curved layer planes lie convex relative to the centre of the node. The counter-rotating cross is thus a four-fold version of the three-fold delta structure of the counter-rotating node.

The processes of the formation, coalescence and deformation of the plastic mesophase establishes the basic elements of the graphite microstructure i.e. the parallel alignment of the aromatic layer planes and the rearrangement of the complex folds in the fibrous regions. The linear stacking discontinuities, that is, the nodal and cross-structures, are essential characteristics of the coalesced mesophase, and the nodal structures at least are found to persist in their basic form upto graphitization temperatures.

The carbonaceous mesophase transformation which plays an intermediate but critical role in determining the morphology of graphitic products is thus essentially a precursor state to all graphitizable aromatic organic compounds. The present work has been undertaken in an attempt to get some information on the structures formed during the relatively short life-time of the plastic mesophase formed during the pyrolysis of benzene, the starting organic compounds of the aromatic group.

Blayden et al.¹⁸ suggested that hetero-atoms might control the carbonising and graphitizing character of large polyaromatic organic molecules. Among the raw materials used for the production of artificial carbons and graphites, there are hydrocarbons including aromatic organic ring compounds which contain a number of hetero-atoms such as H₂, O₂, N₂, S, etc. During Pyrolysis, these hetero-atoms can form in part stable volatile by-products, thus reducing the carbon yield. On the other hand, the hetero-atoms can affect cross-linkage in the compound to be pyrolysed. In this way they will reduce the

vapour pressure and cause coking in the liquid and especially in the solid phase. This effect will increase the carbon yield

Later investigation ^{19,20} indicated that hetero-atoms present in the feedstock material play a significant role in determining the final properties of a graphite, especially the coefficient of thermal expansion.

The simple objective is to produce a graphite which is isotropic in expansion rather than the anisotropic expansion of perfect graphite or the disorder of glassy carbons. Again isotropic conditions also coincide with maximum α_v bulk expansion coefficient according to a highly idealised model of an isotropic cross-linked carbon polycrystal, ^{19,20} as illustrated in fig. 1.4. The general concept of the model which has been outlined is

$$\alpha_v \cong 3\alpha_a + k \alpha_c n^{\frac{1}{2}}$$

where

- α_v = bulk volume coefficient of expansion,
- α_a = coefficient of expansion along a-axis,
- α_c = coefficient of expansion along c-axis,
- and n = hetero-atom concentration.

The behavior of the curve drawn α_v versus $n^{\frac{1}{2}}$ has been diagrammatically shown in fig. 1.5.

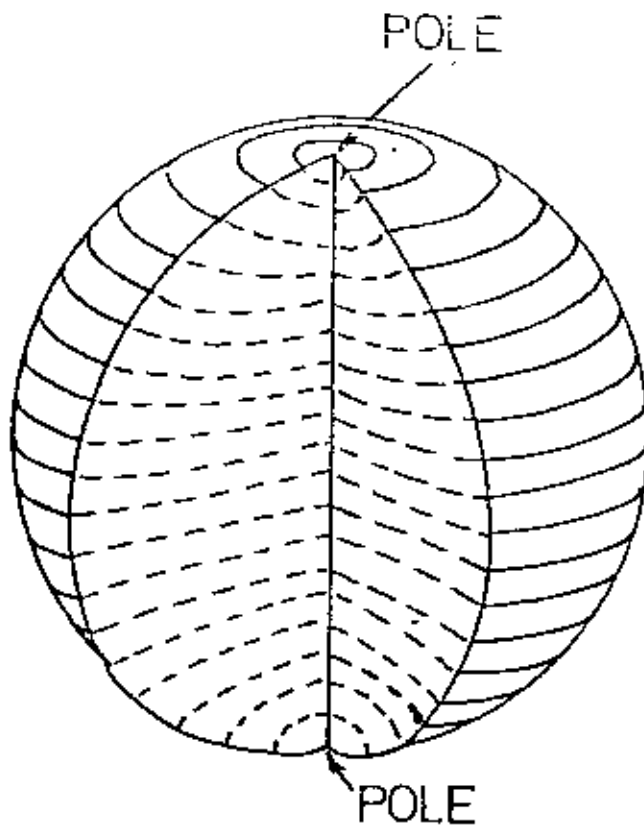


Fig 1.1. MESOPHASE SPHERE WITH SECTION INCLUDING POLAR DIAMETER



BEFORE CONTACT



JUST AFTER CONTACT



SHORT TIME AFTER CONTACT



TYPE OF COMPLEX INTERNAL STRUCTURE FORMED WHEN COMPOSITE OF TWO OR MORE SPHERES CONTRACTS TO ONE LARGE SPHERE

Fig.1.2 REARRANGEMENTS WHICH APPEAR TO OCCUR WHEN TWO SPHERES COALESCE

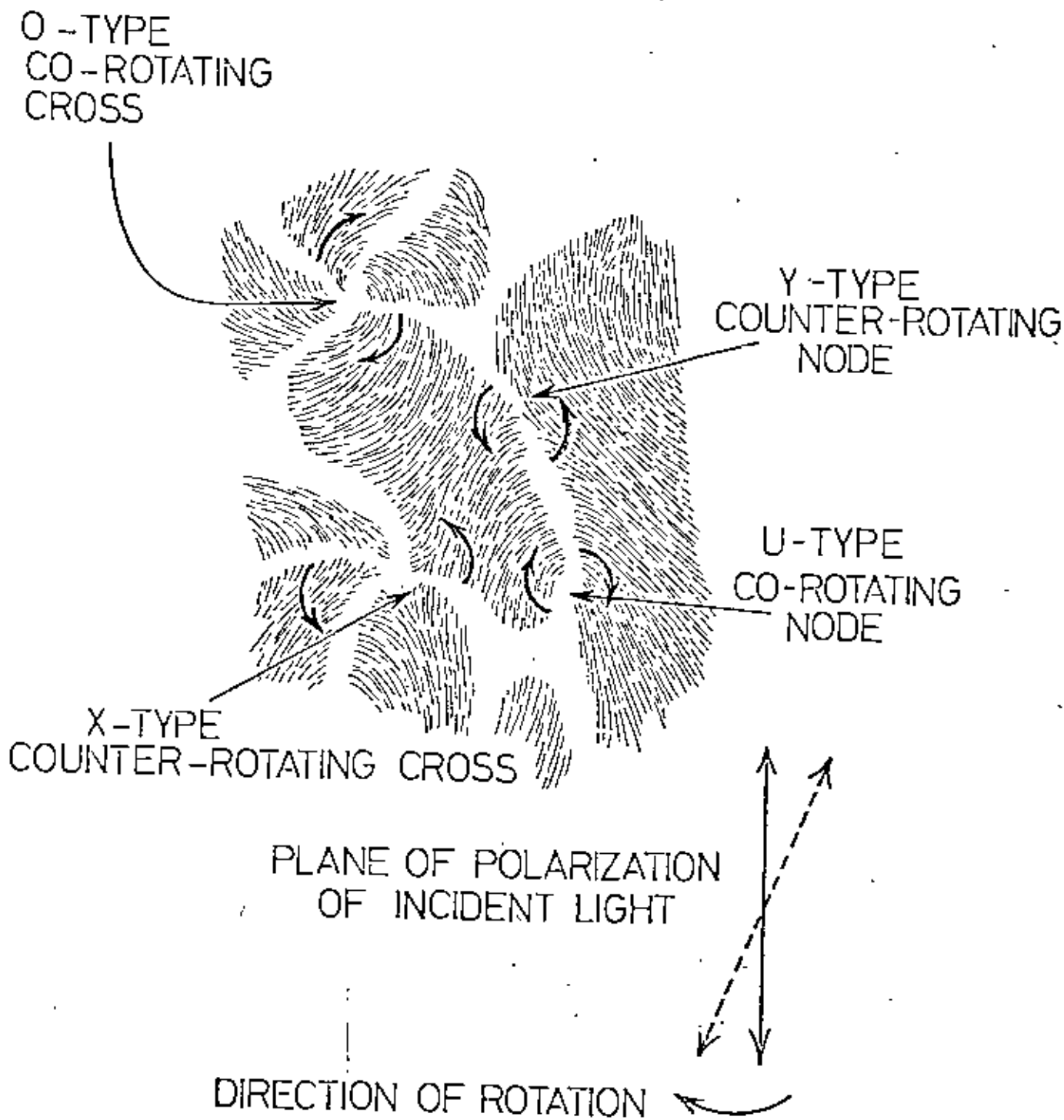


Fig. 1.3. Schematic diagram of the four types of mesophase stacking defects. Extinction contours are shown for the case of crossed polarizers.

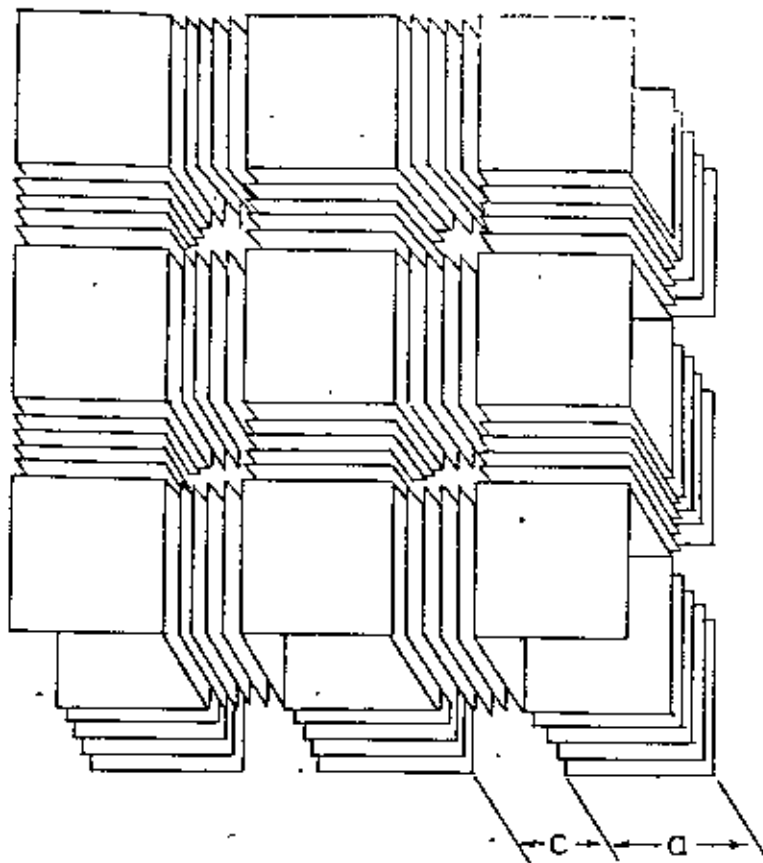


Fig. 14. Simplified model of three-dimensional crosslinked graphite polycrystal.

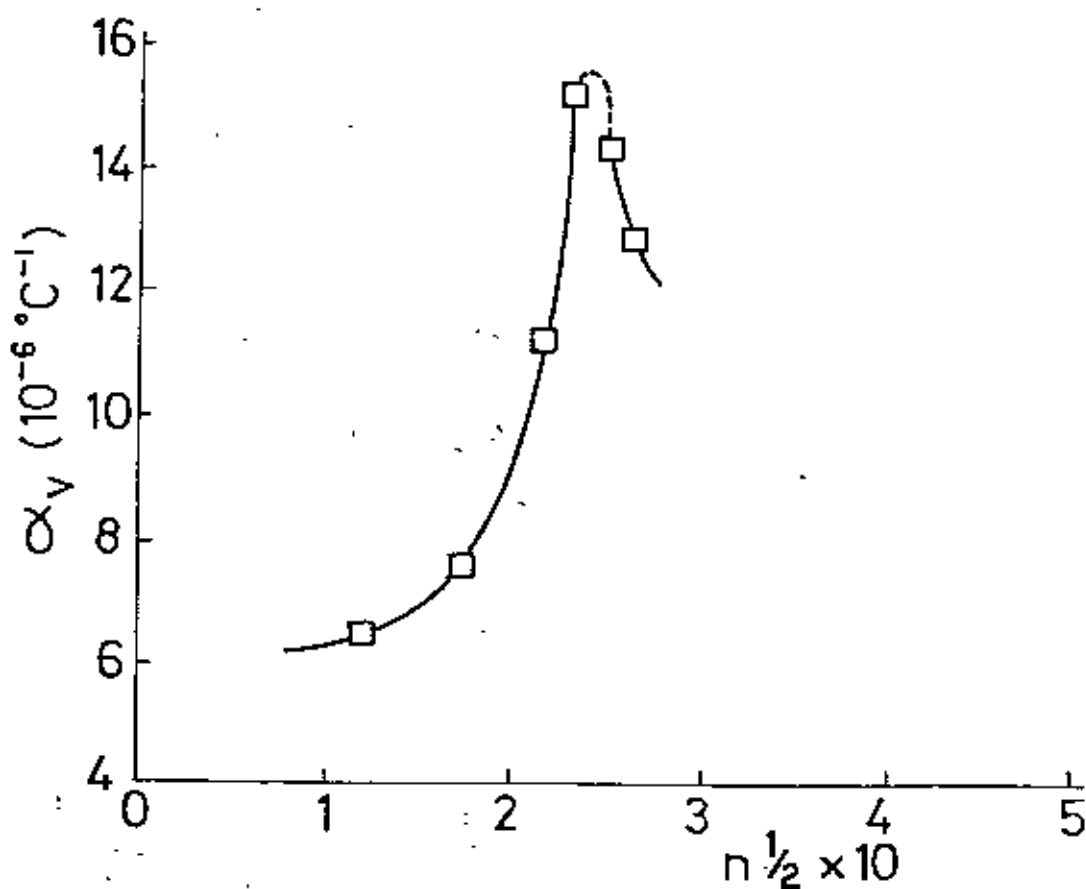


Fig. 15 Relationship between α_V and n for direct sulphur addition to catarex pitch.

REFERENCES

1.1 Taylor, G.H., Fuel, 1961, 40, 465.

1.2 Kipling, J.J., Sherwood, J.N., Shooter, P.V. and Thompson, N.R., Carbon, 1964, 1, 315.

1.3 Kipling, J.J., Sherwood, J.N., Shooter, P.V. and Thompson, N.R., Carbon, 1964, 1, 321.

1.4 Kipling, J.J. and Shooter, P.V., Second Conf. Ind. Carbon and Graphite, Soc. Chem. Ind., 1965, 15.

1.5 Brooks, J.D. and Taylor, G.H., Carbon, 1965, 3, 185.

1.6 Brooks, J.D. and Taylor, G.H., Nature, 1965, 206, 697.

1.7 Kipling, J.J. and Shooter, P.V., Carbon, 1966, 4, 1

1.8 White, J.L., Guthrie, G.L. and Gardner, O., Carbon, 1967, 5, 517.

1.9 White, J.L., Dubois, J. and Soullart, C., J. Chim. Phys., Special volume, April, 1969, 33; Euratom Report 4094 e, 1969.

1.10 Honda, H., Kimura, H., Sanada, Y., Sugawara, S. and Furuta, T., Carbon, 1970, 8, 181.

1.11 Dubois, J., Agace, C. and White, J.L., Euratom Report 4627 e, 1971.

1.12 Honda, H., Kimura, H. and Sanada, Y., Carbon, 1971, 9, 695.

1.13 Walker, P.L., Carbon, 1972, 10, 369.

- 1.14 Sanada, Y., Furuta, T., Kimura, H. and Honda, H.,
Fuel, 1973, 52, 143.
- 1.15 Graham, S.G., Ph.D. Thesis, 1974, Salford University.
- 1.16 White, J.L., In *Petroleum-Derived Carbons* (Edited
by Grady, T.M.O. and Deviney, M.I.), Am. Chem. Soc.
Symp. Ser., 1976, 21, 282.
- 1.17 Hossain, T., *J. Bangladesh Academy of Sciences*, Vol.7,
No. 1 & 2, 1983, 57
- 1.18 Blayden, H.E., Gibson, J. and Riley, H.L., *Inst. of
Fuel, Wartime Bulletin*, 1945, 125.
- 1.19 Hutcheon, J.N. and Jenkins, M.J., *Second Conf.
Ind. Carbon and graphite, Soc. Chem. Ind.*, 1966, 493.
- 1.20 Dollimore, J. and Jenkins, M.J., private communication,
1966.

CARBONISATION AND GRAPHITIZATION

2.1 Introduction

Carbon is the sixth element in the periodic table and it has an atomic weight of 12.011 on the chemical scale. The electron configuration of carbon is $1s^2 2s^2 2p^2$. Of the six electrons in a neutral atom, four in the outer L-shell, $2s^2 2p^2$, are always available for chemical bonding. This bonding is principally carried out by the excitation of one S-electron into a P-state, followed by orbital mixing. Several hundred thousand carbon-containing compounds are known till today, because of this unique atomic structure of carbon which results in its capacity to react chemically with most other elements, as well as to bond with itself. In its elementary form, carbon occurs naturally in 'amorphous' forms as coal, lignite, gilsonite and in more limited quantities in its two allotropic crystalline forms; natural graphite and diamond.

During the pyrolysis of carbon-containing materials to high temperatures, the removal of non-carbon atoms, usually oxygen, hydrogen, nitrogen or sulphur, as well as some carbon constitutes the process what is known as 'carbonisation'. This process is followed by a rearrangement of order within the remaining carbon atoms giving rise to a greater degree of order within the carbon produced which may develop a three-dimensional order. This development of a three-dimensional order gives rise to a structure very close to the well-defined structure of

pure graphite is termed 'graphitization'. In fact, graphitization does not occur in 'graphitizable carbons' until they are annealed above 2500°C . The temperature range from 2500°C to 3000°C is called the 'graphitization temperature range'. The temperature at which graphitization starts, has been found to differ from material to material.

2.2 Different forms of carbon

There are only two allotropic crystalline forms of carbon - graphite and diamond. Both exist in nature or can be produced artificially from many carbon containing materials. The difference in properties between these two allotropic forms is determined by the forces lying within and between crystallites. Diamond is a face-centred cubic material with each carbon atom bonded covalently to four others in the form of a tetrahedron, the interatomic distance being 1.54 \AA . It is the hardest known naturally occurring substance due to the rigidity of the tetrahedral covalent bond lattice of the single macromolecule that forms the perfect crystal. Diamond is metastable to graphite. The conversion of graphite into diamond requires the assistance of catalysts as well as high temperatures and pressures. Though diamond normally has the structure described above, Ergun and Leroy¹ have shown that a hexagonal structure for diamond is possible. Again diamond changes spontaneously at ordinary pressure to graphite above 1500°C ² and Graphite at atmospheric pressure is more stable form of carbon.

Graphitic is a lamellar structure and is the anisotropic

allotropic form of carbon. Its accepted ideal crystal structure is illustrated in fig. 2.1, which was first established by

Bernal³ (1924). It is a stable hexagonal lattice where the

basal planes or layer planes consist of open hexagons with

interatomic C-C distance 1.415 Å. These planes are stacked in

an alternating sequence, the interplanar distance being 3.354 Å.

Crystallographically perfect graphite has a density of

2.266 g/ml, while it is 3.530g/ml for diamond. In this structure

only three of the four valence electrons of carbon form regular

covalent bonds with adjacent carbon atoms. The fourth electron,

which is free, resonates between the valence bond structures.

Strong chemical bonding forces exist in the basal planes, while

weak Van der Waals' forces exist between planes. The bonding

energy between planes is only about 2% of that within the planes^{4,5}.

* The weak forces between layer planes account for (a) the

tendency of graphite materials to fracture along planes, (b) the

formation of interstitial compounds, and (c) the lubricating

compressive and many other properties of graphite, as shown for

the hexagonal graphite structure, the stacking sequence of the

planes is ABAB so that the atoms in alternate planes are

congruent.

A rhombohedral structure has been found to exist in many

graphites where the stacking sequence is ABC ABC (Fig. 2.2).

Lipson and Stokes⁶ in 1942 were able to show that this rhombohedral

lattice, originally proposed by Debye and Scherrer⁷ (1917) fully

accounted for the extra X-ray lines found in some powder photographs of graphites. The proportion of the rhombohedral form may be increased in graphites by grinding⁸ which indicates that the change arises from the movements of the layers carbon networks with respect to one another.

Most naturally occurring graphite is polycrystalline. Perfect single crystals greater than 10 μ m are quite rare, although they can be produced with difficulty. Most synthetic graphites, made by high temperature calcination of pitch/coke blends, are polycrystalline. Single crystals of graphite of large dimension that occurs in some natural deposits can be obtained by pyrolytic deposition of carbon from carbonaceous vapours. Under suitable conditions, the deposit of carbon can take the form of highly oriented layers. Subsequent treatment of this material can produce quite large single crystals of pure graphite, known as 'pyrolytic graphite'.

Apart from diamond and graphite, there exists a third form of carbon which is known as 'amorphous carbon'. Although this name literally means a structureless form of carbon but almost all amorphous carbons possess a small amount of order. The first application of X-ray diffraction methods to amorphous carbons, however, led to the concept that they were also graphitic with their apparently amorphous character which arises from the very minute size of the crystallites. These amorphous carbons can be prepared by the combustion of hydrocarbons in an incomplete supply of air, i.e. carbon blacks, and include soot, charcoal, and lamp blacks.

2.3 Structure of carbons as determined by X-rays.

Carbons can be classified into two distinct and well-defined types - graphitizing or non-graphitizing, soft or hard. Graphitizing carbons may be defined as those which begin to develop three-dimensional order (giving oblique graphite-like X-ray reflections) on heating to temperatures near 1700°C . Such carbons are produced by two main processes: either by deposition from the vapour phase or by solidification from the liquid or plastic state to form cokes.

Substances which produce graphitizing carbons from the liquid or plastic state include vitrinites of medium volatile coking coal, high temperature coal-tar pitch, petroleum bitumen, polymers such as P.V.C and polynuclear aromatic compounds such as naphthacene or dibenzanthrone. The carbons normally obtained by heating these substances are coke-like in appearance and show complex patterns of optical anisotropy when observed under the microscope.

'Non-graphitic carbons' are carbons in which the graphite-like layers lie in parallel groups but are not oriented like the crystalline structure of graphite. The three-dimensional structure of crystalline graphite is not present. On heating certain non-graphitic carbons to sufficiently high temperatures between 1700°C and 3000°C the graphite-like layers show a tendency to change from a 'random layer structure' towards the ordered structure of crystalline graphite. (This can be shown by X-ray powder photography). These intermediate type of

structures in which the three-dimensional graphite structure is partly developed, are called 'graphitic carbons'. A description of their formation has been given by Franklin⁹. Also those carbons which, on heating to temperatures between 1700°C and 3000°C showed a continuous change from a non-graphitic to a graphitic structure were called 'graphitizing carbons' and those which on heating to 3000°C still did not show three-dimensional ordering were called 'non-graphitizing carbons'. These two types can be distinguished in terms of the relation between crystal height and crystal diameter on heat-treatment (Fig. 2.3). L is the average layer distance and M is the mean value of the number of layers per crystallite.

Graphitizing carbons are generally relatively soft, are of high apparent density. They possess little microporosity and are relatively rich in hydrogen or low in oxygen, sulphur and nitrogen. They were termed 'soft carbons' by Mrozowski¹⁰. Franklin considered that, during the early stages of the carbonisation process, the crystallites in the graphitizing carbons were fairly mobile and that in the region of 1000°C, a high proportion of the crystallites lay nearly parallel to each other. Weak cross-linking was supposed to exist between the crystallites. A model (reproduced in Fig. 2.4) was put forward by Franklin¹¹ for the structure of a graphitizing carbon. X-ray data also suggested the movable nature of the whole layers or groups of layers with the rise of the heat-treatment temperature, but the most significant factor was that neighbouring crystallites had

to be nearly parallel. Crystallite growth was considered to occur by the layer planes linking together.

Non-graphitizing carbons are generally hard, are of low apparent density. They have a high microporosity and are relatively low in hydrogen or rich in oxygen, sulphur and nitrogen. They were correspondingly called 'hard carbons' by Mrozowski¹⁰. Again Franklin¹¹ put forward a model (reproduced in fig. 2.5) to account for their structure. In this model she considered that the parallel layer groups which were oriented at all angles, were joined together at their extremities, thus accounting for the microporosity. With the increase of pyrolysis temperatures there was some growth in the basal plane direction by incorporation of disordered carbon atoms at the edges of the crystallites. Other carbon atoms acted as linkages between crystallites.

2.4 The carbonisation process

It has been mentioned by many workers that the early stages of carbonisation (350-600°C) are important in determining the ability to graphitize at high temperature. The following is a summary of the work done by some authors.

Ripling et al¹² described some of the properties of carbons made from a range of polymers and one polycyclic compound (dibenzanthrone). The carbons could be sharply divided

into two groups; those which became graphitic at temperatures of 2700°C or above and those which remained non-graphitic. Kipling has investigated the relationship between fusion during carbonisation process and the ability of the resultant carbon to graphitize subsequently at a higher temperature. It was later suggested^{13,14} that organic materials could only give rise to graphitic carbon if they passed through a fusion stage which had to occur under specific conditions. These specific conditions were such that the polycyclic aromatic structures formed in the residue during carbonisation readily orientate to form graphite. It was also confirmed by using polarized-light microscopy to study low and high temperature carbons¹⁵. Taylor¹⁶ undertook a detailed study of the microscopic changes exhibited by a vitrinite with the progress of carbonisation using optical methods. Observations were made on a thermally metamorphosed coal. The vitrinite, which in its unaltered state was anisotropic, became isotropic and this transition was followed under controlled conditions in the laboratory. The change from anisotropy to isotropy has been found to occur at a temperature slightly below that at which the plasticity became measurable. About 10 to 15°C before the onset of resolidification the change from isotropic plastic vitrinite to anisotropic semicoke was indicated by the appearance of small spherules initially of micron size, in the isotropic vitrinite, forming as a separate phase. These spheres were found to grow in size with the rise of heat-treatment temperature at the expense of the plastic vitrinite

which eventually coalesced to form a mosaic structure about the resolidification temperature.

The spheres, which later became units of the mosaic texture, had an interesting pattern of behavior in singly and doubly polarized light. A particular structure having a strain effect was brought forward to account for this behavior. At first it was believed that this structure was inherently improbable as because the strain effects were in fact of little importance to account for the observed optical properties, and hence a second model which included a stress effect was proposed. However the original structure was later verified to be correct by Brooks and Taylor^{17,18} using electron diffraction and optical microscopic techniques. The three dimensional structure of a simple sphere has been shown in the introductory chapter on page 6 in Fig. 1.1. The layers consist of condensed polycyclic aromatic compounds which are aligned perpendicular to the polar diameter but curve to meet the interface with the isotropic matrix at a high angle. The poles constitute anomalous regions, but this is not sufficiently reflected in the spherical droplet. Spheres were also found to appear on heating bitumen, pitches, PVC, naphthalene and dibenzanthrone, all of which produce graphitizing carbons. This two phase liquid state structural transformation is known as 'carbonaceous mesophase formation' or 'liquid crystal formation'.

Brooks and Taylor showed that the spheres differed little in composition ($C_{100}H_{49}O_{1.4}$) from the isotropic liquid phase ($C_{100}H_{53}O$) and that the spheres had an average molecular weight of about 1700 compared with a molecular weight of about 400 for the isotropic liquid. They concluded that those materials which finally produce graphitizing carbons pass through a fluid state during the early stage of carbonisation which generally occurs in the temperature range 350-600°C. In the final stages of this fluid phase a second phase having anisotropic structures is found to form and this structure persists into the semi-coke beyond. They also concluded that any solid-surface appeared to be a preferred site for mesophase growth and that the nucleating effect of solids increased with their available surface area. It is now thought, however, that nucleation is not the principal mechanism in mesophase formation, but the growth of the anisotropic liquid crystals occurs at the expense of the isotropic liquid phase¹⁹.

White et al²⁰ employed polarized-light micrography to investigate the microstructure of the coalesced mesophase formed in the carbonisation of coal-tar pitch. They noticed that the structural features of the coalesced mesophase were similar to those found in electron micrographs of graphitized materials. Also prominent features in the polarized-light extinction contours were the nodes and crosses which did not move when the plane of polarization of the incident light was rotated. These nodal points were found to correspond to two types of linear defects in the stacking of the aromatic layer planes.

Later White and co-workers²¹ extended their classification of defect structures in the stacking of the mesophase layer planes to four. They are : (a) Co-rotating node, (b) Counter-rotating node, (c) Co-rotating cross, and (d) Counter-rotating cross.

These four types of linear defects were termed co - and counter - rotating nodes and crosses depending on whether the extinction contours moved with or against the direction of rotation of the plane of polarization of the incident light. A description of the four types of linear defects and their formation have been given in the introductory chapter on page 3. These four types of linear defects have also been represented schematically in Fig. 1.3 on page 7 of the same chapter. The notation used there is in opposition to that used by Honda et al²⁴.

White et al. concluded that the processes of the formation, coalescence and deformation of the plastic mesophase established the basic elements of the graphite microstructure, i.e. the parallel alignment of the aromatic layer planes and the rearrangement of the complex folds in the fibrous regions. The linear stacking discontinuities, namely the nodal and cross structures, were essential characteristics of the coalesced mesophase, and the nodal structures at least were found to persist in their basic form upto graphitization temperature. However, they did not appear to be involved in shrinkage cracking.

fold sharpening and the formation of mosaic blocks and kinks which occurred during pyrolysis. Later White et al²² extended their studies to include graphitizable materials such as coal-tar pitch and petroleum coke feedstocks and arrived at similar conclusions.

Honda and co-workers²³ supplemented the works of Brooks and Taylor by examining in much more detail, the effect of temperature and resident times upon the growth and physical properties of the mesophase in pitches and found that temperature and heat-treatment duration were essentially complementary factors.

In a polarized-light study Honda et al²⁴ used crossed polarizers with a gypsum plate to investigate the microstructure of the carbonaceous mesophase formed in pitches during the early stages of carbonisation. By use of this-so-called sensitive-tint technique, changes in pleochroism and in extinction contours for coalesced and for deformed mesophases were observed. This method permitted distinction between crosses and nodes and so enabled four types of linear defects in the stacking of the aromatic layer planes to be identified. These were similar to those seen by White et al²¹ but were now termed as Y-type co-rotating nodes, U-type counter-rotating nodes, X-type co-rotating crosses and O-type counter-rotating crosses. This notation is opposite to that of White²¹ probably because of opposite direction of rotation of the plane of polarization of the incident light. Honda also explained schematically how the

crosses and nodal structures were formed by the coalescence of two simple spherules and the deformation of such coalesced mesophase.

Whittaker and Grindstaff²⁵ found that the rates of formation, growth and coalescence of the mesophase spheres varied from feedstock to feedstock and that the type of molecular structure in the original feedstocks and the type of structures formed on pyrolysis had a significant influence on the resulting coke structure.

Carbonaceous mesophase formation, a liquid-state structural transition of optical anisotropy, has been found to occur in a few aromatic organic compounds^{26,27} as a prerequisite to graphitization. Reflected polarized light micrography using cross-polarizers with a gypsum plate has been found suitable for investigating the microstructures of carbonaceous mesophase.

2.5.1 Pressure effects on mesophase microstructure

Extensive studies on the carbonisation of some organic compounds and coal-tar pitches under extremely high pressures (~ 3 k bar) were performed by Walker et al^{28,29} and by Marsh et al^{30,31}. The structures of the carbonised solid products, obtained by pyrolysis in a sealed tube, were characterised as anisotropic carbonaceous mesophase, whose morphologies change from vesicular to spherical with the rise of pressure. Pressure was also observed to prevent coalescence of the mesophase spheres and thus enhance graphitizability.

Since the first report of carbonaceous mesophase spherules of optical anisotropy by Brooks and Taylor^{17,18} a large number of studies were made on the nucleation, growth and coalescence processes of mesophase spherules^{35,37}. Most of the studies showed that in the individual mesophase spherule flat aromatic molecules lie parallel to each other in the interior and perpendicular to the surface of the spherule near the surface and thus confirmed the findings of Brooks and Taylor.

2.5.2 Different types of mesophase spherules

lower part.

mesophase without insolubles is found to be deposited in the upper part of the pyrolysis vessel whereas a highly ordered like carbon black. The separated insolubles accumulate in the conventional coal-tar pitches and of artificial insolubles rise to a pronounced segregation of original insolubles and graphitizability of the residues. Increasing pressure gives It was also observed that increasing pressure improves pre-order also lowers the temperature at which pyrolysis is completed. Increasing pressure does not only increase the coke yield but petroleum pitches^{33,34} under pressure upto 200 bar showed that Some results on studies with conventional coal-tar and pressures of approximately 100 bar maintained upto 550°C. It was observed that maximum coke yields are achieved at from conventional pitches was studied by Fitzer and Terwiesch³². The effect of a gas pressure upto 100 bar on coke yield

Most recently mesophase spherules with structures other than that proposed by Brooks and Taylor have been reported. Honda and his co-workers³⁸ reported a second-type mesophase spherules having different optical properties from those of the Brooks-Taylor spherules. They proposed a structural model in which the outer layers lies parallel to the spherule surface but having a similar layer alignment like that of the Brooks-Taylor-type around the central region (Fig. 2.6B). Similar mesophase spherules were also observed by Kovac and Lewis³⁹ and Imamura et al⁴⁰. Hutteringer⁴¹ and also Imamura and Nakamizo⁴² reported the third-type mesophase spherules with all the layers lying in concentric circles about the centre of the spherules (Fig. 2.6C). The structure of a fourth-type spherule (Fig. 2.6D) was put forward by Imamura, Nakamizo and Honda⁴³. The structure of this type was almost similar to that of the Brooks-Taylor type and it is now believed that the fourth-type spherule is a metastable phase of the Brooks-Taylor type. Novel anisotropic mesophase features having a flower-petaloid texture were reported by Mochida et al⁴⁴.

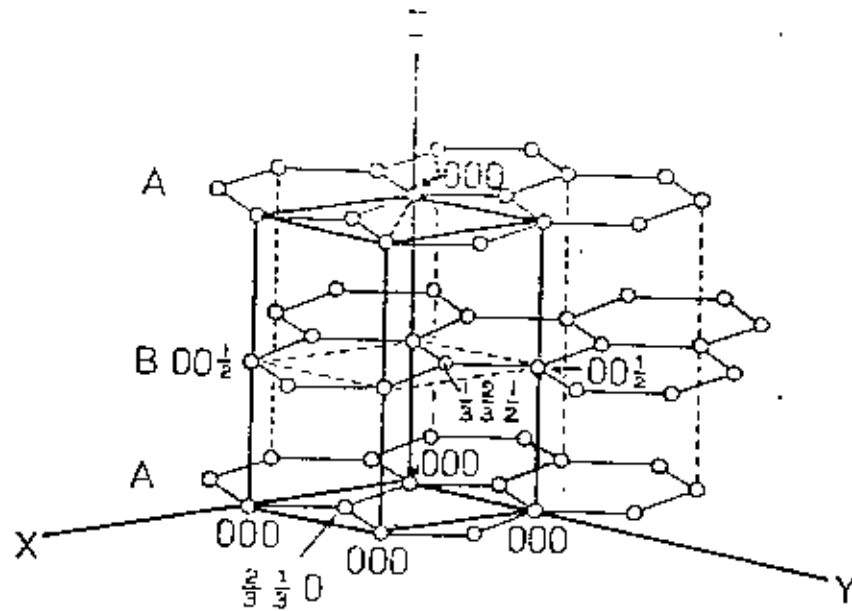


Fig. 2.1. The ideal graphite crystal structure with the hexagonal unit cell with crystal axes and lattice co-ordinates.

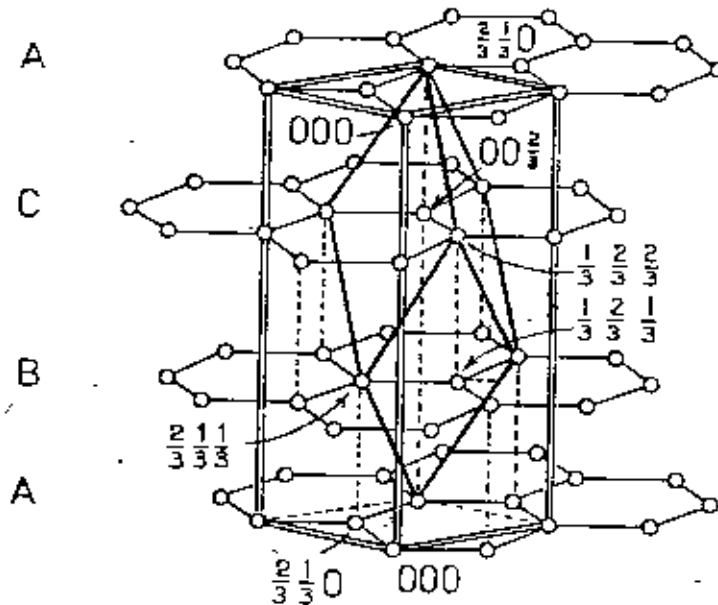
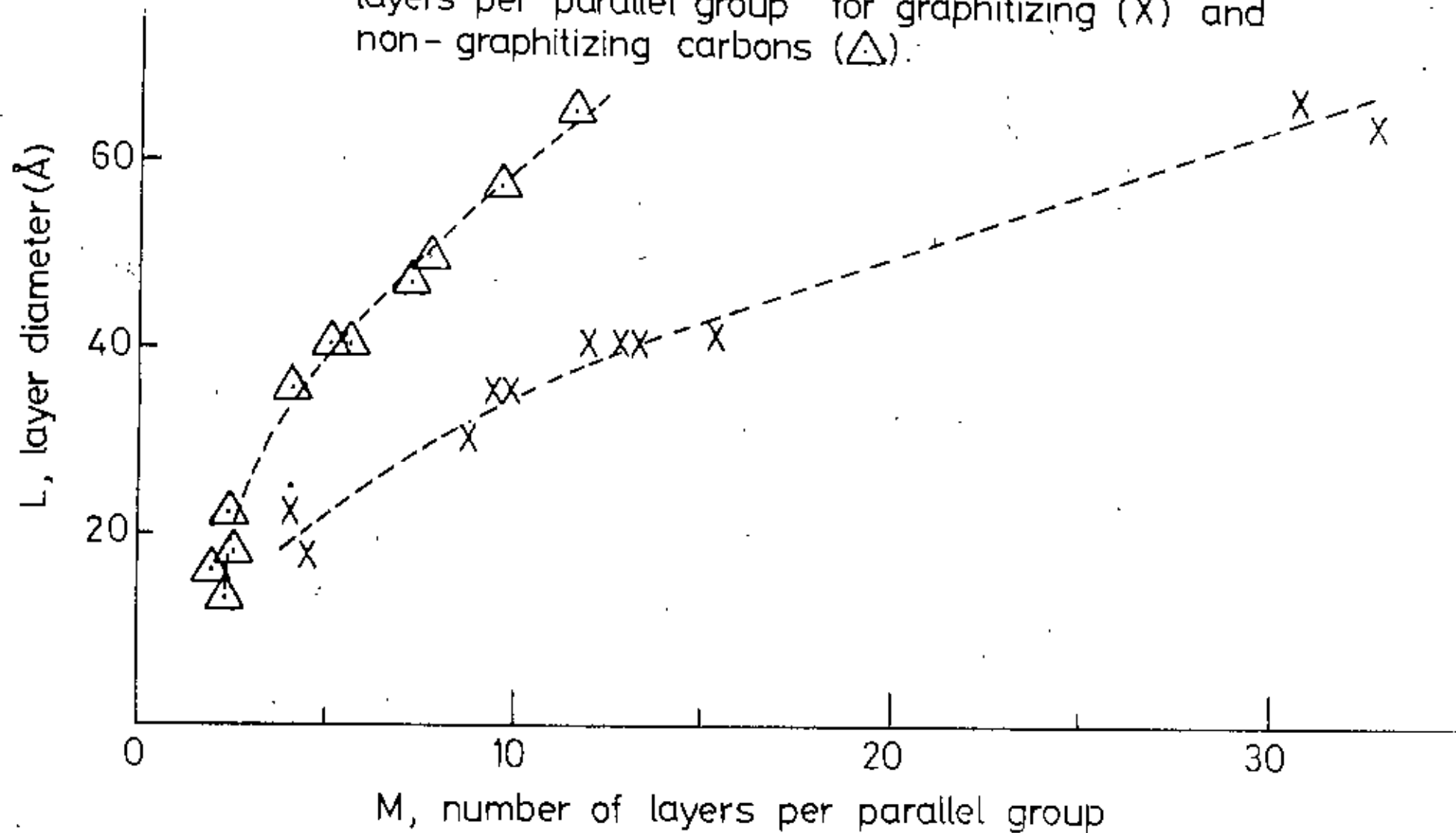


Fig. 2.2. The rhombohedral structure, showing the true unit cell and the atomic co-ordinates in the approximate hexagonal cell, shown in double lines.

Fig.2.3. Relationship between the layer diameter and the number of layers per parallel group for graphitizing (X) and non-graphitizing carbons (Δ):



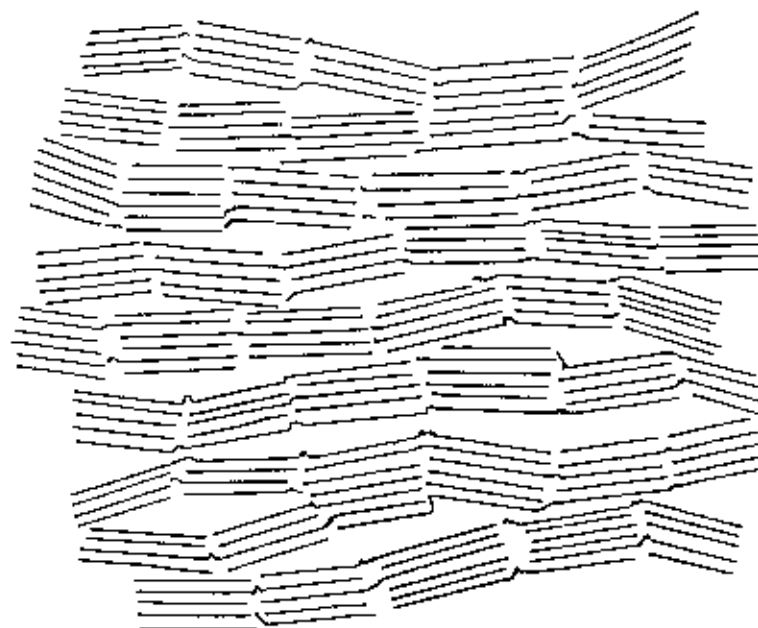


Fig. 2.4. Schematic representation of the structure of a graphitizing carbon.

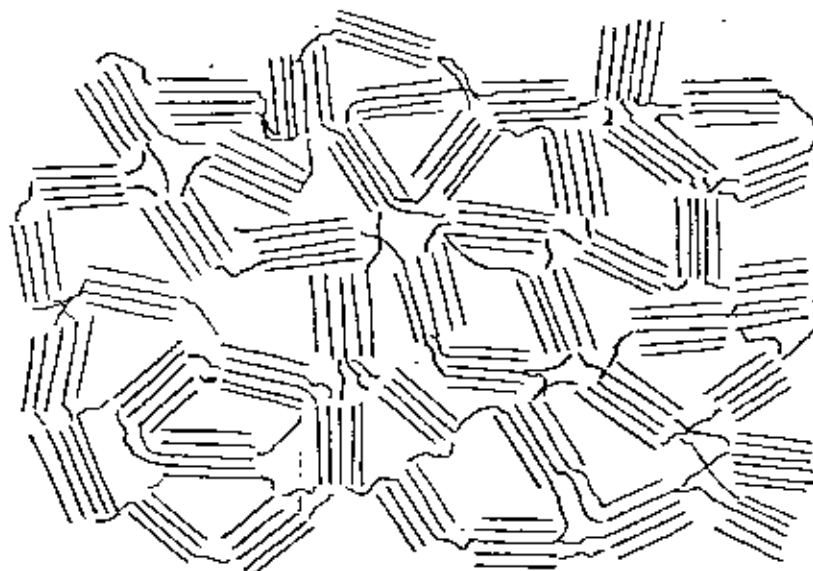
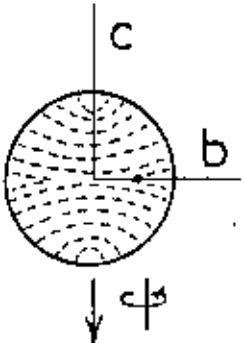
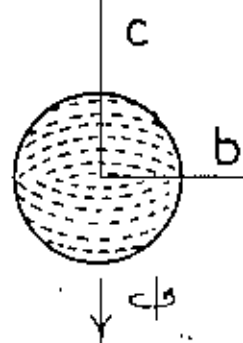
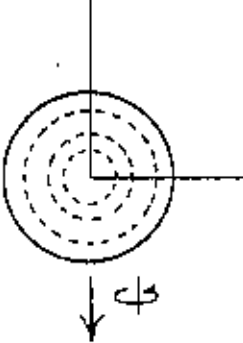
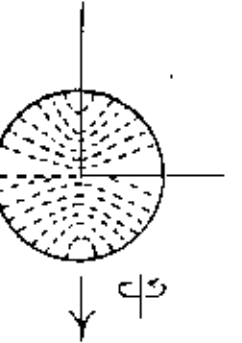
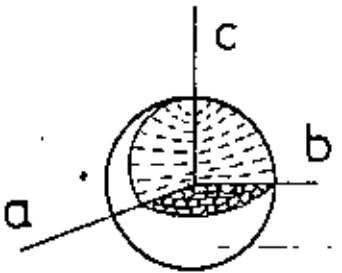
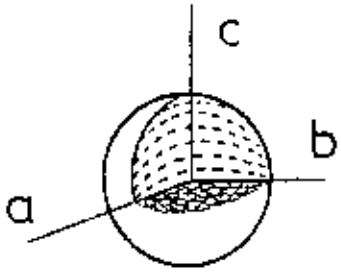
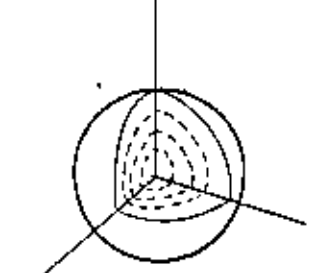
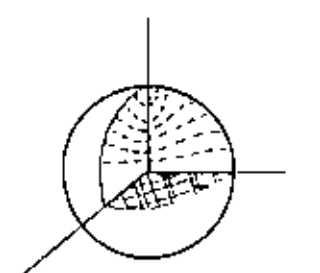


Fig. 2.5. Schematic representation of the structure of a non-graphitizing carbon.

	Brooks-Taylor type	2nd Type	3rd Type	4th Type
SECTION				
MODEL				

(A)

(B)

(C)

(D)

Fig. 2.6. Schematic structural sketches of sections and three-dimensional models for (A) Brooks-Taylor type, (B) 2nd type, (C) 3rd type, and (D) 4th type spherules.

REFERENCES

- 2.1. Ergun, S., Leroy, E.A., *Nature*, 1962, 195, 765.
- 2.2. Seal, M., *Nature*, 1960, 185, 522.
- 2.3. Bernal, J.D., *Proc. Roy. Soc. A*, 1924, 106, 749.
- 2.4. Girifalco, L.A. and Lad, R.A., *J.Chem.Phys.*, 1956, 25, 693.
- 2.5. Brennan, R.O., *J. Chem. Phys.*, 1952, 20, 40.
- 2.6. Lipson, H. and Stokes, A.R., *Proc.Roy.Soc.A*, 1942, 181, 101.
- 2.7. Debye, P. and Scherrer, P., *Physikal Z.*, 1917, 8, 291.
- 2.8. Bacon, G.E., *Acta Cryst.*, 1950, 3, 320.
- 2.9. Franklin, R.E., *Acta Cryst.*, 1951, 4, 253.
- 2.10. Mrozowski, S., *Proc. First and Second Conf. on Carbon, Buffalo, 1953*, 31.
- 2.11. Franklin, R.E., *Proc.Roy.Soc.A*, 1951, 209, 196.
- 2.12. Kipling, J.J., Sherwood, J.N., Shooter, P.V. and Thompson, N.R., *Carbon*, 1964, 1, 321.
- 2.13. Kipling, J.J., Sherwood, J.N., Shooter, P.V. and Thompson, N.R., *Carbon*, 1964, 1, 315.
- 2.14. Kipling, J.J. and Shooter, P.V., *Second Conf. Ind. Carbon and Graphite, Soc. Chem. Ind.*, 1965, 15.
- 2.15. Kipling, J.J. and Shooter, P.V., *Carbon*, 1966, 4, 1.
- 2.16. Taylor, G.H., *Fuel*, 1961, 40, 465.
- 2.17. Brooks, J.D. and Taylor, G.H., *Nature*, 1965, 206, 697.
- 2.18. Brooks, J.D. and Taylor, G.H., *Carbon*, 1965, 3, 185; *Physics & Chemistry of Carbon*, 4, 243.
- 2.19. Walker, P.L., *Carbon*, 1972, 10, 369.
- 2.20. White, J.L., Guthrie, G.L. and Gardner, J.O., *Carbon*, 1967, 5, 517.

- 2.21. White, J.L., Dubois, J. and Souillart, C., *J. Chim. Phys.*, Special Volume, April, 1969, 33; *Euratom Report 4094e*, 1969.
- 2.22. Dubois, J., Agace, C. and White, J.L., *Euratom Report 4627e*, 1971; *J. Metallography*, 1970, 3, 337.
- 2.23. Honda, H., Kimura, H., Sanada, Y., Sugawara, S., and Furuta, T., *Carbon*, 1970, 8, 181.
- 2.24. Honda, H., Kimura, H. and Sanada, Y., *Carbon*, 1971, 9, 695.
- 2.25. Whittaker, M.P. and Grindstaff, L.I., *Carbon*, 1972, 10, 165.
- 2.26. Graham, S.G., Ph.D. Thesis, 1974, Salford University
- 2.27. Hossain, T., *J. Bangladesh Academy of Sciences*, Vol.7, No.1 & 2, 1983, 57.
- 2.28. Hirano, S., Dacheille, F. and Walker, P.L., *J. High Temperature-High pressures*, 1973, 5, 207.
- 2.29. Whang, P.W., Dacheille, F. and Walker, P.L., *J. High Temperature-High pressures*, 1974, 6, 127, 137.
- 2.30. Marsh, H., Dacheille, F., Melvin, J. and Walker, P.L., *Carbon*, 1971, 9, 159.
- 2.31. Marsh, H., Foster, J.M., Hermon, G. and Iley, M., *Fuel*, 1973, 52, 234, 243, 253.
- 2.32. Fitzer, E. and Terwiesch, B., *Carbon*, 1973, 11, 570.
- 2.33. Hüttinger, K.J. and Rosenblatt, U., *Proc. Fourth Conf. Ind. Carbon and Graphite*, 1974, Soc. Chem. Ind., 1976, London, 50.
- 2.34. Hüttinger, K.J. and Rosenblatt, U., *Carbon*, 1977, 15, 69.

- 2.35. White, J.L., Air Force Report, No. SAMSO-TR-74-93, 1974.
- 2.36. Marsh, H., Fuel, 1973, 52, 205.
- 2.37. Singer, L.S. and Lewis, R.T., Abstracts of the 11th Biennial Conf. Carbon CG-27, 1973, 207, Gatlinburg.
- 2.38. Honda, H., Yamada, Y., Oi, S. and Fukuda, K., Extended Abstracts of the 11th Conf. Carbon, 1973, 219, Gatlinburg.
- 2.39. Kovac, C.A. and Lewis, I.C., Extended Abstracts of the 13th Conf. Carbon, 1977, 199, Irvine; Carbon, 1978, 16, 433.
- 2.40. Imamura, T., Yamada, Y., Oi, S. and Honda, H., Carbon, 1978, 16, 481.
- 2.41. Hüttinger, K.J., Carbon, 1972, 72, 5.
- 2.42. Imamura, T. and Nakamizo, M., Carbon, 1979, 17, 507.
- 2.43. Imamura, T., Nakamizo, M. and Honda, H., Carbon, 1978, 16, 487.
- 2.44. Mochida, I., Miyasaka, H., Fujitsu, H. and Takeshita, K., Carbon, 1977, 15, 191.

CHAPTER - IIITHE POLARISING MICROSCOPE AND OPTICS OF CRYSTALS3.1. Introduction

The use of polarized-light technique enables us to determine quantitatively the optical properties of transparent, translucent and opaque materials by studying their influence upon reflected as well as transmitted polarized light. Polarized-light technique was initially restricted to mineralogy, but in recent years it is being widely applied in metallurgy, chemistry, biology and various branches of industrial technology. Various aspects of this technique have been described in detail by a number of authors. Hallimond¹ has discussed the design and use of the polarizing microscope. Conn and Bradshaw² have described its application to metals and ores. Mott and Haines³ have discussed its application to the examination of a number of anisotropic metals. Marshall⁴ and Dale⁵ have discussed optics of crystals. Hartshorne and Stuart⁶ have given a good description for the microscopic examination of uniaxial and biaxial crystals under polarized light. A review of the use of polarizing microscopy in organic chemistry and biology is also given by Vickers⁷.

Polarized-light microscopy has been found well-suited to studies of carbonisation and graphitization because (a) the strong optical anisotropy, characteristic of the graphite crystal, begins with the parallel alignment of mesophase molecules and (b) the high viscosity of the mesophase permits microstructures formed in the plastic mesophase to be cooled to room temperature with little apparent disruption. Thus the polarized-light response on a section polished at room temperature can be used to identify the orientation of the intersections of mesophase layers with the plane of the section. Most microstructures are brought out with best contrast when the polarizers are crossed. Under this condition the extinction contours define the loci of layers lying either parallel or perpendicular to the plane of polarization of the incident light and the specific orientation can be distinguished for any particular region by the use of sensitive-tint plate.

3.2. The polarizing microscope

The polarizing microscope is essentially an ordinary compound microscope provided with calcite polarizing prisms, or, more usually now, discs of 'Polaroid' (or some other make of polarizing filter) above and below the stage, and some convenient means of altering the orientation of the object (usually in one plane only) with reference to the plane of vibration of the light incident upon it. Provision is also made for the insertion of auxiliary lenses and compensators into the path of the light through the instrument.

Because of widely varying applications the polarizing microscope has undergone many modifications, but in principle all types are the same and do not differ essentially from one another. However, the arrangement of the main components of a typical modern polarizing microscope are described below. The incident light passes through the Polaroid disc, the polarizer, and is thus constrained to vibrate in one plane only. The polarizer can be rotated in its own plane and the angle of rotation can be read against a fixed mark from divisions engraved on the metal ring in which it is mounted. A second Polaroid disc, the analyser, is mounted in the body tube of the instrument. The analyser can be rotated or withdrawn from the field of view to enable a sample to be viewed in unpolarized light. When both the polarizer and analyser are in the 0° - position (as marked on the scale) they are said to be in 'crossed position', and they will not permit light to reach the eyepiece so long as the medium between them is entirely isotropic. This is because light emerging from the polarizer is completely extinguished by the analyser according to the principle underlying the well-known Malus's experiment in optics.

The specimen under investigation, mounted in a quick-setting acrylic resin or on a glass slide, is placed on a mechanical stage. This specimen, which can be held in position by means of a clamp attached to the stage, is capable of movement in two directions in the plane of the stage. To permit easy return to a certain specimen point the coordinate positions

can be read against millimetre scales. The stage can be rotated in its own plane and is provided with centering screws and 'click stops' at intervals of 45° . The angle of rotation of the stage can be measured on a degree scale. The stage is also provided with a clamp to arrest the motion if so desired.

Above the objective lens is a slot in the body tube of the instrument, through which the compensator or tint plate is inserted. The tint plate, which is a gypsum plate (sometimes called first-order red plate) is placed at an angle of 45° to the vibration planes of the polarizer and the analyser when they are in the crossed position.

Also contained in the microscope body is the Bertrand lens which can be swung into or out of the field of view. This lens and the eye piece act together to constitute a low-power microscope which can be focussed on the upper focal plane of the objective. The chief purpose of this combination is, however, to give an enlarged image of the interference figures which are formed in this plane under certain conditions. Above the Bertrand lens is an iris diaphragm, or a pinhole stop, the purpose of which is to isolate the interference figure of the crystal occupying the centre of the field of view when several are present.

The condensing lens system is situated between the rotating stages and the polarizer. Its primary function, as in the compound microscope, is to bring the incident light to a focus in the plane of the specimen.

The eye piece lens system, fitted to the microscope body is of the binocular type, having a certain magnification. This together with the different objectives produces the overall magnification.

The illumination of the microscope is provided by a low - voltage 15 watt quartz-iodide bulb, the power supply of which is controlled from a regulating transformer. This lamp generally operates on 6 V, 15 watt a.c. supply and contains a fixed condenser. The bulb is fitted in a well ventilated housing with a circular opening for the emission of light.

The body tube of the microscope allows a camera adaptor to be fitted after the analyser. The adaptor is supplied with a definite magnifying eye piece. The camera used for photography is a 35 mm Kaw ES-2.

3.2.1. Modes of observation in a polarizing microscope

Two modes of observations are available in a polarizing microscope: orthoscopic or conosopic.

3.2.1.1 Orthoscopic arrangement

The orthoscopic arrangement may be regarded as an ordinary microscope arrangement (Fig.3.1) in which the crystal is illuminated by a series of essentially parallel, normally incident rays all of which travel along the same crystallographic direction within the crystal. In this type of observation there are three combinations of polarizer and analyser that enable three different sets of observations and measurements to be made.

Firstly, both the polarizer and analyser being removed, observations can be made on colour, crystalline form, cleavage and fracture, together with the determination of the refractive index of isotropic crystals.

Secondly, with the polarizer inserted, the principal refractive indices of anisotropic crystals can be determined. Observations on pleochroism (which is the variation in colour or tint resulting from differential absorption of white light) and twinkling (which is the variation in relief when a crystal having a large double refraction is rotated in an immersion medium whose refractive index is near to one of those of the crystal) may also be made with just the polarizer inserted.

Lastly, with the polarizer and analyser inserted in the crossed position, distinctions can be made between isotropic and anisotropic substances and measurements of extinction angles can be made.

Most of the observations on the polarizing microscope are performed with both the polarizer and analyser inserted in crossed position. The origin of some of the effects seen through the microscope are discussed in a later section of this chapter but here it may be useful to review them.

extinguishes when the traces of its vibration directions being brightest at 45° from the extinction position. The section positions of darkness the crystal will become illuminated, dark, or extinguished at intervals of 90° , and between these crystal on the stage in either cases will cause it to become rays travelling in different velocities. Rotation of such a principal directions at right angles to each other, the two by a polished anisotropic surface is polarized in the two travelling with different velocities. Similarly, light reflected rays vibrating in planes at right angles to one another, and polarizer is doubly refracted on entering the crystal, the two crossed polars, the plane polarized light emerging from the Alternately, when an anisotropic substance is placed between vibration, and the field remains dark as if the stage is empty. It does not interfere in any way with the direction of light substance is placed on the microscope stage between the polars, direction, the wave surface being sphere, and so, when such a isotropic substances light vibrates with equal ease in every

The reason for this difference in behavior is that in in certain definite positions will become dark. will appear coloured on rotation in most orientations and only their orientations. On the other hand, anisotropic substances dark, like the rest of the field of the microscope whatever be namely, isotropic and anisotropic substances. The former remain all non-opaque substances can be divided into two groups, in accordance with their behavior between crossed polars,

become parallel to those of one of the polars, for in such positions, the light from the polarizer is not resolved in the crystal, but passes on to the analyser unchanged as if there is no crystal on the stage, and hence darkness results. The colours shown in the positions of illumination are known as 'polarization colours'.

The polarization colours observed through the microscope depend on the relative retardation or optical path difference, i.e. the retardation of the ordinary ray relative to the extraordinary ray. For any crystal section the amount of retardation of one wave behind the other depends on the difference in wave velocity beams in a direction normal to the plane of the section. The retardation also depends on the thickness of the crystal plate. Since the wave velocities are related inversely to their respective refractive indices, the relative retardation of the section is given by the formula: $R = (n_1 - n_2)t$, where ' $n_1 - n_2$ ' is the difference between the two refractive indices for the ordinary and extraordinary rays, i.e. its birefringence and ' t ' the thickness of the plate. The phase difference between the two components of velocity on emergence from the crystal is given by $R \times 360/\lambda$; R being the relative retardation, λ the wavelength of incident light. If the sample is viewed in white light and at the same time its thickness is varied from zero to a finite quantity, a series of different colours will be seen. This is because the increasing thickness introduces a phase difference between the two components of velocity and

consequently constructive and destructive interference occurs at different thickness for different wavelengths. The colours from zero thickness upwards are arranged in orders, the Newton colour scale, each one terminating and including red. As the thickness is increased still further, the colours become further and further complex, owing to the overlapping of the extinction bands for different parts of the spectrum, the fifth and sixth orders consisting mainly of pale pinks and greens. In still higher orders these colours merge into white.

For bireflecting substances the two reflectances belonging to the principal directions in a surface may also vary independently according to the wavelength of light used. In white light the two directions then present different characteristic tints. This is sometimes called 'reflection pleochroism', since it has some analogy with pleochroism in transmitted light. The latter, however, depends substantially on the absorption, while the reflectance (ratio of the intensity of the reflected light to that of the incident beam) is determined by both absorption and refractive index. As the stage is rotated under polarized illumination the reflected light changes in tint through the admixture in varying proportions of the two component tints, each of which is seen unmixed when the vibration direction of the incident light coincides with the corresponding principal direction. The changes obtained in this way are very characteristic. In a uniaxial crystal there are two principal colours, for light vibrating parallel or perpendicular to the crystal axis and in inclined sections the tints remain the same. In a biaxial crystal there are three principal colours and the effects for inclined sections are more

complicated. An important aspect of these variations is that the difference between the reflectances for the two principal directions, i.e. the bireflection for the section, though small, often varies greatly with the wavelength. This is termed 'dispersion of the bireflection'. It causes very distinctive colour effects when the section is examined with the two polars at or near the crossed position.

3.2.1.2. Conoscopic arrangement

The passage of light through a polarizing microscope when it is used as a conosccope to observe a specimen on the stage of the microscope is indicated in fig. 3.2. The conoscopic arrangement requires, in addition to the polarizer and analyser, the insertion of an Amici-Bertrand lens and a substage condensing lens. The former converts the microscope into a low-power telescope focussed at infinity. The latter causes the object on the stage to be illuminated by a cone of light rather than by a bundle of near-parallel rays as it is with orthoscopic case. Important additional information may be obtained by passing a strongly convergent beam of light through the crystal when it is possible, by various means, to examine the optical character in many directions at one and the same time. This is done by viewing between crossed polars, not the image of the crystal, but another optical image formed in the principal focus of the objective by the strongly convergent beams of light. This image is called the 'interference figure'. Each point in the field corresponds to a given direction through the crystal. In effect, the Bertrand lens and the eyepiece constitute a system used to examine the pattern in the back focal plane of the objective.

The interference figures produced in a conosccope can be classified into two broad divisions: those formed by the uniaxial crystals and those formed by the biaxial crystals. The former pattern consists of concentric circles known as 'isochromes' onto which is superposed a pattern in the shape of a maltese cross, the arms of which are known as 'isogyres'. This pattern is produced assuming that the section of the crystal is normal to the optic axis, or in the basal section. On rotation of the stage, the pattern remain unchanged provided that the optic axis is centred and perpendicular to the stage. If a section of the crystal parallel to the optic axis is used then the isogyres only retain a broad cross shape when the optic axis is parallel to one or other of the polars. Rotation of the stage causes the isogyres to move in and out giving rise to 'flash figures'. These phenomena are dealt with in detail later in section 3.3 of this chapter.

In a biaxial crystal there are two optic axes, the lines bisecting their enclosed acute angle is called the 'acute bisectrix'. The interference figure obtained when viewing a section normal to the acute bisectrix consists of two 'eyes' or melatopes, which mark the points of emergence of the optic axes, surrounded by bands of equal retardation, coloured in white light. On to this pattern are superimposed the isogyres which form a cross when the trace of the optic axial plane (i.e. the line joining both melatopes) lies parallel to either polar, that arm of the cross passing through the melatopes being narrower than

the other. Rotation of the crystal away from this position causes the cross to break up into two hyperbolic brushes which are centred on the melatopes. The isogyres revolve in a direction opposite to the movement of the stage. The origin of the biaxial interference figures given by a section normal to the acute bisectrix as described above is discussed later in section 3.3 of this chapter.

3.2.2. Types of illumination used in polarizing microscope

There are three types of illumination usually used with the polarizing microscope. These are: Bright field (with and without polars), Dark field and phase contrast. Bright field illumination is that one where the empty area surrounding any particular specimen being observed under the microscope appears bright. This can be achieved in two different ways.

Firstly, when both the polarizer and analyser are removed from the microscope. This is the situation for the normal compound microscope.

Secondly, when both polars are inserted in the crossed position together with a compensator or tint plate. The tint plate is made of a flake of clear gypsum (or selenite ground), cleaved to a thickness such that the plate produces a path difference (i.e. retardation) of one wavelength for yellow light near 575 nm wavelengths. The plate is 0.062 mm thick and extinguishes the yellow light so as to produce an interference colour near first-order red in white light. The gypsum plate assists

in the determination of exact extinction positions since any slight rotation from the extinction position results in a change from the lower to higher-order colours, blue or yellow, which is immediately obvious to the observer. The basic principle of a tint plate is further described in section 3.4 of this chapter.

Dark field illumination is that one where the empty space surrounding any particular specimen, appears dark, and is obtained when both polarizer and analyser are in crossed position with the tint plate removed. Due to the direction of illuminating rays emanating from a dark field condenser, only those portions of the light diffracted by the specimen pass into the objective, the undiffracted rays being extinguished by the crossed polars.

A method intermediate between dark field and bright field examination is provided by de-centering the beam of incident light, as shown in fig. 3.3, which results in a relatively small portion of the direct light being accepted by the objective.

Phase contrast illumination is achieved with the aid of a special objective lens containing a flat plate into which is machined a circular groove. The difference between the thickness of the plate and the depth of the groove is of the required size to produce a phase difference of 180° between a light ray passing through the plate and one passing through the groove. Each objective is used in conjunction with one of the annular discs contained in the condenser so that only an annulus of light from the condenser reaches the phase plate in the upper

local plane of the objective illuminating only the groove. When a specimen is observed the diffracted rays pass through the centre of the phase plate, and interfere with the undiffracted rays passing through the annulus. This effect therefore changes small phase differences (caused by absorption in different thickness of the sample, which cannot be detected by the eye) into large amplitude differences (which are easily detected). This makes it possible to see detail in a crystal which would normally be transparent in reflected as well as in transmitted light. The illumination of the field from dark to bright can be adjusted by means of an iris diaphragm contained in the objective lens close to the phase plate.

3.3. Optics of crystals

In dealing with crystals we must generalise the material equations $\underline{J} = \sigma \underline{E}$, $\underline{D} = \epsilon \underline{E}$, $\underline{B} = \mu \underline{H}$ to take account of anisotropy.

For anisotropic media such as crystals we have to introduce the dielectric tensor ϵ_{kl} and when dealing with absorbing crystals we further have to introduce the conductivity tensor σ_{kl} .

Combining Maxwell's equations and the general material equations Fresnel⁸ arrived at the formula for the propagation of light in crystals leading eventually to the concept of the ordinary ray, O-ray and the extraordinary ray, E-ray travelling at different speeds in the crystal. These provide the explanation of many of the phenomena observed in crystals for example bireflection and double refraction in a uniaxial crystal such as calcite.

The electromagnetic equations may be solved⁸ to give the interference conditions for a uniaxial crystal when viewed between crossed nicols or polarizers and in converging light. However a simple geometric model based on the O- and E - rays leads directly to the same result.

If we view the basal section of a uniaxial crystal in converging polarized beam of light, all the rays not travelling along the optic axis are doubly refracted (Fig.3.4). At the upper surface there emerge at all points rays O' and E' derived from a given pair of incident parallel rays EE, which from there onwards travel along the same path, vibrating in planes at right angles to one another. One of these rays will have been retarded behind the other by an amount which depends upon the direction of their paths through the crystal. When the retardation of one ray behind the other is exactly one wavelength or any whole multiple of one wavelength, darkness results due to interference. All emergent rays so allied to one another lie on the surfaces of an infinite number of geometrically similar cones coaxial with the optic axis (Fig.3.5) and the locus of their focal points in the interference figure is a circle. This gives rise to the series of concentric rings, called 'isochromes' in the interference pattern (Fig.3.6).

The O-ray vibrates in the plane containing the ray and a line normal to both the ray and to the optic axis, whilst an E-ray vibrates in the plane containing the ray and the optic axis. The traces of these planes of vibration are shown

in fig. 3.7 by small double-headed arrows. The O-rays vibrate tangentially, and the E-rays radially. It is obvious that along the directions PP' and AA' which represent the vibration planes in the polarizer and analyser respectively, extinction will result, and at 45° to these directions, between the dark rings, the interference figure will be most brightly illuminated. This pattern in the form of a maltese cross is shown in fig. 3.6. The arms of the maltese cross are called 'isogyres'. In the central portion of the field the rays are normal to the section and travel parallel to the optic axis and so the field there remains dark. The pattern in fig. 3.6 is a typical interference figure.

In the basal section rotation does not distort the cross but usually optic normal sections are presented by uniaxial crystal under microscope. This results in a figure which is very similar to that of a biaxial optic normal interference figure, and consists of four series of hyperbolic isochromatic bands which are disposed symmetrically in quadrants, and which rotate with the stage. The bands are frequently very diffuse in white light. As the stage is rotated diffuse hyperbolic isogyres enter the field, form a broad cross in the centre when the optic axis is parallel to one or other of the crossed polarizers, i.e. when the crystal is in the extinction position for parallel light, and then swing out again in the direction of the optic axis. These isogyres move very rapidly and only occupy the centre of the field during the rotation of the stage through

a few degrees, giving the impression of a momentary darkening of the whole field, for, which reason the figure is often called a 'flash figure'.

When rays of convergent light enter the section of a biaxial crystal not along the optic axis, double refraction takes place. Those rays the wavefronts of which travel along the optic axis are brought to a focus in the interference figure at two points called the 'metatopes', which, being extinguished by the analyser, appear dark. All other rays emerging from the crystal are made up of two components, differing in phase and vibrating in directions at right angles to one another (just as in the uniaxial case described before), and therefore resulting in interference in the analyser. Emergent rays for which the retardation is the same lie on conical surfaces surrounding each optic axis, the sections of the cones being nearly circular when the inclination to the optic axis is small, and becoming more pear-shaped as this inclination increases; at still greater inclinations the surfaces merge so as to surround both optic axes. The relative arrangement of representative surface corresponding to retardations of λ , 2λ , 3λ , etc. for a given wavelength of light is illustrated in fig. 3.8. Each surface (together with its allied parallel surfaces) produces a ring of focal points in the interference figure similar in shape to its trace upon a horizontal plane. Such an interference figure consisting of two eyes or metatopes surrounded by coloured bands when viewed under white light is shown in fig. 3.9.

Crystals and glasses which appear coloured by reflection or transmission owe thus to the fact that they absorb one or more bands of wavelengths in the visible spectrum to an appreciable degree. Absorption consists in a progressive decline in the amplitude, and hence the intensity, of the light as it enters more and more deeply in the medium, the energy thus lost being in most cases converted to heat. The absorption of the light leads to Fresnel's equations becoming complex. The solution to these equations is well known in the case of reflection from a metallic surface, however they are not so well known for absorbing crystals. Born and Wolf⁸ derive the expressions for the case of a partially absorbing partially transmitting material.

In anisotropic crystals the absorption depends on the vibration direction of the light. Thus the two polarized components into which a ray of monochromatic light is resolved on entry suffer in general different degrees of absorption, and when white light is used the transmission colours for the two components may therefore differ considerably. Similar is the case with reflection colours. This phenomenon is known as 'pleochroism' and observations on this constitute the most important practical application of absorption in the study of crystals using polarizing microscope.

3.4 Basic principle of a tint plate

Tint plates or compensators are often used to assist in the identification of interference colours shown between crossed polars. These are crystal plates or wedges of known optic orientation and relative retardation, suitably mounted so that

they can be inserted into the microscope slot just below the analyser, intercepting the light beam. If the direction of the slot through the tube is at 45° to the vibration direction of the polars in their crossed position then the compensator must be mounted so that one of its vibration directions is parallel to the plate when it is inserted.

The basic principle of a tint plate is shown in fig.3.10. The stage of the microscope is turned so as to bring one of the vibration directions of the specimen parallel to the slot i.e. at 45° to an extinction position. The compensator plate is inserted and it is noted whether the effect of this is to (a) raise or (b) lower in Newton colour scale, the original colour shown by the specimen. If (a) (the additive effect) the corresponding vibration direction of the specimen and compensator must be parallel. If (b) (the subtractive effect) the vibration direction of the specimen and compensator are in opposition.

The most common compensators are quarter wave mica plate (also called the quarter undulation plate), first-order red or unit-retardation plate (sometimes called the gypsum plate) and the simple quartz wedge.

The quarter-wave mica plate is made of a sheet of muscovite mica cleaved to such a thickness that one transmitted component is retarded a quarter of a wave of yellow light behind the other, i.e. by about 145 nm. By itself between crossed polars the plate gives a pale grey interference colour.

The first-order red plate may be made of a cleavage sheet of gypsum (also called selenite) and is thus sometimes called the gypsum plate. The thickness is such that the relative retardation between the two transmitted components is one wavelength of yellow light ($\approx 575 \text{ nm}$). Between crossed polars it gives violet-red interference colour at the end of the first order and is usually called the first-order red or Red I plate. It is also known as the sensitive red or sensitive tint plate because, if it suffers a very small subtractive effect there is very marked change to orange or yellow, while if it suffers a very small additive effect the red colour is raised to indigo or blue. The plate is sometimes made of cleavage sheet of mica or a plate of quartz ground to the right thickness. In general, the first-order red plate is more suitable for specimens showing a very low colour since, owing to the sensitive colour of the plate, additive and subtractive effects are sharply distinguished.

3.5. Optical studies of the carbonaceous mesophase spheres

The theoretical background for work with reflected polarized-light was provided largely by the aid of the mathematical treatment due to Drude⁹ (1887). This was followed by practical applications to microscopy initiated by Wright¹⁰ (1919). Wright gave a summary of the theory, starting from the Maxwell's equations, and dealing with the special cases of normal incidence on a surface normal to an optical symmetry plane. When the reflected light can be represented by two plane polarized components at right angles, subject to a phase difference, the cases were dealt with more directly by Woodrow,

Mott and Haines¹¹.

Apart from a general remark by Taylor¹³ concerning the remarkable reflectance pleochroism of carbons, coal and graphites it has generally been assumed that the reflected light microscopy is analogous to the transmitted one. The fundamental equations for reflectance pleochroism have not been reviewed in the carbon literature since 1928 despite the predominance of the use of reflected-light microscopy technique. The transmission-light microscopy observations of the mesophase spherules have in broad outline been related to the reflectance experiments.

The usual current solution has been to assume the complementary nature of reflection and transmission and the simple proof of the pleochroic effects has been put forward for example by Gray and Cathcart¹² making observation on pyrolytic carbon deposits.

Making observations on pyrolytic carbon (PyC)-coated fuel particles they noted maltese cross patterns when the microscope was in the orthoscopic mode and not the conoscopic mode. Fig.3.11 shows a schematic representation of a PyC-coated particle. The thin lines are the 'c' axes of the PyC fibres; in this case the c-axis coincides with the optic axis. When a beam of plane polarized-light, incident normally on a hexagonal crystal, is reflected from a surface not perpendicular to the 'c' axis, the reflected beam is resolved into two

components, \underline{R}_S and \underline{R}_P . The electric vectors of these two components vibrate perpendicular and parallel, respectively to the principal plane of the crystal (the principal plane is parallel to the 'c' axis). These can be expressed in terms of the incident vectors as follows:

$$\underline{R}_P = \underline{E}_P \frac{(n_p - 1)}{(n_p + 1)}$$

$$\underline{R}_S = \underline{E}_S \frac{(n_s - 1)}{(n_s + 1)}$$

where n_p and n_s are the refractive indices parallel and perpendicular to the principal plane.

There are four directions in the PyC coating in which the incident electric vector is either perpendicular or parallel to the principal planes of the PyC fibres. In these directions either \underline{E}_P or \underline{E}_S must be zero. The electric vector of the reflected light, therefore, can have only one component, and the reflected beam must be plane polarized with the same azimuth of polarization as the incident beam. Light reflected from these areas will be extinguished by the analyser, hence dark bands will be seen on the specimen in these regions.

Everywhere else on the specimen the incident electric vector will have components parallel and perpendicular to the principal planes and, due to absorption in the PyC these two components will undergo both a relative amplitude reduction

and a phase retardation on reflection resulting in elliptically polarized light which is not extinguished by the analyser. These areas will be light.

Mesophase spheres also show a characteristic maltese cross pattern in orthoscopic light. Taylor¹³ has put forward a characteristic structure to account for this (see fig. 3.12). The behavior of the spheres in singly and doubly polarized light is shown schematically in figs. 3.13 and 3.14.

At the earliest stage at which they can be resolved, the spherical bodies are strongly pleochroic. Their absorption of plane-polarized light varies with orientation from being very strong (colour almost black) to very weak (colourless or pale yellow). Analogous behavior is observed in reflected light. However, the pleochroism of the spherical bodies is not quite as simple as that in a pleochroic crystal. As the spherical bodies grow larger it can be seen that the pleochroism is not uniform but that dark bars move across the sphere, unite, and then move out again (Fig. 3.13). Between crossed nicols, the spherical bodies, when small, behave essentially as single crystals, lightening and darkening four times per stage revolution. As the bodies grow larger the simple extinction gives way to the sequence shown in fig. 3.14.

Honda, Kimura and Sanada¹⁴ employed the so-called 'sensitive tint method' in an attempt to get further information about the structures. From the changes in pleochroism and extinction contours for the mesophase spherules, they concluded that a simple mesophase spherule is optically a uniaxial positive liquid crystal belonging to the hexagonal system with a straight extinction.

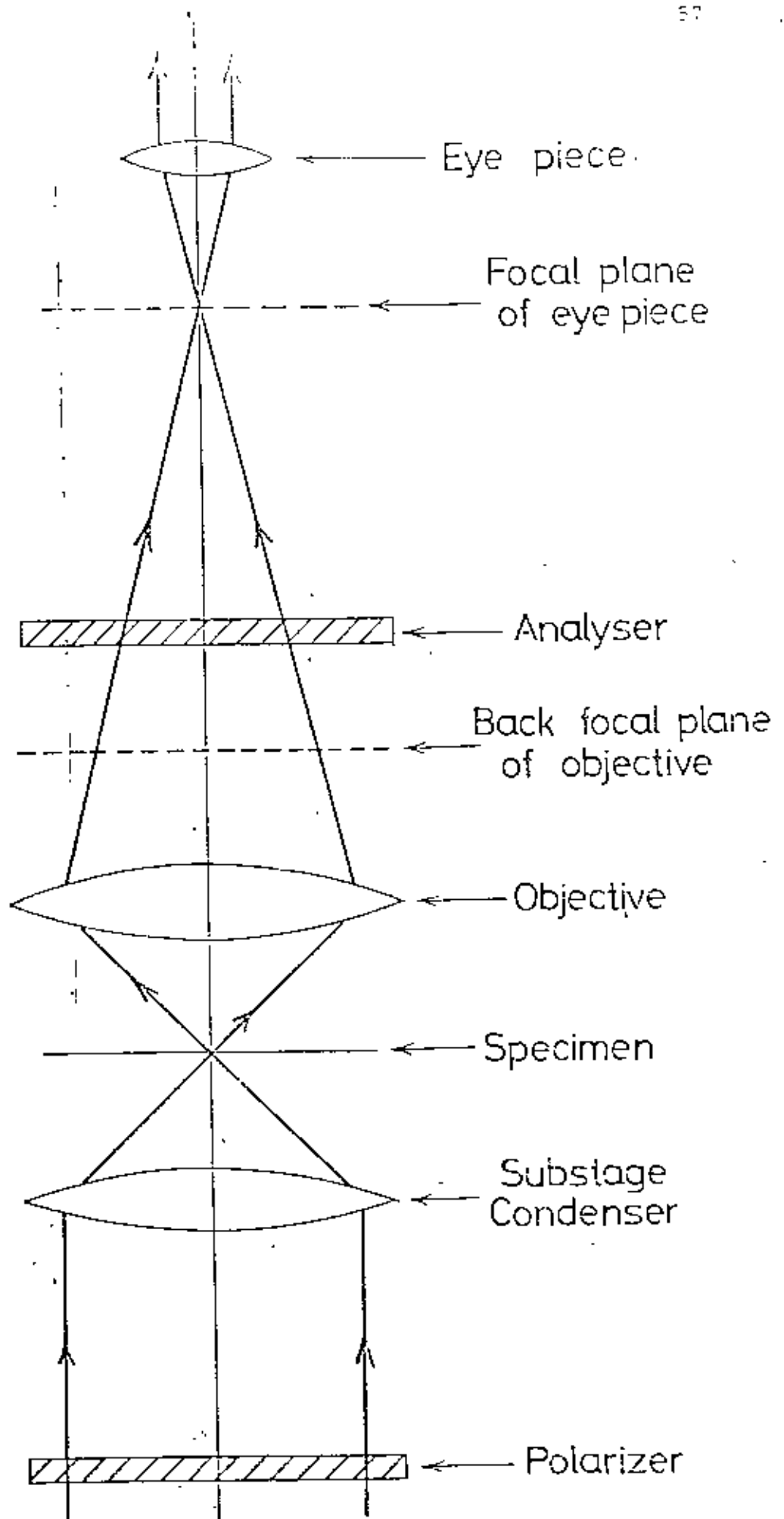


Fig . 3.1. Polarizing microscope in orthoscopic mode.

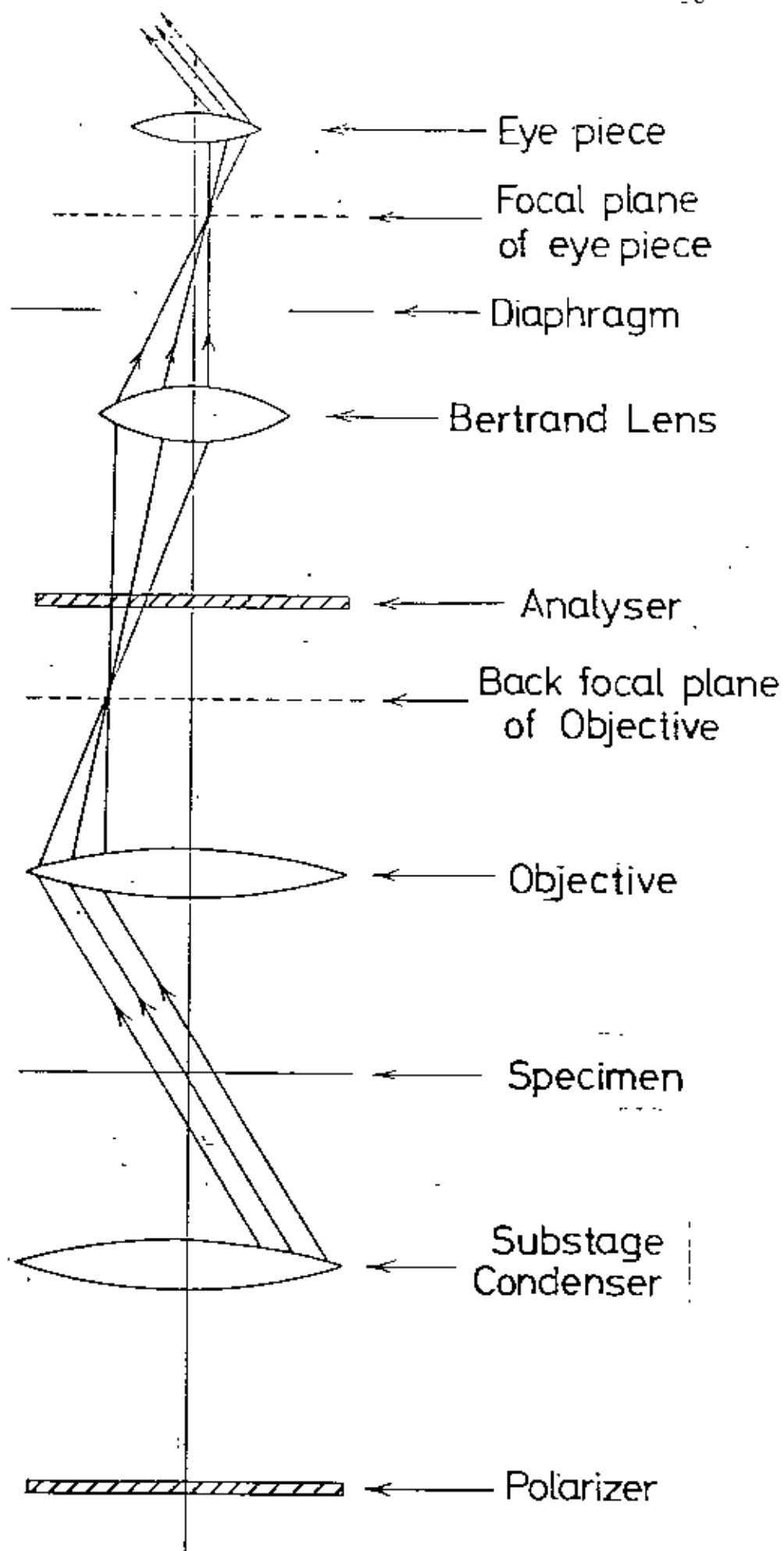


Fig. 3.2. Polarizing microscope in conoscopic mode.

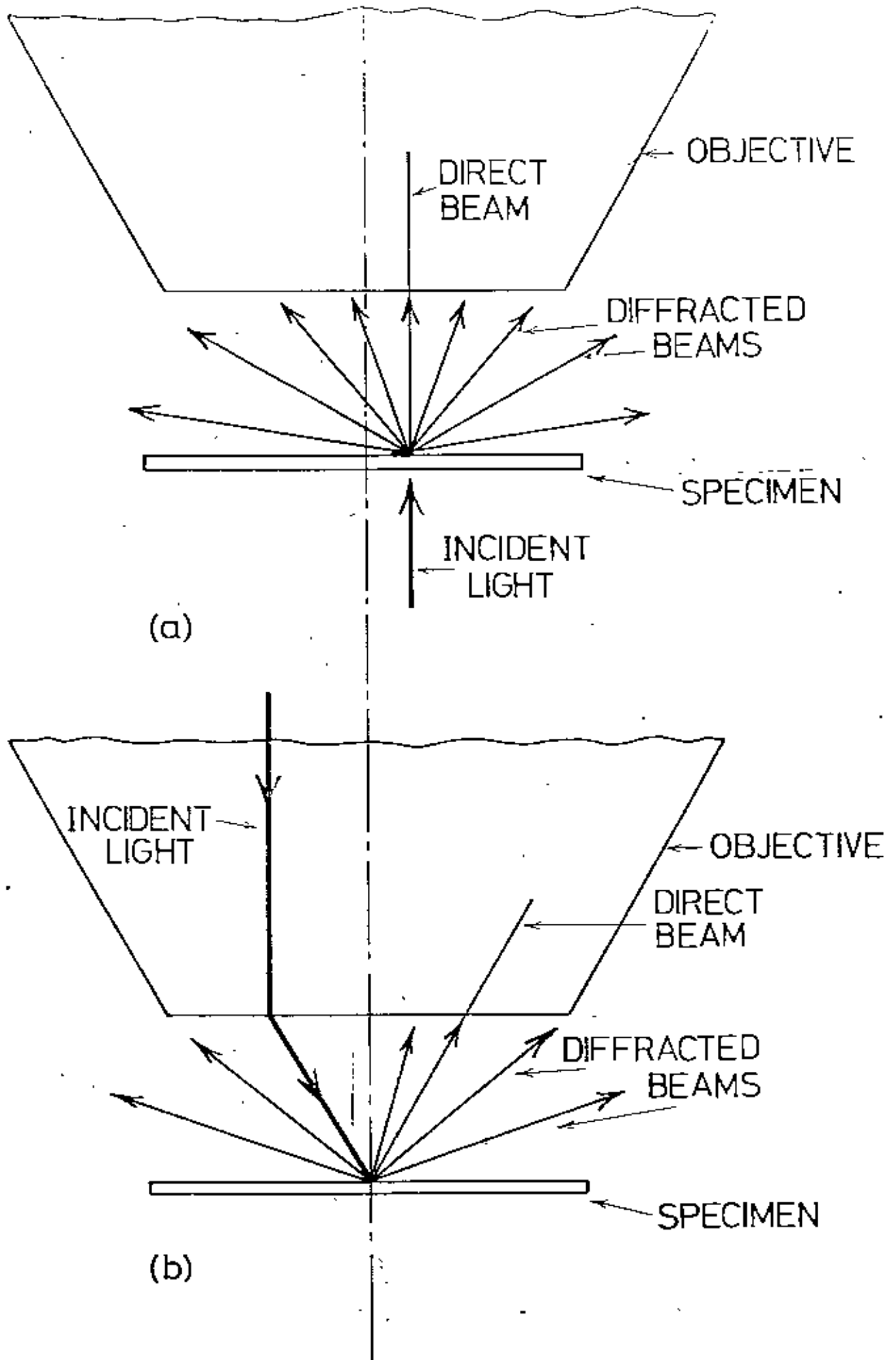


Fig. 3.5. Illumination provided by a de-centred incident beam (a) For transmitted light (b) For reflected light.

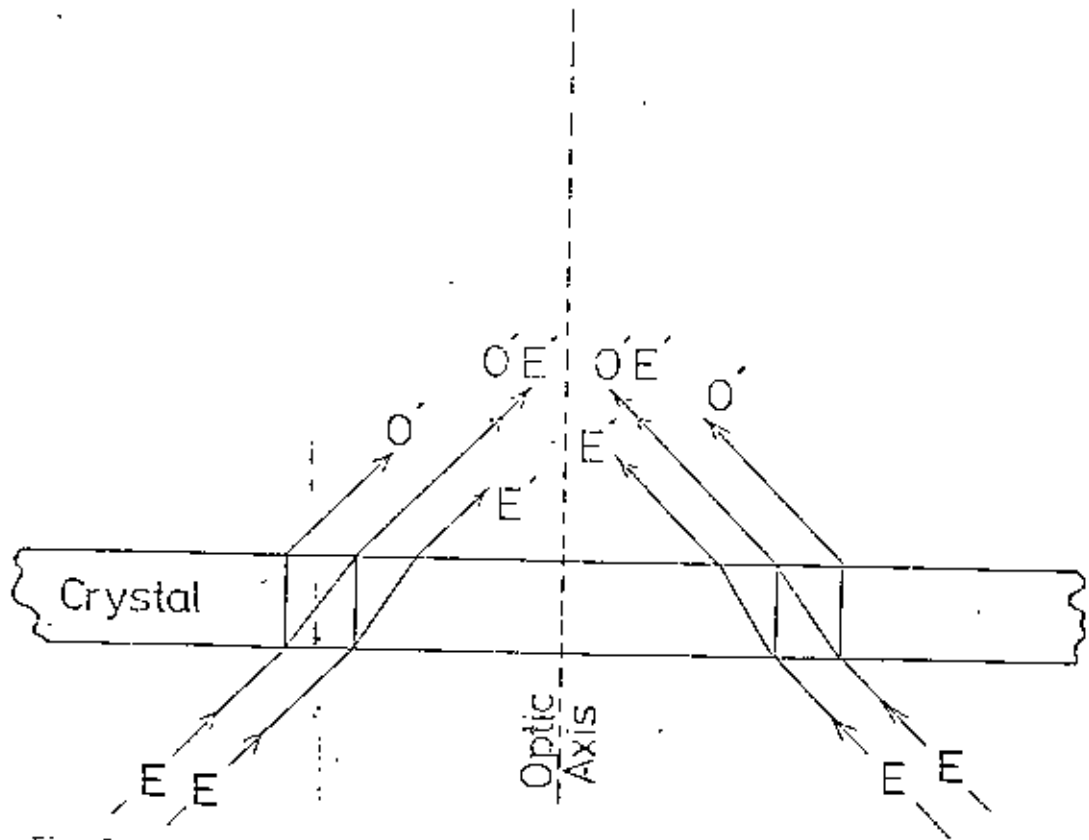


Fig. 3.4. Passage of convergent polarized light through a uniaxial crystal nonaxial to the optic axis.

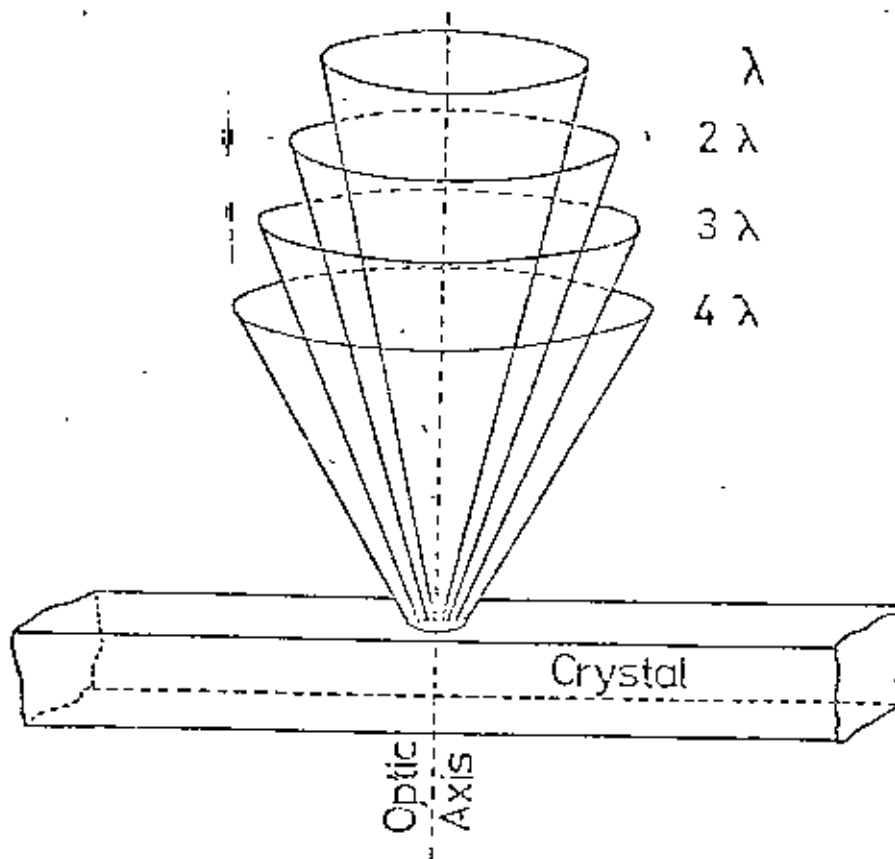


Fig. 3.5. Cones of equal retardation around the optic axis of a uniaxial crystal.

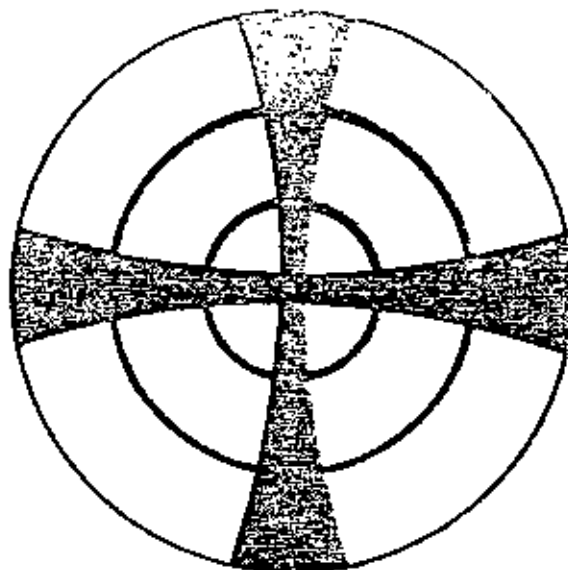


Fig. 3.6. Typical interference figure for uniaxial crystal.

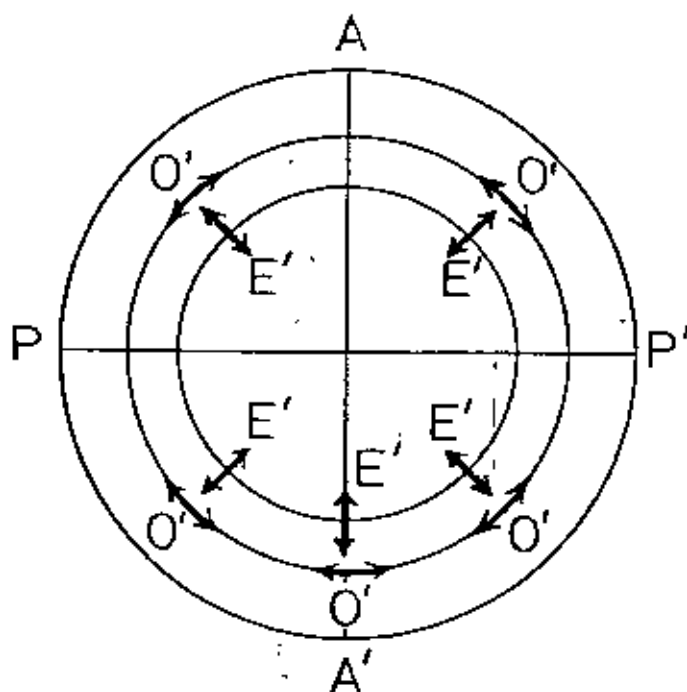


Fig. 3.7. Directions of vibration of O- and E-rays (AA' , PP' -vibration planes in polarizer and analyser).

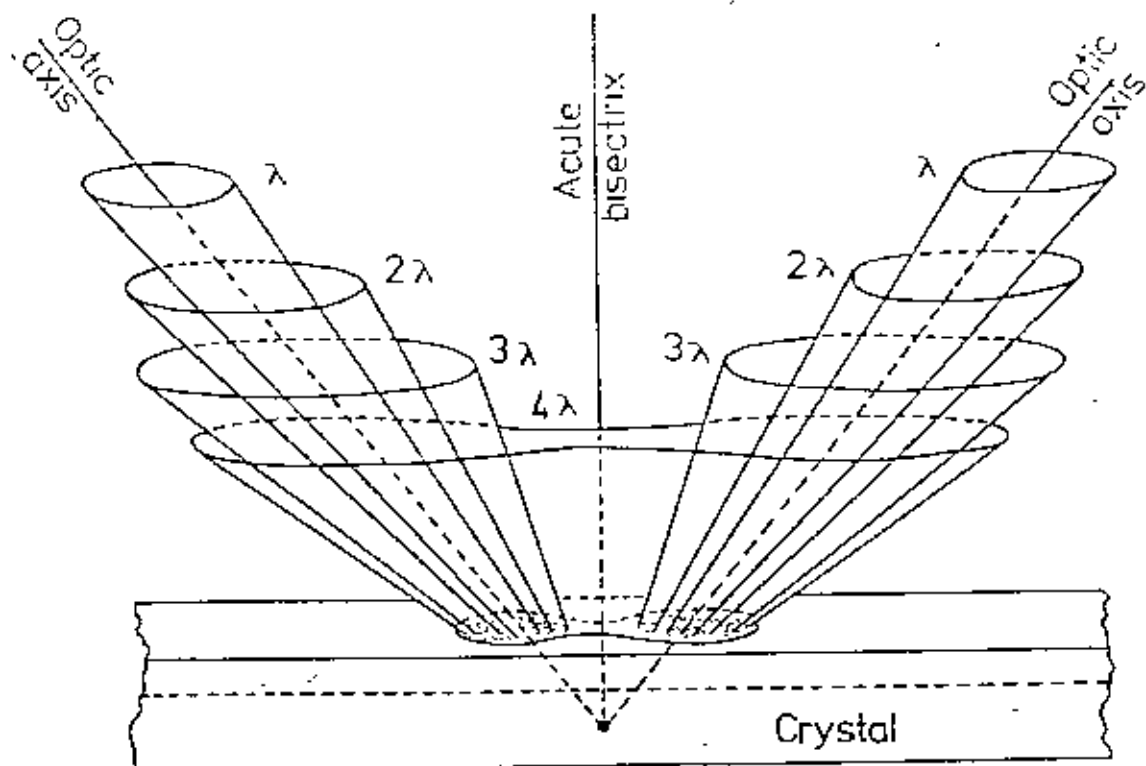


Fig. 3.8. Surfaces of equal retardation around the optic axes of a biaxial crystal.

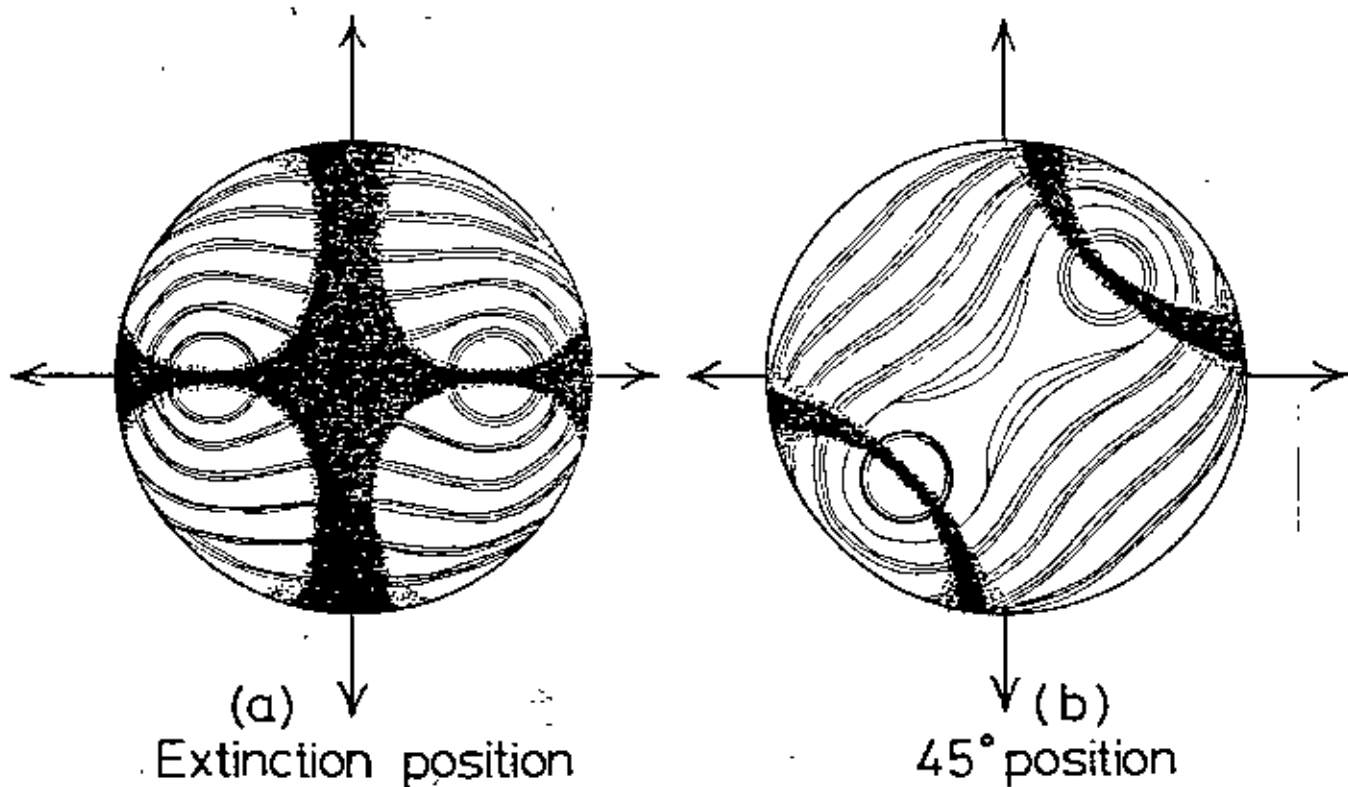


Fig. 3.9. Biaxial interference figure given by a section normal to the acute bisectrix.

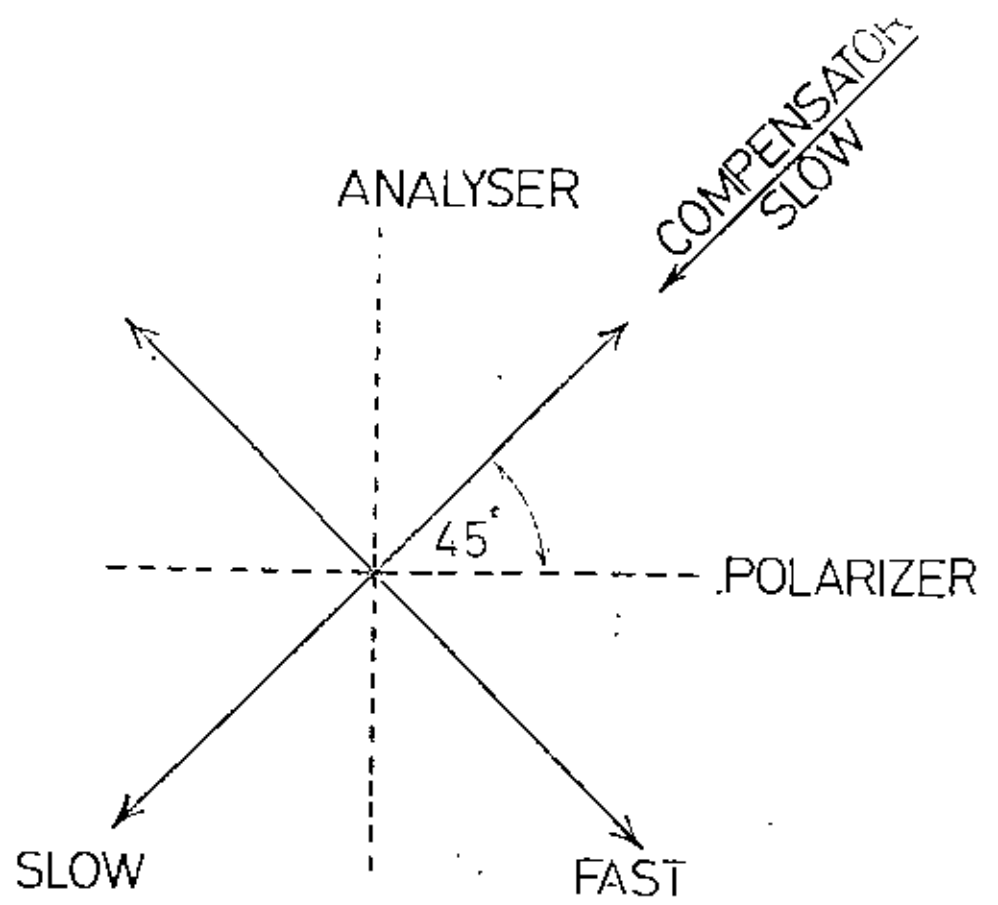


Fig. 10 (a) Additive effect; colours raised.

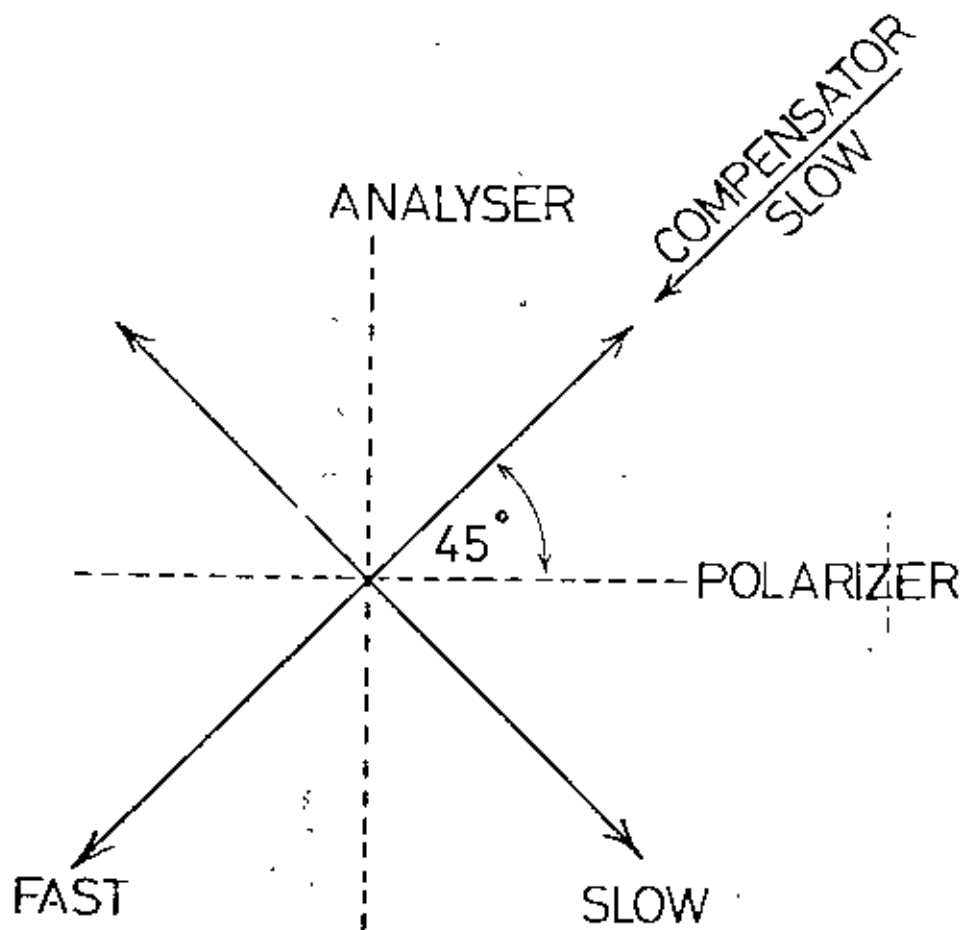


Fig. 10 (b) Subtractive effect; colours lowered.

62457

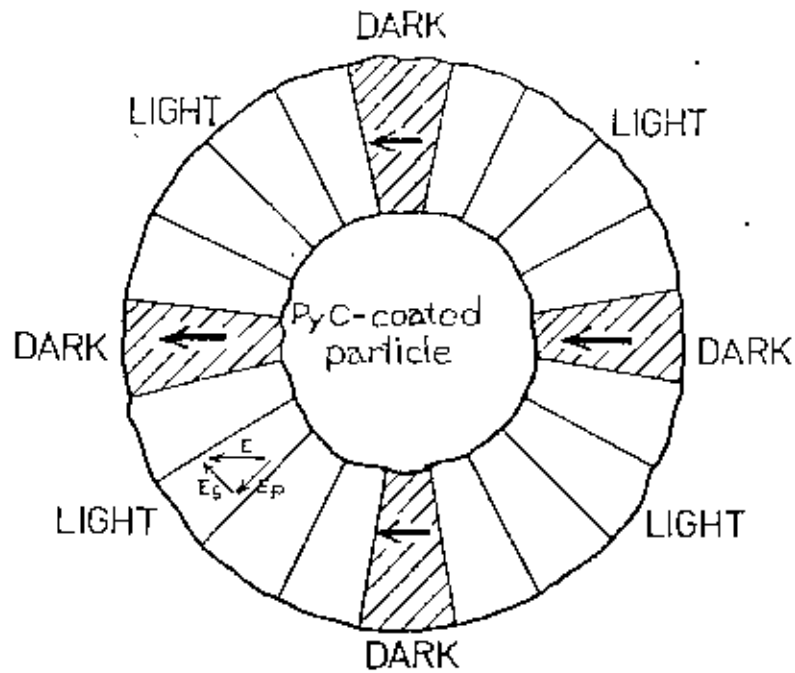


Fig. 3.11. Schematic representation of the median plane of a PyC-coated particle. The 'c' axes of the fibers are indicated by thin straight lines. Resolution of the incident electric vector 'E' is shown in the bottom left. The dark areas represent areas of the PyC where the incident E vector is either parallel or perpendicular to the principal planes (i.e. either E_s or E_p is zero).

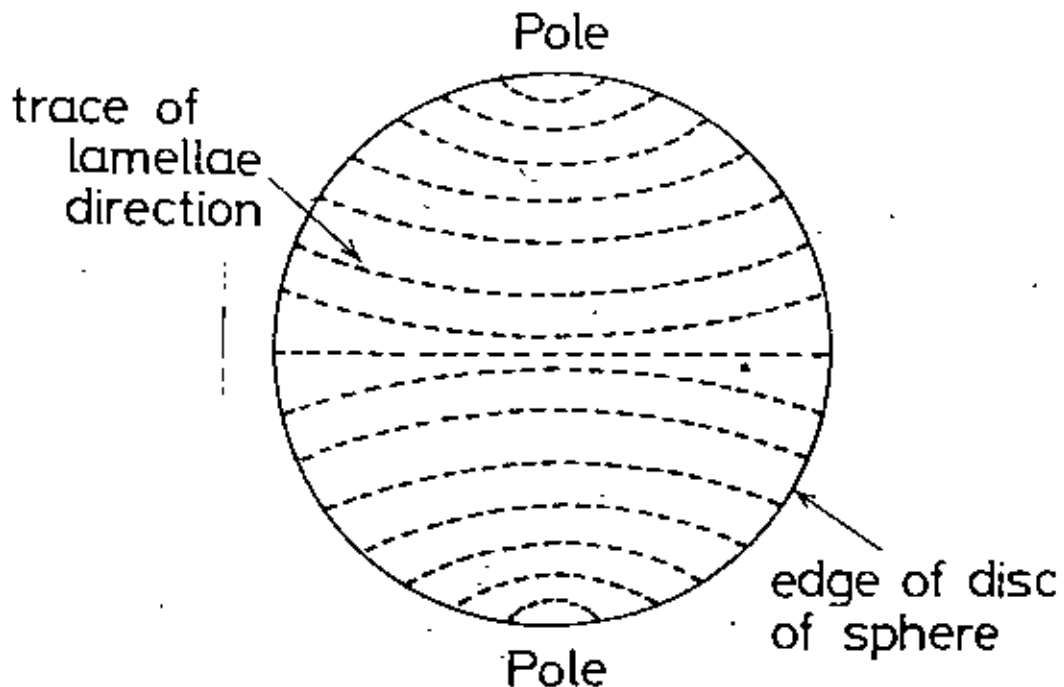


Fig. 3.12. Fine structure which would account for observed optical effects.

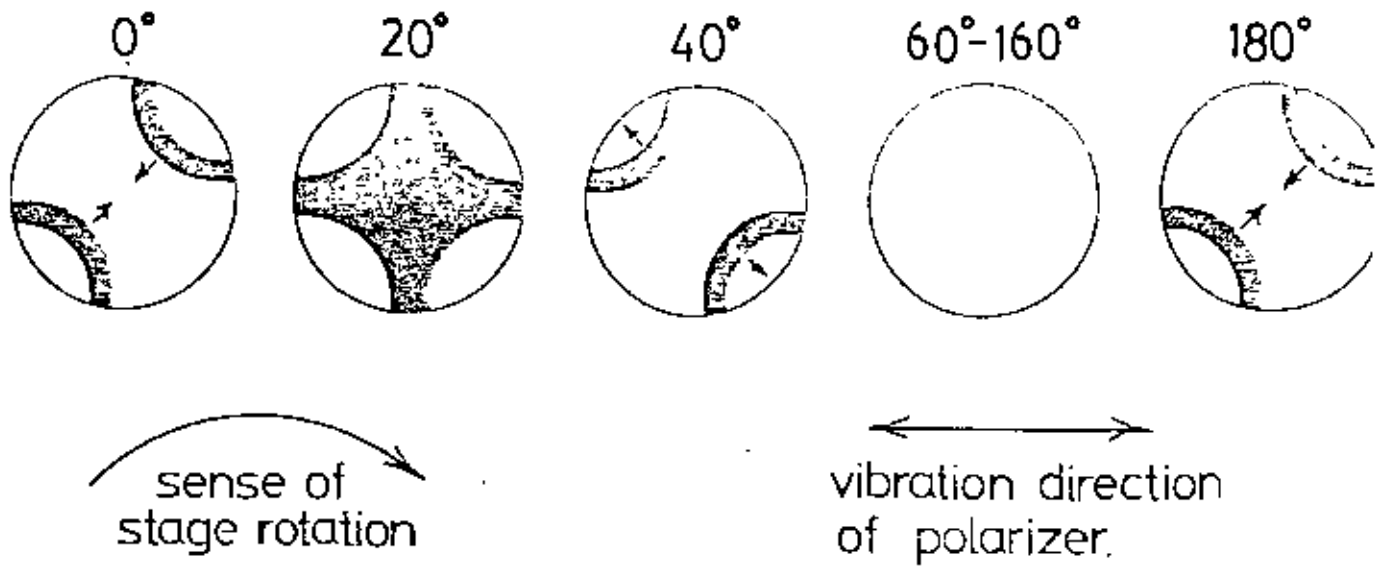


Fig. 5.13. Pleochroic phenomena observed when symmetrically oriented spherical body is rotated with respect to plane of polarized light.

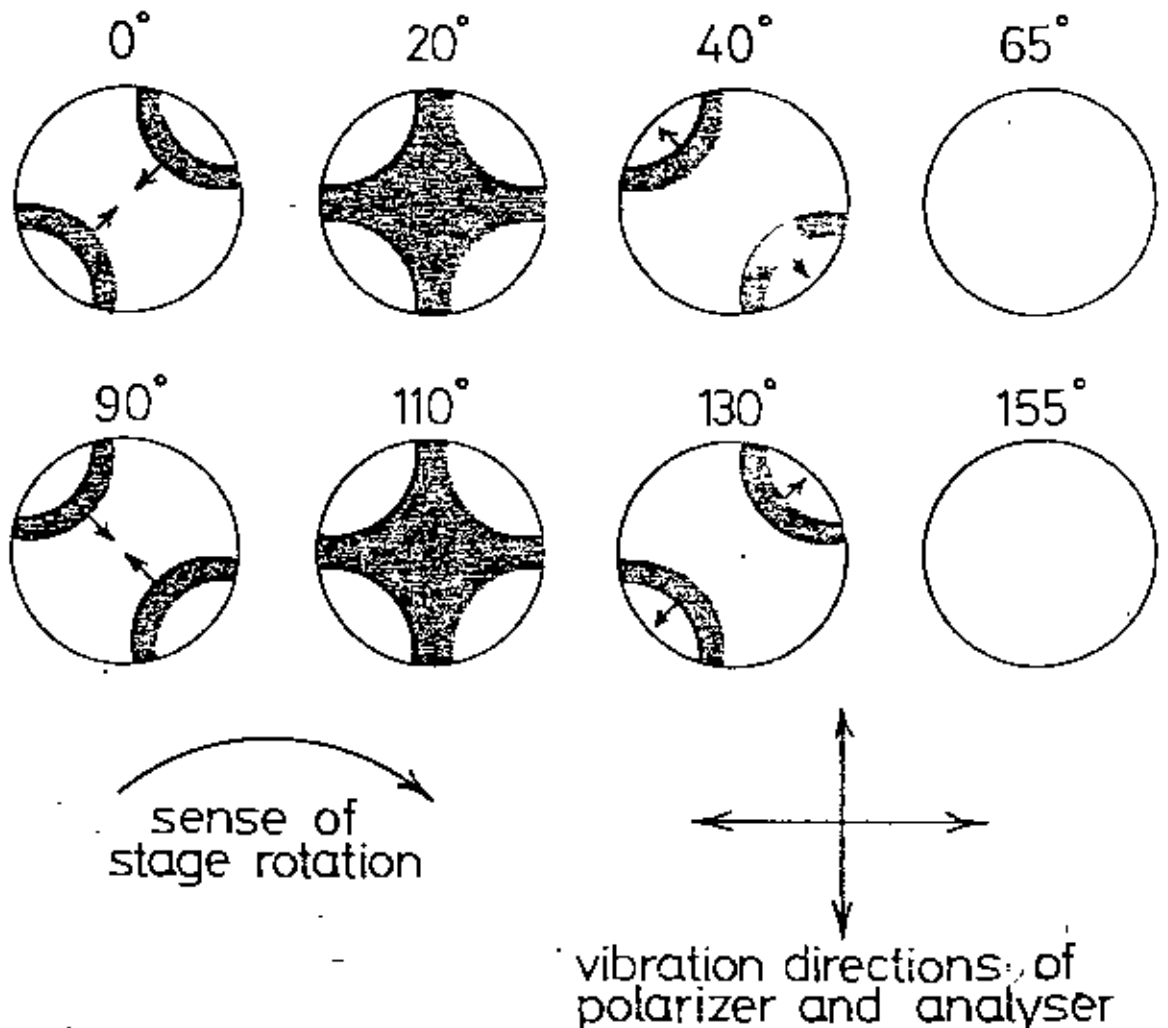


Fig. 3.14. Phenomena observed when symmetrically oriented spherical body is rotated between crossed polars.

REFERENCES

- 3.1. Hallimond, A.F., *The Polarizing Microscope*, Vickers Instruments, York, 1970.
- 3.2. Conn, G.K.T. and Bradshaw, F.J., *Polarized Light in Metallography*, Butterworths, London, 1952.
- 3.3. Mott, B.W. and Haines, H.R., *J.Inst.Met.*, 1952, 80, 629.
- 3.4. Marshall, C.E., *Introduction to Crystal Optics*, Cooke, Troughton and Simms, York, 1953.
- 3.5. Dale, A.B., *The Form and Properties of Crystals*, Cambridge University Press, London, 1932.
- 3.6. Hartshorne, N.H. and Stuart, A., *Crystals and the Polarizing Microscope*, Edward Arnold Ltd., London, 1970.
- 3.7. Vickers, A.E.J., 'Polarizing Microscopy in Organic Chemistry and Biology' in *Modern Methods of Microscopy*, Butterworths, London, 1956, 103.
- 3.8. Born, M. and Wolf, E., *Principles of Optics*, Chapter XIII, Pergamon Press, 1964.
- 3.9. Drude, P., *Ann.Phys.*, 1887, 32, 584.
- 3.10. Wright, F.E., *Proc. Amer. Phil. Soc.*, 1919, 58, 401.
- 3.11. Woodrow, J., Mott, B.W. and Haines, H.R., *Proc.Phys. Soc.*, 1952, 65, 603.
- 3.12. Gray, R.J. and Cathcart, J.V., *J.Nuclear Materials*, 1966, 19, 81.
- 3.13. Taylor, G.H., *Fuel*, 1961, 40, 465.
- 3.14. Honda, H., Kimura, H. and Sanada, Y., *Carbon*, 1971, 9, 695.

THE THERMAL ANALYSIS

CHAPTER - IV

4.1 Introduction

Differential thermal analysis (DTA) first proposed by Le Chatelier (1887)¹ has been found to be a useful technique in the fields of metallurgy, ceramics, geology, and chemistry. However, recently this technique is being widely applied in the investigations of polymers and inorganic solids. The study of thermal behavior of carbonising materials by DTA was first introduced by Nakamura and Atlas.² The theoretical basis and manifold applications of DTA have been elaborately described by Smothers, Chiang and Mackenzie^{3,4}.

DTA gives a continuous thermal record of reactions that occur in a sample, although it does not indicate what these reactions are nor does it sort out simultaneously occurring reactions. By comparing the temperature in a sample with the temperature in an inert reference material such as anhydrous alumina when both are heated at a uniform rate in a furnace, temperature regions where heat is absorbed (endothermic reactions) or evolved (exothermic reactions) by the sample can

be observed. The exothermic and endothermic reactions are generally shown in the DTA trace as positive and negative deviations respectively from a base line.

Additional informations such as thermogravimetric analysis (TGA), X-ray diffraction, infrared absorption spectroscopy, visual phase examinations, polarized-light micrography, etc. are necessary to supplement the DTA curve for correct interpretation of the thermogram peaks. The formation of the carbonaceous mesophase of a graphitizable organic compound generally occurs in the temperature range $350^{\circ}\text{C} - 600^{\circ}\text{C}$. The actual temperature interval in which the mesophase develops in the carbonisation of a particular organic compound may be a few degrees or it may be tens of degrees. This obviously causes practical difficulties in determining the exact temperature interval of mesophase formation for the samples under investigation. A combination of differential thermal analysis and polarized-light micrography^{5,18} has proved a valuable approach to the determination of the temperature interval of mesophase formation.

4.2 DTA apparatus

Differential thermal analysis is the process of correctly noting the difference in temperature between a thermocouple embedded in the sample under test and a thermocouple surrounded by a standard inert substance, such as aluminium oxide, while both are being heated at the same rate. These temperature differences are due to the phase transformations or chemical reactions occurring in the sample which involves rejection or absorption of heat.

The basic design of the DTA apparatus Fig. 4.1a with block diagram (Fig. 4.2b) has been fully described by Lewis

and Edstrom^{6,7}. The DTA thermocouple assembly consists of two matched chromel-alumel thermocouples which are supported in a porcelain tube held in position inside a furnace combustion tube. The sample and reference containers are nickel or inconel cups with a thermocouple well extending into the centre of the cup from the bottom. This arrangement protects the thermocouple junctions from being contaminated with the sample or reference material. The sample and reference cups are also isolated from each other and this arrangement facilitates weighing before and after heating so that weight changes can be readily determined. Approximately, 0.1 g anhydrous alumina is used in the reference cup and the sample weights varies over a range 0.05 g to 0.125 g, depending on their packed density. Normally, a heating rate of 10°C/min. is employed.

All experiments are carried out at atmospheric pressure in a continuous flow of a purified inert gas, usually argon, nitrogen or helium. Gases are normally purged into the furnace chamber at the lower end through a purification train in which oxygen and water are removed by heated copper wool and exhausted from the top into a condensate trap for collecting the condensable volatile products. The condensable volatile reaction products along with the unchanged starting material, if any, are thus swept by the flow of inert gas into a KBr-filled condensate trap⁸ placed in the exhaust end of the furnace. The non-condensable gases then pass through a sulfuric acid bubbler which seals the system and prevents back diffusion of air.

Normally, the DTA thermograms on carbonisation are obtained by heating continuously to 750°C at which the residue is essentially carbon.

4.3 Thermal behavior of carbonising and graphitizing materials

It has already been mentioned that in differential thermal analysis, the rejection or absorption of heat by any material during pyrolysis is recorded and indicated by exothermic or endothermic peaks in the DTA trace. The reaction temperature and the rate of reaction together give the characteristic thermal curve of that particular material. By the application of differential thermal analysis to a number of organic solids, Varma⁹ successfully found their melting and boiling points correct to $\pm 3^{\circ}$. One of the attractive features of the method was the convenience of obtaining the temperatures of sublimation, decomposition, elimination of water of crystallisation, etc. which are difficult by other methods.

Lewis and Edstrom^{6,7} in an attempt to investigate the thermal reactivity of polynuclear aromatic hydrocarbons used differential thermal analysis to categorise the high temperature behavior of those hydrocarbons as either thermally 'reactive' or thermally 'unreactive'. The thermally 'reactive' species possess sufficient reactivity in an atmospheric pressure system to undergo a condensation sequence in the liquid phase and yield measurable amount of polymerised carbonaceous residue at 750°C . The thermally 'unreactive' entities have sufficient stability so that such condensation reactions do not occur prior to complete

volatilisation. Hence, for those compounds no carbonaceous residues are observed at 750°C. For such materials DTA offers a convenient method of measuring melting and boiling points. Depending on the physical characteristics of the apparatus, either the initial inflection point of the endotherm, the endothermic minima, or the endothermic minima minus the temperature difference between the reference and sample couples, may give the appropriate result. However, the initial inflection point of the melting endotherm has been found to be the most reliable method for ascertaining the melting points for the respective compounds. The melting points thus determined for some of the aromatic hydrocarbons are shown in table 4.1 and the respective literature values^{10,11} are also listed for comparison. In most cases the agreement is quite good. The boiling endotherms on the other hand are generally broader and have no specifically defined inflection temperature. The shape of the boiling endotherm reflects the increasing vapour pressure of the sample with increasing temperature. The gradual approach to the boiling endothermic minima indicates slow but increasing vaporisation. The calculated values of the boiling points listed in table 4.1 are the corrected endothermic minima. Here the corrected endothermic minima means the endothermic minima minus the temperature difference between the reference and sample couples. The boiling points calculated as above gives good agreement with literature values^{10,11}.

The thermograms of thermally 'reactive' aromatics which undergo thermal condensation leading to some carbonaceous-residues at 750°C , differ quite markedly from those of the 'unreactive' category. The major melting endotherms are, however, still evident. The boiling endotherms are observed to be either completely absent or largely diminished in those thermograms. In a large number of cases an exothermic peak indicative of polymerisation or condensation is usually observed. In nearly every instance new chemical species in addition to the starting material are obtained in the condensed distillate.

Differential thermal analysis for the carbonisation of a good number of polymers in nitrogen flow were reported by Dollimore and Heal¹². From the DTA results with certain exceptions in the case of chlorinated polyvinyl chloride and chlorinated rubber, it is generally observed that an exothermic portion of the DTA curve somewhere in the initial stage of decomposition, indicates that the resulting product will be a non-graphitizing carbon. Two competing reactions are often found to occur: cross-linking producing an exothermic reaction, and chain stripping and associated reactions, which produce endothermic peaks. The second type often allows the formation of oriented aromatic rings, which produces graphitizable carbons. It should be noted that the exothermic reactions may be preceded by some reaction of secondary importance, such as loss of absorbed water or other volatile impurities. Bearing these facts in mind, it would seem that the appearance of an exothermic reaction, somewhere in the

initial polymer decomposition region ensures that the resulting carbon has non-graphitizing properties. At nearly 600°C and above it is well known that semi-coke becomes coke¹³.




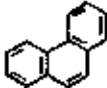
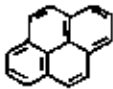
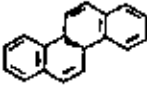
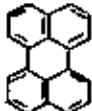
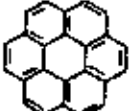
In a thermal analysis study by Lapina and Ostrovskii¹⁴ the essential characteristics of the carbonisation process of graphitizable and non-graphitizable materials were obtained as a result of the investigation of the carbonisation process of various classes of organic polymer substances and the structure of the resulting carbon as well. For graphitizable materials endothermal processes of destruction are typical while for non-graphitizable ones exothermal processes of cross-linking are observed.

Graham⁵ (1974) used differential thermal analysis to determine the temperature interval of carbonaceous mesophase formation. The samples under study were the mixtures of acenaphthylene and sulphur. Samples which did not pass through carbonaceous mesophase transformation due to prolonged heating at 300°C , have been heat-treated in an atmosphere of dry nitrogen in the Stanton differential thermal analyser and their respective thermograms obtained (Fig. 4.2). Characteristic of the curves is the presence of an initial large endotherm due to melting of the tarry substance which is then followed by small fluctuations before a smooth trace returns. These fluctuations (indicated by dotted lines in fig. 4.2) are characteristic of almost all the samples with the exception of the sample having S/H ratio of 3/8 from which they were absent. The temperature regions in which these fluctuations appeared, remained constant

for the samples having S/H ratios up to $2/8$. Graham concluded that the temperature at which all the fluctuations terminate was nothing but the temperature of complete coalescence in the case of carbonaceous mesophase. This had also been verified by polarized-light microscopy, by viewing through it a sample heat-treated to similar temperature. He further added that the fluctuations in the DTA trace was due to the formation of gases within the sample during pyrolysis.

Differential thermal analysis has also been employed by Hossain and Dollimore¹⁵ to locate the temperature intervals of mesophase formation in the case of a few graphitizable aromatic organic compounds such as naphthalene, anthracene, phenanthrene and chrysene. Selected samples, withdrawn during the initial thermal treatment and which has not yet passed through the carbonaceous mesophase transformation due to prolonged heating at 400°C , have been heat-treated in the stanton differential thermal analyses (Model - Stan data 5 - 50). These samples (0.1 g) were heated in the inconel head to 700°C with dry alumina being employed as the inert material in the reference cell. The DTA was determined on Dupont unit, with pen recording. The DTA traces so obtained (Fig. 4.3) for the different aromatic compounds were used to determine the temperatures to which the original parent samples had to be heated in order to obtain the mesophase spherules which usually appear in the initial stages of carbonaceous mesophase.

Table 4.1

COMPOUND	STRUCTURE	MELTING POINT (°C)		BOILING POINT (°C)	
		Literature ¹⁶	DTA	Literature ¹⁶	DTA
BENZENE C ₆ H ₆		5.4	—	80.4	—
NAPHTHALENE C ₁₀ H ₈		80.287	77	217.955	245
ANTHRACENE C ₁₄ H ₁₀		216.04	215	339.9	350
PHENANTHRENE C ₁₄ H ₁₀		99.15	93	338.4	348
PYRENE C ₁₆ H ₁₀		150.6	146	393	386
CHRYSENE C ₁₈ H ₁₂		255.8- 255.3	260	448	460
PERYLENE C ₂₀ H ₁₂		270	295	460	505
CORONENE C ₂₄ H ₁₂		438 - 440	438	525	600

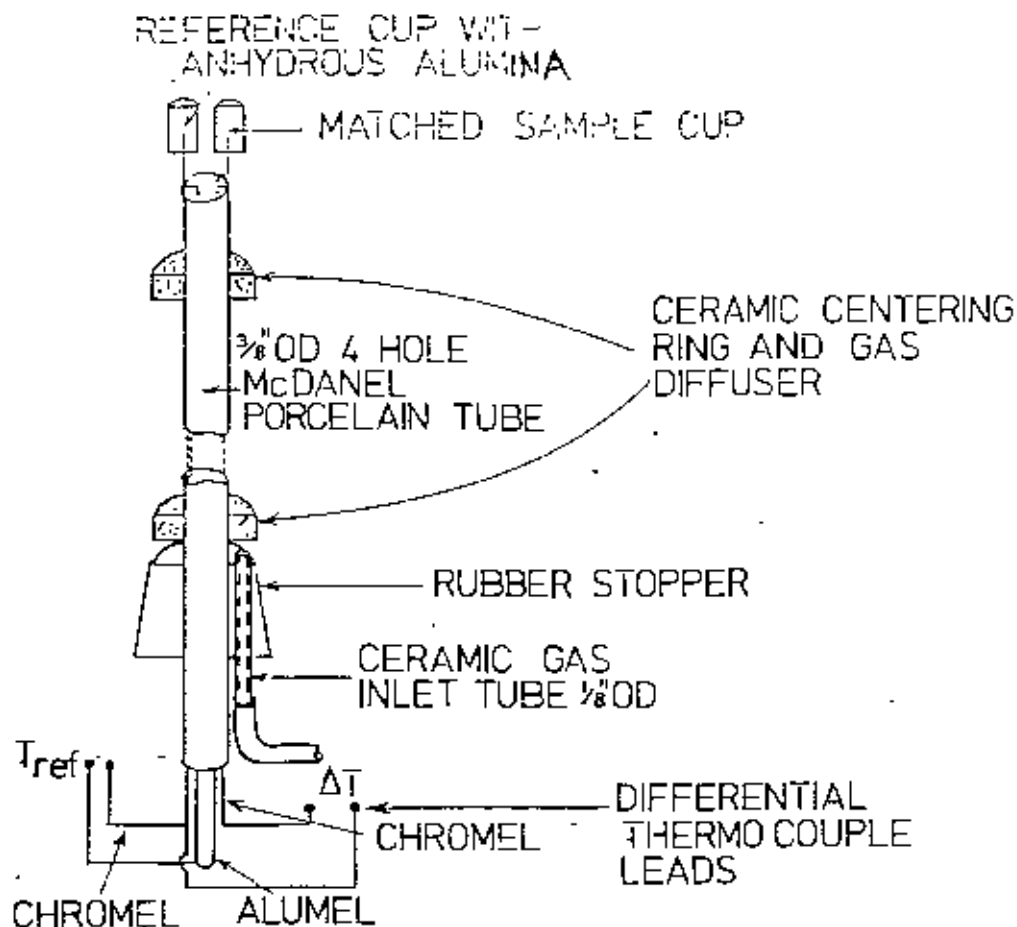


Fig. 4.1 (a) DTA thermocouple assembly

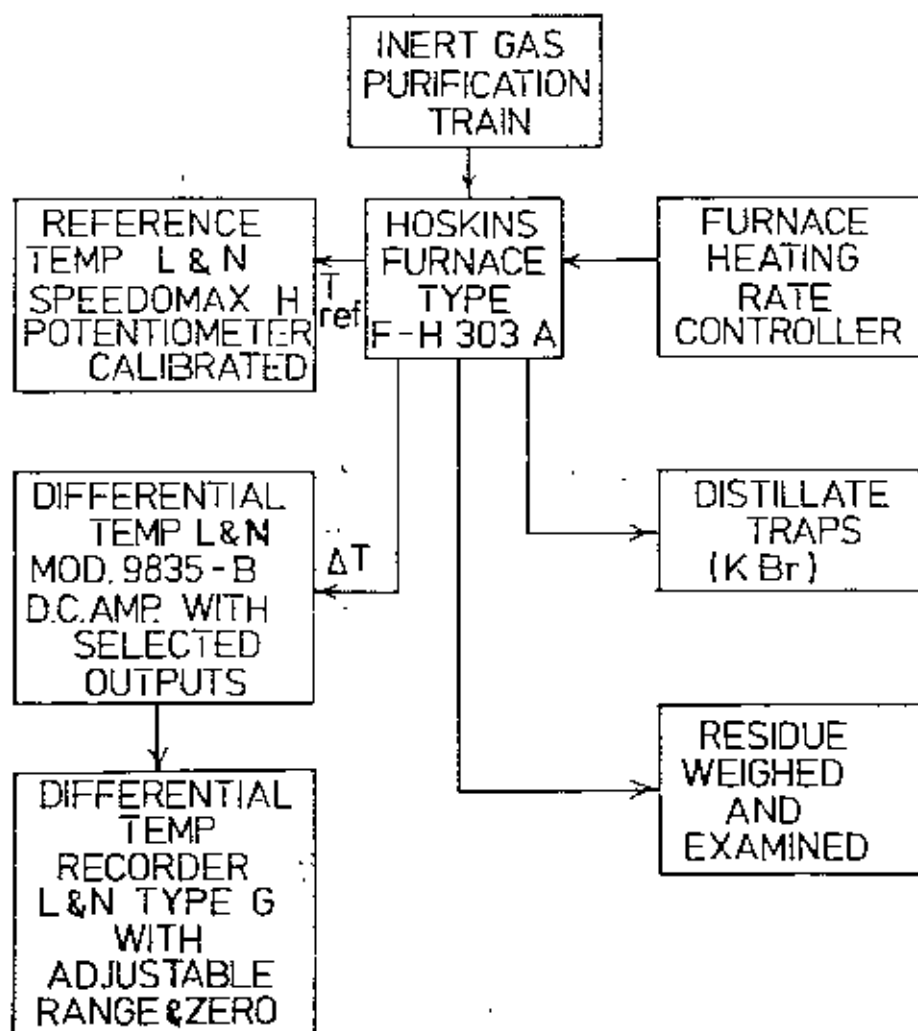


Fig. 4.1 (b) Block diagram of DTA apparatus

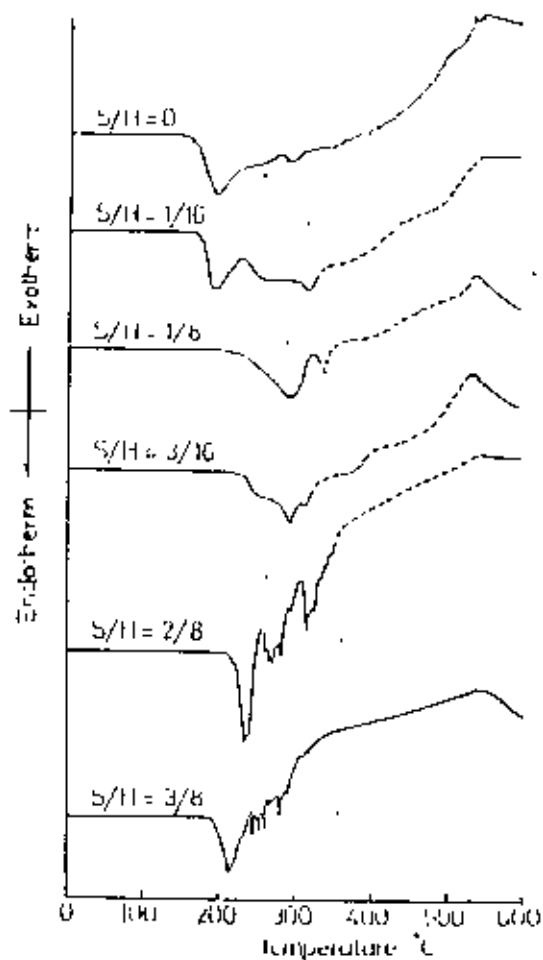


Fig. 4.2 Differential thermal analysis traces of partially refluxed acenaphthalene sulphur mixtures.

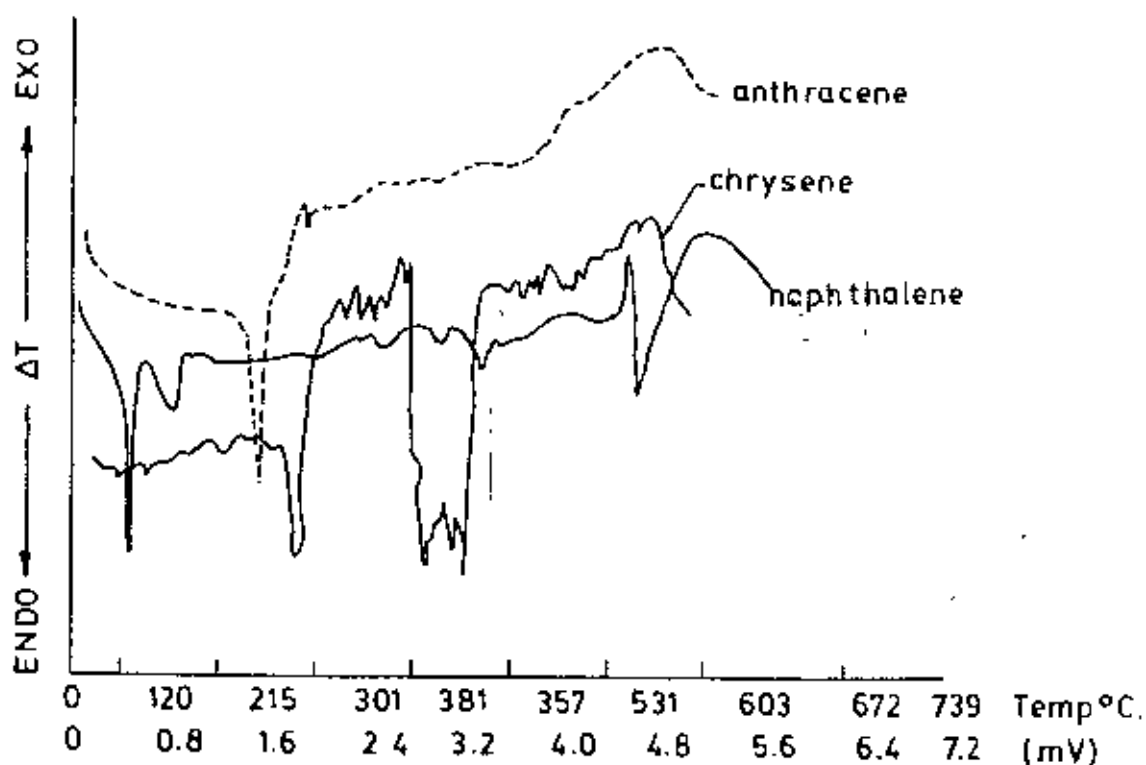


Fig. 4.3. DTA Trace of partially carbonised aromatic organic compounds.¹⁵

REFERENCES

- 4.1. Chatelier, H.Le., *Bull.Soc.franc. mineral*, 1887, 10, 204.
- 4.2. Nakamura, H.H. and Atlas, L.M., *Proc. fourth carbon conf.*, Pergamon Press, London, 1960, 625.
- 4.3. Smothers, W.J. and Chiang, Y., *Differential Thermal Analysis, Theory and Practice*, Chemical Publishing Company, New York, 1966.
- 4.4. Mackenzie, R.C. (Ed.), *The Differential Thermal Investigations of Clays*, Mineralogical Soc., London, 1957.
- 4.5. Graham, S.G., Ph.D. Thesis, Salford University, England, 1974.
- 4.6. Lewis, I.C. and Edstrom, T., *Proc. Fifth Carbon Conf.*, Pergamon Press, London, 1962, 413.
- 4.7. Lewis, I.C. and Edstrom, T., *J.Org.Chem.*, 1963, 28, 2050.
- 4.8. Leggon, H., *Anal. Chem.*, 1961, 33, 1295.
- 4.9. Varma, M.C.P, *J. App. Chem.*, 1958, 8, 117.
- 4.10 *The Coal Tar Data Book*, The Coal Tar Research Association, Leeds, England, 1965.
- 4.11 Bulletin 606, U.S. Bureau of Mines, 1963, Anderson, H.C. and Wu, W.R.K., *Properties of Compounds in Coal - Carbonisation products.*
- 4.12 Dollimore, D. and Heal, G.R., *Carbon*, 1967, 5, 63.
- 4.13 Papkov, V.S. and Slonimskii, G.L., *Vysokomol. Soyed.*, 1966, 8, 80; A10, 1968, 1204 (Translated in *Polymer Science USSR*, 1966, 8, 84; 1968, 10, 1402.

- 4.14 *Lapina, N.A. and Ostrovskii, V.S., Thermal Analysis, 2, Proc. Fourth ICTA Budapest, 1974, 407.*
- 4.15 *Hossain, T. and Dollimore, J., Chemical Engineering Research Bulletin, 5, 1981, 25.*
- 4.16 *Hossain, T. Ph.D. Thesis, Salford University, 1981, 91.*
-

CHAPTER - VPYROLYSIS CHEMISTRY OF BENZENE5.1 Introduction

Organic compounds are the main and almost exclusive raw materials for the production of artificial carbons and graphite. By pyrolysis, these carbon compounds are converted to solid carbon as the main product and to different volatile compounds as by-products. Such thermal decompositions below approximately 1000°C are carried out by a great variety of technical processes. In such processes, the pyrolysis is controlled by a few reaction parameters such as temperature, heating rate, residence time at the pyrolysis temperature, and possibly the total gas pressure. The low-temperature stage of pyrolysis, especially below 700°C , has the greatest influence on both the carbon yield and the carbon properties. In all such technical cases, the primary importance is to achieve a high carbon yield which is again determined by the mechanism of the pyrolysis. The pyrolysis must be directed towards the formation of carbon-free volatile by-products and towards avoiding the formation of volatile stable carbon compounds. Thus, the carbon yield can be influenced by the choice of the compound to be pyrolysed, by its thermal and chemical pretreatment, as well as by the reaction conditions prevailing during the pyrolysis.

The practical problem is, therefore, carbon yield and in the case of low yield, pyrolysis of the compound inside an

ordinary carbonising furnace with a stream of nitrogen or other inert gas should be invariably avoided. Some aromatic organic compounds sublime off and give off hetero-atoms before it carbonises and some are found to be evaporated leaving no carbonaceous residue at all. In those cases it becomes necessary to heat the organic samples in sealed tubes in order to obtain appreciable yields.¹ This is because increased gas pressures of evaporated hydrocarbons lead to high carbon yields. Again, as the vapour pressure of the compound being carbonised inside the sealed tube is not known, it is always preferred to take a heavy-walled glass tube or quartz tube so that the tube can stand the increased pressure of the pyrolysis gases. Even then the tube may burst and so some safety enclosure round the tube should be taken as a precautionary measure against any blow or blast. Nevertheless, opening of the carbonised sealed tube is another practical problem. Due to heavy pressure inside, it cannot be opened ordinarily by cutting with a diamond edge or with a tungsten blade without adopting any safety measure against the blow or blast if any. It is, therefore, advised to open the tube inside a strong safety box. Alternately, the tube can be opened without the aid of a safety box provided it is immersed in a Dewar containing liquid nitrogen for at least an hour before opening. The second process involves a thermal shock and should be avoided.

In the sealed tube technique of pyrolysis mentioned before, heating of the sample is first carried out under normal pressure and then under increasing pressure caused by the pyrolysis gases.

Besides the sealed tube technique, the following pyrolysis techniques are adopted alternatively :

- (a) pyrolysis in autoclaves, where the pressure can be regulated during the whole reaction time.
- (b) Liquid pyrolysis in an open crucible with continuous removal of the gaseous by-products; this is mostly used for reactions carried out under normal pressure.
- (c) Gas cracking in a steady-state tubular flow reactor with relatively fast heating of the evaporated starting material and in most cases with quenching of the volatile products.
- (d) The hot wire method as a special arrangement of the flow system.

5.2. Aromatic hydrocarbons

Any organic compound which undergoes substitution reactions of carbon-hydrogen (C-H) bonds is said to be aromatic. With the advent of wave-mechanics it was shown by W. Huckel² (1937) that a planar cyclic compound which has $(4n+2)\pi$ electrons (where n is an integer) should possess a resonance energy, and therefore undergo aromatic reactions. Thus to be aromatic, a molecule must have 2($n=0$), 6($n=1$), 10($n=2$), 14($n=3$), 18($n=4$).....
..... n electrons. Huckel's $(4n+2)$ rule applies to monocyclic systems like benzene and other compounds which have very little resemblance chemically to benzene. It has also been suggested

that the $(4n+2)$ rule should be applied to the peripheral (conjugated) π -electrons of polycyclic condensed systems such as naphthalene, anthracene, phenanthrene, etc. (see fig. 5.1)³. Huckel's rule stimulated a large amount of research on aromaticity and, so far, no exceptions have been found. A further test for aromaticity is that such compounds sustain diamagnetic ring currents in the presence of magnetic fields. In general an aromatic organic compound should fulfil the following requirements:

- (a) The Huckel's $(4n+2)$ rule is obeyed.
- (b) All the compounds undergo electrophilic substitution reactions (nitration, sulphonation, etc.).
- (c) The compounds show delocalisation of the π -electrons by supporting a diamagnetic ring current (This can be shown by N.M.R.).

The word aromatic is derived from the Greek word 'aroma' meaning 'fragrant smell'. Most of the aromatic organic compounds have one thing in common : a pleasant odour.

Most aromatic hydrocarbons are colourless solids or colourless liquids and are lighter than water (average density = 0.8). They are non-polar materials, immiscible with water, but readily soluble in non-polar solvents such as ether, petroleum ether, carbon tetrachloride.

The high stability of the aromatic organic compounds is due to resonance energy⁴ which increases with the increasing molecular size of the ring system. (see table 5.1).

The two industrial sources of aromatic hydrocarbons are the two main reservoirs of fossil organic compounds, coal and oil. The other main source of organic compounds, living matter, does not contain a high proportion of aromatic materials.

When coal is heated in the absence of air to 1000 - 1300°C it is partly broken down into simpler volatile compounds which distil out of the oven. The residue, coke, is used for iron smelting. The volatile materials consist of coke oven gas (50% hydrogen, 30% methane and small quantities of other gases), light oil, coal-tar and ammonia. The light oil and coal-tar are refined by fractional distillation and specific chemical reactions. Well over a hundred different aromatic compounds have been obtained from coal-tar.

The second major route to aromatic hydrocarbons is by the dehydrogenation of petroleum feed-stocks. This route was developed during the second world war, when coal-tar process could not give sufficient toluene for the manufacture of TNT explosive (2,4,6-trinitrotoluene). The aliphatic hydrocarbons are passed over a copper catalyst at 650°C when dehydrogenation and cyclisation reactions occur.

5.2.1 Benzene

Benzene, having molecular formula C_6H_6 , is a colourless, mobile and highly refractive liquid (b.p. 80.4°) with a sharp smell. It has a specific gravity 0.87 (at 20°). Solidified benzene melts at 5.4° . It is highly inflammable and burns with a smoky luminous flame. Benzene is practically immiscible with water but miscible with many organic liquids such as ether, alcohol, etc. It is a good solvent for fats, resins, gums, rubber, etc as also for iodine, phosphorus, sulphur, etc. Two parts of benzene vapour in about 100 part of air may prove fatal if inhaled; absorption of benzene, liquid or vapour, through the skin has toxic effects. Though unsaturated, it is remarkably stable.

A consequence of the aromaticity of benzene is that all the carbon-carbon (C.C) bond lengths are the same, and all the positions equally reactive, as is not usual, with polycyclic aromatic compounds. Physico-Chemical evidence, e.g., heat of combustion, etc., points towards benzene being a resonance hybrid of mainly two resonating structures I and II (Fig.5.2). These structures are called Kekule's forms^{5,6}. According to Kekule (1872), the carbon atoms in the benzene ring are continually in a state of vibration, and due to this vibration, each C-C pair has a single bond half of the time and a double bond the other half. In general, there are 'n+1' principal resonating structures for an aromatic organic compound containing 'n' benzene rings.

Resonance between the two structures largely contributes to the greater stability of the benzene molecule as well as it explains the intermediate bond length of 1.39\AA (intermediate between C-C single and C=C double bond lengths). The resonance energy of benzene is nearly 36 Kcal mole and so it is a very stable compound.

5.3. Pyrolysis of Benzene

The pyrolysis of benzene, first described by Berthelot, leads to biphenyl, which is produced today on a large industrial scale using this method. In this process, terphenyls and polyphenyls appear as by-products. The mechanism with formation of phenyl radicals as intermediates is shown in Fig.5.3. In a sealed tube, biphenyl formation has been observed as beginning below 300°C . The dependence of the biphenyl yield on temperature and experimental arrangement⁸, is presented in Table 5.3⁹. In the pyrolysis of benzene, the formation of naphthalene has never been observed.

Table 5.1

Resonance energies of polycyclic aromatic compounds⁴

Compound	Resonance energy (K cal mole ⁻¹)
Benzene, C_6H_6	36
Naphthalene, C_{10}H_8	61
Anthracene, $\text{C}_{14}\text{H}_{10}$	83.5
Phenanthrene, $\text{C}_{14}\text{H}_{10}$	91.9
Chrysene, $\text{C}_{18}\text{H}_{12}$	116.5

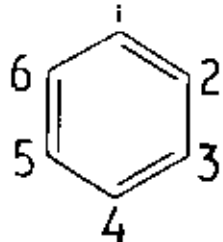
Table 5.2

Gas-phase carbonisation of benzene naphthalene, anthracene and chrysene⁷

Temperature °C	% carbon converted to coke contact time in sec			
	2	10	20	40
	<i>Benzene</i>			
800	1	3	6	8
900	3	19	33	39
1000	35	59	69	73
1100	80	91	94	96
	<i>Naphthalene</i>			
800	0	2	4	7
900	11	43	52	60
1000	38	76	83	90
	<i>Anthracene</i>			
800	21	67	83	90
900	32	79	89	95
1000	72	96	98	99
	<i>Chrysene</i>			
800	4	13	20	25
900	30	65	77	84
1000	76	88	93	98

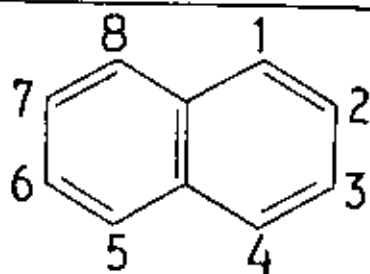
Table 5.3Formation of Biphenyl from Benzene⁹⁾

<i>T</i>	<i>P</i> , liters/hr	Yield of biphenyl, wt %
685°C	0.846	14.6
	0.423	22.4
	0.282	26.2
	0.212	27.8
	0.141	29.2
	0.121	29.4
	0.106	29.4
	0.0282	29.4
	0.0141	29.4
760°C	2.75	13.7



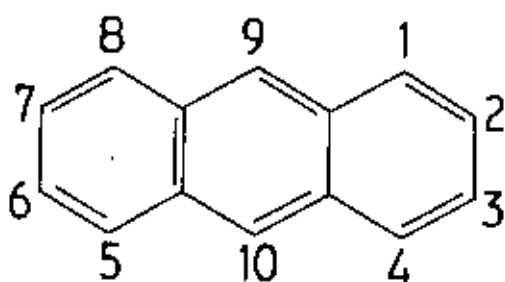
6π electrons = $(4 \times 1 + 2)$; aromatic

Benzene, C_6H_6



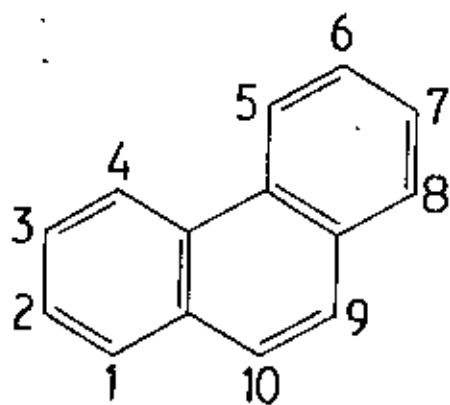
10 electrons = $(4 \times 2 + 2)$; aromatic

Naphthalene, $C_{10}H_8$



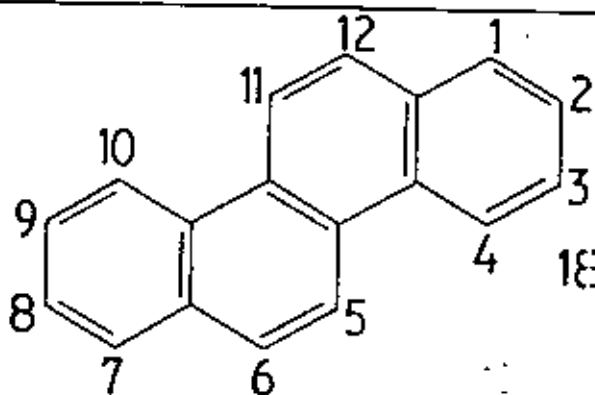
14 electrons = $(4 \times 3 + 2)$; aromatic

Anthracene, $C_{14}H_{10}$



14 electrons = $(4 \times 3 + 2)$; aromatic

Phenanthrene, $C_{14}H_{10}$



18 electrons = $(4 \times 4 + 2)$; aromatic

Chrysene, $C_{18}H_{12}$

Fig. 51 Simple aromatic organic compounds obeying Huckel's $(4n+2)$ rule.

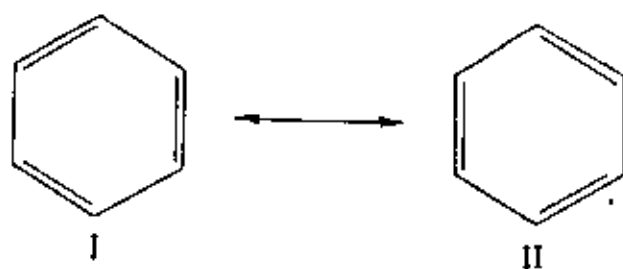


FIG. 5.2 TWO RESONATING STRUCTURES OF BENZENE

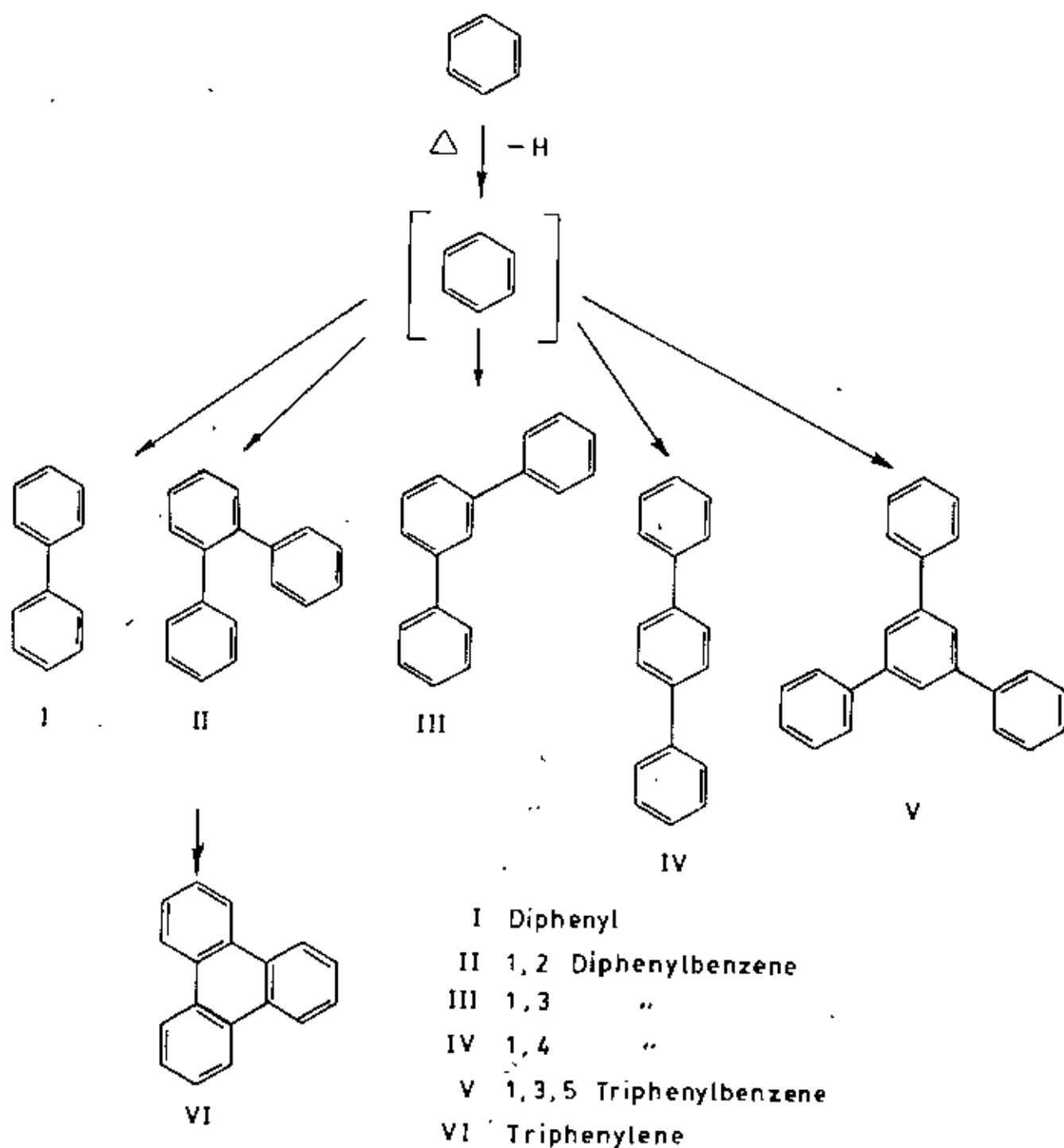


Fig. 5.3 Pyrolysis of benzene.

REFERENCES

- 5.1. Fitzer, E., Mueller, K. and Schaefer, W., *Chem. Phys. Carbon*, 7, 255.
- 5.2. Hückel, Z. *Elektrochem.*, 1937, 43, 752, 827;
- 5.3. Pinar, I.L., *Organic Chemistry*, 1976, 1, 577, Longmann, London and New York.
- 5.4. Wheland, G.W., *Resonance in Organic Chemistry*, 1955, John Wiley, New York.
- 5.5. Kekule, *Ber. dtsh. Chem. Ges.*, 1872, 162, 77;
- 5.6. Badger, G.M., *The structures and Reactions of the Aromatic Compounds*, Cambridge University Press, 1957, 4.
- 5.7. Brooks, D.T., *The Chemistry of Petroleum Hydrocarbons*, 1955, 2, 114, Reinhold Publishing Corporation, New York.
- 5.8. Hougen, O.H. and Watson, K.M., *chemical process principles*, vii.III, Wiley, New York, 1900, p847.
- 5.9. Fitzer, E., Mueller, K and Schaefer, W., *Chemistry & Physics of carbon*, 4, 278.

6.1. Introduction

The importance of the carbonaceous mesophase formation

as a prerequisite to graphitization has been discussed in

the introductory chapter as well as in section 2.5. In the

present study the mesophase formation during carbonisation of

benzene has been examined and polarized-light photomicrographs

of the sample during mesophase formation has been taken in

order to study the nucleation, growth and coalescence processes

of the mesophase spherules at different heat-treatment

temperatures. Thermal analysis of the partially carbonised

sample has been carried out to get the information about the

graphitizability of the sample as well as to locate the

temperature interval of mesophase formation. A particle size

analysis of the mesophase spherules has been carried out using

polarized-light microscopy in order to find out the size of

the spherules at different heat-treatment temperatures. The

mean spherulite diameter of a graphitizing organic compound

when it passes through the carbonaceous mesophase bears a

relationship with the crystallite parameters of the

corresponding graphite produced. No first order correlation

exists but generally it has been observed that a reduction in

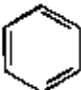
spherulite size corresponds to a small or secondary decrease

in the X-ray parameters. The latter study is left at this stage.

6.2. Experimental

6.2.1 Sample

Benzene, the simplest aromatic hydrocarbon, manufactured by E. Merck (India) Limited was used in this study. It had a purity greater than 99.5%.

Sample	Structure	Melting point of Solidified Benzene °C	Boiling point °C
Benzene		5.4	80.5

6.2.2 The safety device for opening sealed tubes containing heat treated organic samples.

A heavy pressure is developed when an aromatic organic compound is heat-treated inside a sealed tube because of the presence of H_2 and other hydrocarbon gases which are generally evolved during pyrolysis. The safety device, that has been worked out in the opening of the carbonised sealed tube having no risk of explosion, consists of a mechanical contrivance of cutting the tube inside a strong closed box by means of a diamond edge or tungsten blade. The external wall of the safety box is made of 16 SWG aluminium sheet and its design plan is illustrated in fig.6.1. The portion of a 16 SWG aluminium hinged lid carrying a makralon viewing panel constitute the roof of the box. A spring loaded plunger carrying the diamond edge or tungsten blade is fitted at the lid. The plunger thus slides up and down when pressed and released and its circular motion is restricted by screw in slot.

The sealed tube containing the heat-treated sample is always placed in a horizontal position, inside the safety box with the lid closed, such that when the plunger is pressed down, the diamond edge or tungsten blade at its tip touches the tube at the central position.

This is secured in the following way : The tube is allowed to rest on two 1" ϕ Tufnol rollers fitted with two 3/16" ϕ M.S. spindles which are in turn fitted to a 10 SWG aluminium frame work clamped firmly on the floor of the box. The ends of the tube passes into rubber caps provided at the ends of two other spring loaded plungers, placed in the same height at the two opposite side walls of the box. These plungers carrying the sealed tube in horizontal position is capable of clockwise or anticlockwise rotation.

By pressing the lid plunger down and holding it in such a position that the diamond tip or tungsten blade is in touch with the tube, a complete rotation is given to the tube by rotating the side plungers placed at the two opposite walls. The sealed tube will thus be found to be cut at the centre. A strong push is then applied on the cutting area by means of a rigid rod having a sharp edge and the tube will be found to open very easily without any blow or blast because of the incumbent pressure of the pyrolysis gases inside. To facilitate near vision of the tube from outside, the makralon portion of the hinged lid having the size 11" x $4\frac{3}{4}$ " x 3 mm is slanted to make an angle of 30° with the vertical wall. A 3" ϕ exhaust with a gauze is fitted at one corner of the safety box for clearance of the onrushing gas.

6.2.3 Increasing pressure developed inside pyrolysed sealed tube accelerates carbonisation process.

Extensive studies on the influence of very high pressures on the carbonisation of pure organic compounds, pitches and coal were undertaken by a number of workers^{1,2} and it was established that increasing pressure not only increases the coke yield but also lowers the temperature at which pyrolysis is completed.

Little information seems to be available in the open literature as to the amount of pressure that is developed on pyrolysis of a certain amount of vapourising pure organic sample inside a sealed tube. In such technique of pyrolysis, heating of the sample is first carried out under normal pressure and then under increasing pressure caused by the pyrolysis gas. It is this increasing pressure which accelerates the carbonisation process with a big yield. In view of the above fact, the sealed tube method of pyrolysis was adopted in the case of benzene..

6.2.4 Thermal analysis

Carbonaceous mesophase formation has earlier been stated to occur generally in the temperature range 350°C - 600°C. The actual temperature interval in which the mesophase develops in the carbonisation of a particular compound may be only a few degrees or it may be tens of degrees. This naturally causes difficulties in locating the exact temperature intervals of mesophase formation in benzene during carbonisation.

Thermal analysis is an important tool to ascertain the temperature interval of mesophase formation. A small amount (about 0.7 g) of the sample was taken in a heavy-walled pyrex tube, 2.5 mm in thickness and 16 mm in internal diameter. The tube along with the sample inside was sealed at both the ends and again placed inside a steel bomb fitted with screw caps at both the ends. The sample was then heat-treated inside a solenoidal furnace at a fixed power input to the bomb upto 450°C , at which temperature the sample was kept for a long duration. During heating the pressure inside the sealed tube increased primarily because of the presence of H_2 and other hydrocarbon gases which were evolved. After allowing the tube to cool to room temperature, the sealed tube was opened inside a safety box, the design details of which has been given in article 6.2.2.

The heat-treated sample was then removed from inside the tube, dried and then ground in a pestle and mortar.

Selected sample, withdrawn during the initial thermal treatment and which had not yet passed through the carbonaceous mesophase transformation due to prolonged heating at 450°C , have been heat-treated in a pyrex tube into which is dipped a chromel-Alumel thermocouple as in fig. 6.2 to measure the reaction-temperatures including the temperatures of phase transformations in the different stages of pyrolysis. The couple is connected to a sensitive potentiometer capable of reading in millivolt. The temperature of one of the junctions is maintained

at 0°C by placing it in melting ice. The temperature of the other junction is gradually increased by heating the pyrex tube containing the sample directly by a burner and the e.m.f.s of the couple at suitable intervals are recorded. The thermo-e.m.f.s. are calculated from the knowledge of the balancing lengths. The temperatures at the different phase transformations and reactions are obtained from the e.m.f.-temperature chart (Table 6.1) of the thermocouple used. The thermal curves so obtained (Figs. 6.3 & 6.4) for the sample under study were used to determine the temperature to which the parent sample had to be heated in order to obtain mesophase spherules.

6.2.5 Micrographic preparation of samples for mesophase observation.

Mesophase samples for polarized-light micrography and particle size analysis were obtained by heating the selected original samples (0.7 g) individually in sealed tube inside the solenoidal furnace as before to the desired temperature at which investigation was necessary. A heating rate of $10^{\circ}\text{C}/\text{min.}$ was adopted by the temperature controller. The sample was heated to carbonise at a fixed temperature for a fixed duration. The sample was then allowed to cool and on reaching the room temperature the sealed tube was opened inside the safety box as before. The sample was then separated from the tube, dried and then embedded in a cold-setting mounting resin, placed on a Lucite or Plexi-glass.

The mounted sample was then ground on progressively finer grades of water proof silicon carbide paper progressing from 120 to 800 grit to expose the carbonised residue in the way described as follows :

The silicon paper in the form of a disc was fixed on the top of a rotator and the sample was allowed to be rubbed by the silicon paper when the disc was kept on rotation. Light but steady pressures were applied on the sample while it was being rubbed by the carbide paper. The direction of polish was maintained constant except for reversals made at regular intervals by lifting and rotating the sample by 180° at hand, accordingly the sample was not moved about the wheel but was only moved laterally between the centre and the periphery. The sample was washed with tap water before using the another comparatively finer grade of carbide paper. The best results were found to be achieved by using fresh paper for each sample and by grinding somewhat further than what was necessary at each grit level to remove the scratches from the preceding paper. After the final grinding on 800-grit paper, the surface of the sample appeared bright independent of the level of heat-treatment.

Subsequent polishing was done with Metadi diamond lapping compounds (6 micron size followed by 1 micron size) on a wet polishing silk cloth supplied by Buchler Limited, U.S.A. in the way described as follows:

The coarse grade Dialap diamond compound was spread over the polishing silk cloth fixed on one of the rotating discs of the Shimadzu polisher and the sample was kept on rubbing for about five minutes and then thoroughly washed with tap water. The finer grade diamond compound was then spread over another polishing silk cloth fixed on the other rotating disc of the polisher and the sample was again kept on rubbing for another five minutes.

Final polishing of the sample was carried out by high purity Linde Alpha Alumina powder. The powder was first wetted with distilled water and the sample was then rubbed gently by it with hand in the same direction for about ten minutes. The final polishing resulted in a highly polished surface having a bright lustre, characteristic of carbonaceous mesophase which proved suitable for observation by polarized-light microscopy.

6.2.6 Polarized-light microscopy

Samples prepared in the above manner were observed and photographed with a Reichert "METAVENT" polarizing microscope (plate 6.1) using reflected polarized-light. Photographs of the mesophase spheres and of subsequent heat-treated samples were obtained using FUJIFILM NEOPAN SS Black & White 135 mm. 36 exp. film. The coloured mesophase spheres could be produced by the insertion of a gypsum plate inclined to the analyser at an angle of 45° and placed between the analyser itself and the sample under observation. The analyser and polarizer remains

cross with respect to each other. This is the so-called sensitive tint technique^{3,4}. The light source of the microscope was 6V, 15W. low-voltage halogen bulb. An exposure time of 15 minutes per photograph was used. A suitable area of each specimen was photographed so that a good number of mesophasic spherules could be counted and a representative particle size analysis obtained.

6.3. Results & discussions

6.3.1 Different types of carbons obtained by sealed tube pyrolysis of benzene.

The sealed-tube pyrolysis of benzene at different heat-treatment temperatures and durations gives rise to a large variety of carbons and four physically different appearing carbons have been found to be so far identified. Most of the carbons have one thing in common that the deposit of carbon is a closely adhering films of silver grey colour. The first of these, shown in plate 6.2, is the hard grey plated carbon which are similar in appearance to that obtained from anthracene⁵ by sealed-tube pyrolysis. The second type, shown in plate 6.3 is also similar to that obtained from gas phase pyrolysis of anthracene. The third type and fourth type are shown as an admixture in plate 6.4. A remarkable feature of the carbon is that they look like carbon needles or thin carbon feathers. In times they thicken and become a thick film of massive type. Besides, we see spongy mass of brownish black carbons or a typical soot of carbon black.

6.3.2 Thermal analysis

Thermal analysis curves of partially carbonised benzene on heat-treatment at 8 hours and 12 hours duration are presented in figs. 6.3 and 6.4 respectively. Thermal analysis data on which these thermal curves are based on is given in tables 6.1 - 6.3. Characteristic of these curves is the presence of an initial large endotherm usually seen in graphitizable organic compounds, which is then followed by small fluctuations in the trace before a smooth trace returns. The temperature region in which these fluctuations appear casts an idea about the temperature intervals of mesophase formation.

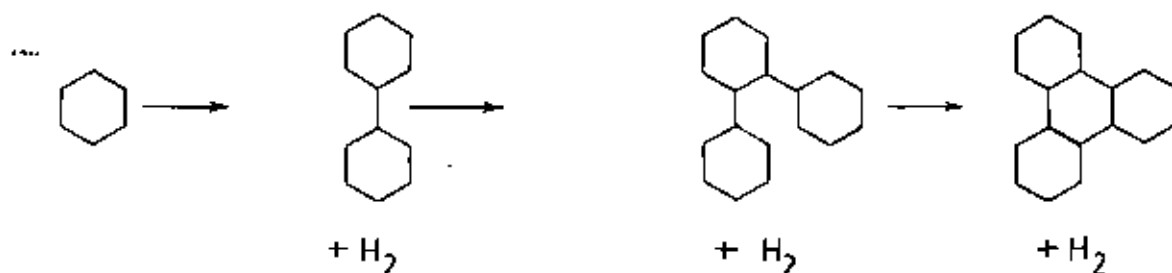
The thermal curves obtained for the two different benzene samples can be interpreted in terms of carbonaceous mesophase formation. The maximum point of extreme right in the curves represents the temperature at which the fluctuations terminate and the curve changes direction sharply. Observation, by polarized-light microscopy, of a benzene sample heat-treated to this temperature revealed that the mesophase had completely coalesced. Similar observations of the sample heat-treated to slightly lower temperatures showed the mesophase in various stages of development. It would appear, therefore, that the extreme K.H.S. turning point in the thermal curves of benzene represents the temperature at which coalescence of the mesophase is complete. The temperature is 570°C for benzene. Similar observations were observed for benzene heat-treated to a different duration. It is interesting to note that the

temperature representing complete coalescence of the mesophase does not alter from 570 °C for the two benzene samples. The temperature at which the mesophase spherules start to develop has not been ascertained and polarized-light microscopy reveals that such spherules appears at 540 °C. It is presumed that very minute spherules appear in this case and it is difficult to analyse them quantitatively by polarized-light microscopy. However, the analysis is not quite difficult when they grow in size with the rise of temperature and heat-treatment duration.

The actual fluctuations in the curves may arise through the formation of gases within the sample. This may result in the sample being lifted away from the thermocouple momentarily thus causing a small peak to occur in the curve. This process may then repeat itself, till the sample is decomposed to produce a mosaic having complete coalescence of the mesophase.

6.3.3 Heat-treatment temperature, duration and also pressure together promote the growth of mesophase formation.

The aromatic hydrocarbons undergo stepwise condensation^{6,7} of the aromatic structures with the elimination of hydrogen until a non-volatile carbon remains. The early stages of such condensations are well-known, particularly for benzene, which has been found to produce the following condensation products.



The conversion of benzene to carbon is catalyzed by the presence of contact surfaces, especially coke or carbon. No doubt the hydrocarbons are absorbed on such surfaces, and undergo dehydrogenation, forming biradicals or even other complex condensation products. The biradicals are eventually converted to carbon giving rise to essentially two main gaseous products hydrogen and methane and with the gradual increase of temperature and resident time methane is again split up to form carbon. As more and more carbons are produced, the vaporising pressure is consequently reduced. When the vapour pressure of the product becomes negligible at high temperatures it is thus classified as carbon. The increase of carbon-yield with the increase of temperature and heat-treatment duration during mesophase formation is well-illustrated in Table 6.4 as well as in fig.6.5.

The variation of pressure inside the sealed tube with temperature at different heat-treatment duration during mesophase formation is well documented in table 6.5 as well as in fig.6.6.

The increasing pressure inside the sealed tube thus enhances the carbonisation process. It is well known⁷ that pressure increases the viscosity of liquids. Thus the effect of pressure will not only reduce considerably any tendency of bubble formation, but also reduce disorder produced by convection currents within the system (because of enhanced viscosity).

The observed mesophase structures arise from a rather unique combination of temperature, soaking time and pressures, all the three parameters promoting the growth of the nematic liquid crystal type of structure and subsequent chemical condensation and increase of density.^{8,9}

Increasing pressure enhances molecular condensation reactions as well as the viscosity of the system. The enhanced viscosity affect both diffusion and coalescence rates. As the temperature is more increased, the isotropic liquid phase is entirely removed but the viscosity and surface tension of the spheres is such as to prevent coalescence. Coalescence is consequently stopped at the temperature of semi-coke formation.

6.6.4 Polarized-Light Photomicrograph

Photomicrograph of the selected mesophase spheres and of subsequent heat-treated samples are presented in plates 6.5 to 6.8. The results of the particle size analysis carried out on the spherules which develop in the carbonaceous mesophase of benzene are shown separately in tables 6.6 — 6.11 and are represented in histogram form in Figs. 6.7-6.10 & in Fig. 6.11. The histograms show the variations between different heat-treated samples more clearly. They clearly indicate an increase in the average spherulite size with the increase of temperature. Typical mesophase spherules for benzene are found to appear at 540°C (plate 6.5). These spherules coalesce to produce bulk

mesophase which consists of larger spherules at 550° & 560°C. This is shown in plates 6.6 & 6.7. Finally complete coalescence takes place to form a mosaic at 570°C (plate 6.8). The spherules

appear to link up to form branch like chains. This may arise from different surface tension - viscosity effects. From the typical coalesced mesophase of benzene, it is presumed that very minute spheres appear in this case during heat-treatment, for which they are not observed at first instance. From the

appearance of the microstructures it also appears that benzene is poor graphitizable organic compound compared to anthracene, phenanthrene, chrysene⁵ and its graphitizability power is

possibly after naphthalene in the group.

6.4 CONCLUSIONS

If we review the criteria of a graphitizable organic compound, we can summarize:

(a) Organic materials which ultimately give rise to graphitizing carbons pass through an anisotropic plastic stage known as 'mesophase transformation' during carbonisation in the temperature range 350 - 600°C during which large planar aromatic molecules become aligned in a parallel array to form the optically anisotropic liquid crystal. The term 'mesophase' (Greek mesos = intermediate) is used for the substances of which the spheres and the mosaic before solidification are formed

In the initial stages of nucleation and growth, the mesophase appears as spherules and as carbonisation progresses, the growing mesophase spherules coalesce and change in shape in forming relative complex bulk mesophase and plastic flow pattern. Thus, three mechanisms - the mesophase transformation itself, the coalescence of the initial spherules to bulk mesophase and the plastic flow before hardening - act to establish the principal features of the lamelliform morphology of a graphitizable coke. The formation of a carbonaceous mesophase as a prerequisite to graphitization is, therefore, very much significant.

(b) The nucleation, growth and coalescence processes of the mesophase spherules establish the basic elements of the graphite microstructure. The nodal and cross structures are essential features of the coalesced mesophase, and the nodal structures at least are found to persist in their basic form up to graphitization temperatures.

(c) For graphitizable organic materials endothermal processes of destruction are generally seen to occur in the initial stage of the thermal curves. In the case of an organic compound under heat-treatment two competing reactions are often found to occur: cross-linking producing an exothermic reaction, and chain stripping and associated reactions which produce endothermic peaks. The second type often allows the formation of oriented aromatic rings, which give rise to graphitizable

carbon. So an exothermic portion of the thermal curve somewhere in the first stage of decomposition indicates that the resulting product will be a non-graphitizing carbon.

The polarized-light photomicrographs (plates 6.5 - 6.8) obtained for the simplest aromatic organic compound (Benzene) at different heat-treatment temperatures and durations indicate that it satisfies the first criteria of graphitization, e.g. it passes through the carbonaceous mesophase transformation and hence it is graphitizable.

Again, the thermal curves obtained for the compound under study (figs. 6.3 to 6.4) clearly indicate that endothermal processes of destructions in the initial portions of the curves are typical in the sample and so it is ~~graphitizable~~ graphitizable. Of considerable interest is the relationship between the thermal analysis traces of partially carbonised samples and the formation of carbonaceous mesophase. This is entirely a new phenomenon which appears to arise because of bubble formation occurring in the sample at the temperature of the formation of the mesophase spherules.

The particle size analysis carried out on the spherules formed in the sample while passing through the carbonaceous mesophase transition, gives some definite informations regarding the size of the spherules in the nucleation and in the subsequent growth to bulk mesophase. Since graphites are formed from materials which pass through a carbonaceous mesophase transformation, generally in the temperature interval of 350 to

600°C, the possibility arises of a relationship between the size of the mesophase spherules formed from a sample and the properties of the corresponding graphite produced. The search for such a correlation is left for future study. Generally a reduction in spherulite size corresponds to a small or secondary decrease in the X-ray parameters¹¹.

As to the pressure influence on the pitch coking process, carbonisation in a sealed tube generally produce a higher carbon yield compared with coking in an open crucible. On the other hand, a gas pressure during pyrolysis causes a poor microstructure in the residue. High gas pressures of evaporated hydrocarbons lead to high carbon yield and to hard carbons. Coking in a sealed tube provides the condition for a combined liquid and gas-phase pyrolysis. The result is a markedly inferior prearrangement of the carbon atoms in the semi-coke. However, in the case of reflux carbonisation, a disturbance of the graphitizability has been found to be observed.

The work of White et al.^{12,13}, Dubois et al.¹⁴ and Honda et al.³ has provided details of how the anisotropic spherules of the mesophase coalesce and grow into macro-order (μm) in graphites. Many X-ray investigations have described the regions of perfect micro-order (\AA) of a near perfect graphite lattice. What has received less attention is the relation between the form birefractance of the mesophase

spherules and the order of the graphite lattice. Taylor¹⁵ and Schmidt¹⁶ stated that optical anisotropy is always the expression of structural anisotropy and most work on the carbonaceous mesophase implies or proves that the mesophase is a laminar structure^{17,18}.

Table No. 6.1

Nickel-Chromium, Nickel Aluminium Thermocouples *
 (Chromel Alumel Couples & T₁-T₂ alloy couples)
 e.m.f in millivolts (absolute). Cold junction at 0°C.

Temp. °C	0	10	20	30	40	50	60	70	80	90
0	0.00	0.40	0.80	1.20	1.61	2.02	2.43	2.85	3.26	3.68
100	4.10	4.51	4.92	5.33	5.73	6.13	6.53	6.93	7.33	7.73
200	8.13	8.54	8.94	9.34	9.75	10.16	10.57	10.98	11.39	11.80
300	12.21	12.63	13.04	13.46	13.88	14.29	14.71	15.13	15.55	15.98
400	16.40	16.82	17.24	17.67	18.09	18.51	18.94	19.36	19.79	20.22
500	20.65	21.07	21.50	21.92	22.34	22.78	23.20	23.63	24.06	24.49
600	24.91	25.34	25.76	26.19	26.61	27.03	27.45	27.87	28.29	28.72
700	29.14	29.56	29.97	30.39	30.81	31.23	31.65	32.06	32.48	32.89
800	33.30	33.71	34.12	34.53	34.93	35.34	35.75	36.15	36.55	36.96
900	37.36	37.76	38.16	38.56	38.95	39.35	39.75	40.14	40.53	40.92
1000	41.31	41.70	42.09	42.48	42.87	43.25	43.63	44.02	44.40	44.78
1100	45.16	45.54	45.92	46.29	46.67	47.04	47.41	47.78	48.15	48.52
1200	48.89	49.25	49.62	49.98	50.34	50.69	51.05	51.41	51.76	52.11
1300	52.46	52.81	53.16	53.51	53.85	54.20	54.54	54.88		

* From - Technical Data on Fuel by SPIERS.

Table No. 6.2

Thermal Analysis Data of Partially Carbonised
Benzene on Heat-treatment at 450°C For a
Duration of 8 hrs.

Time in min.	Wire No	Balancing length in cm	Total length in cm.	F.m.f in mV.	Corresponding temp. in °C
0	7	95.0	795.0	19.78	483
1	7	55.0	755.0	18.78	458
2	7	50.0	750.0	18.66	455
3	7	43.5	743.5	18.50	450
4	7	35.0	735.0	18.29	448
5	7	30.0	730.0	18.16	443
6	7	35.0	735.0	18.29	448
7	7	30.0	730.0	18.16	443
8	7	35.0	735.0	18.29	448
9	7	45.0	745.0	18.54	454
10	7	56.5	756.5	18.82	458
11	7	67.5	767.5	19.10	466
12	7	63.5	763.5	19.00	465
13	7	55.0	755.0	18.78	458
14	7	55.0	755.0	18.78	458
15	7	62.0	762.0	18.96	463
16	7	70.0	770.0	19.16	468
17	7	74.0	774.0	19.26	470
18	7	80.0	780.0	19.41	475
19	7	85.0	785.0	19.53	477
20	7	85.0	785.0	19.53	477
21	7	80.0	780	19.41	475
22	7	75.0	775.0	19.28	471
23	7	70.0	770.0	19.16	468
24	7	80.0	780.0	19.41	475
25	7	95.0	795.0	19.78	454
26	8	15.0	815.0	20.28	495
27	8	27.0	827.0	20.58	502
28	8	25.0	825.0	20.53	501
29	8	19.0	819.0	20.38	498
30	8	10.0	810.0	20.15	493
31	8	14.0	814.0	20.25	495
32	8	21.0	821.0	20.43	498
33	8	23.0	823.0	20.48	499
34	8	25.0	825.0	20.53	500

Table 6.2 (Continued)

Time in min	Wire No.	Balancing length in cm	Total length in cm.	E.m.f in mv.	Corresponding temp in °C
35	8	34.5	834.5	20.76	483
36	8	50.0	850.0	21.15	513
37	8	60.0	860.0	21.40	520
38	8	55.0	855.0	21.27	518
39	8	54.0	854.0	21.25	517
40	8	55.0	855.0	21.27	518
41	8	60.0	860.0	21.40	520
42	8	61.0	861.0	21.42	521
43	8	53.5	853.5	21.24	516
44	8	50.0	850.0	21.15	513
45	8	60.0	860.0	21.40	520
46	8	70.0	870.0	21.65	526
47	8	80.0	880.0	21.90	532
48	8	95.0	895.0	22.27	540
49	9	20.0	920.0	22.89	554
50	9	20.0	920.0	22.89	554
51	9	21.0	921.0	22.92	556
52	9	30.0	930.0	23.14	561
53	9	35.0	935.0	23.26	564
54	9	44.0	944.0	23.49	569
55	9	50.0	947.0	23.56	570
56	9	47.5	947.5	23.57	570
57	9	45.0	945.0	23.51	570
58	9	42.0	942.0	23.44	568
59	9	39.0	939.0	23.36	566
60	9	35.0	935.0	23.26	564

Table 6.3

Thermal Analysis Data of Partially Carbonised Benzene on Heat-treatment at 450 °C for a Duration of 12 hrs.

Time in min.	Wire No.	Balancing length in cm.	Total length in cm.	E.m.f in mV	Corresponding temp. in °C
0	8	27.5	827.5	20.59	503
1	8	13.5	813.5	20.24	494
2	7	95.0	795.0	19.78	454
3	7	84.0	784.0	19.51	476
4	7	67.5	767.5	19.10	466
5	7	55.0	755.0	18.78	458
6	7	38.0	738.0	18.36	447
7	7	30.0	730.0	18.16	443
8	7	58.0	758.0	18.86	460
9	7	80.0	780.0	19.41	475
10	7	85.0	785.0	19.53	477
11	8	00.0	800.0	19.90	485
12	8	10.0	810.0	20.15	493
13	8	05.0	805.0	20.03	488
14	7	87.0	787.0	19.58	478
15	7	75.0	775.0	19.28	471
16	7	75.0	775.0	19.28	471
17	7	80.0	780.0	19.41	475
18	7	98.0	798.0	19.85	485
19	7	90.0	790.0	19.66	480
20	7	92.5	792.5	19.72	482
21	7	95.0	795.0	19.78	483
22	8	04.5	804.5	20.02	488
23	8	14.5	814.5	20.26	494
24	8	15.0	815.0	20.28	495
25	8	15.0	815.0	20.28	495
26	8	20.0	820.0	20.40	520
27	8	23.0	823.0	20.48	499
28	8	25.0	825.0	20.53	501
29	8	24.0	824.0	20.50	500
30	8	25.1	825.1	20.53	501
31	8	32.0	832.0	20.70	504
32	8	39.0	839.0	20.87	507

Table 6.3 (Continued)

Time in min.	Wire No.	Balancing length in cm.	Total length in cm.	E.m.f in mV	Corresponding temp. in °C
34	8	25.0	825.0	20.53	500
35	8	21.0	821.0	20.43	498
36	8	25.1	825.1	20.53	500
37	8	37.0	837.0	20.82	506
38	8	46.0	846.0	21.05	510
39	8	50.0	850.0	21.15	513
40	8	46.5	846.5	21.06	511
41	8	55.0	855.0	21.27	518
42	8	64.0	864.0	21.50	522
43	8	76.0	876.0	21.80	528
44	8	90.0	890.0	22.14	538
45	9	100.0	900.0	22.39	543
46	9	10.1	910.1	22.64	548
47	9	07.0	907.0	22.57	546
48	8	95.0	895.0	22.27	540
49	9	100.0	900.0	22.39	543
50	9	10.0	910.0	22.64	548
51	9	27.5	927.5	23.08	559
52	9	35.0	935.0	23.26	564
53	9	43.0	943.0	23.46	568
54	9	46.0	946.0	23.54	569
55	9	50.0	950.0	23.64	571
56	9	47.5	947.5	23.57	570
57	9	44.5	944.5	23.50	570
58	9	40.0	940.0	23.39	567
59	9	38.0	938.0	23.34	566
60	9	33.5	933.5	23.23	562
61	9	30.0	930.0	23.14	561
62	9	25.0	925.0	23.01	558

Table No. 6.4

Conversion of Benzene to carbon in % during mesophase formation.

No. of Observation	Temp. in °C	Duration in hours	Wt. of the sample taken	Wt. of the carbonised sample + Hc gas along with tube in gm.	Wt. of the tube after breaking in gm.	Wt. of the carbon in gm.	% of carbon obtained
1	540	6	0.704 gm	23.44	23.249	0.191	27.13
2		8	0.704 gm	23.450	23.23	0.220	31.25
3		10	0.704 gm	23.455	23.217	0.238	33.80
4	550	6	0.704 gm	23.445	23.167	0.278	39.48
5		8	0.704 gm	23.46	23.157	0.303	43.03
6		10	0.704 gm	23.465	23.137	0.328	46.59
7	560	6	0.704 gm	23.475	23.141	0.334	47.4
8		8	0.704 gm	23.485	23.101	0.384	54.54
9		10	0.704 gm	23.50	23.091	0.409	58.09
10	570	6	0.704 gm	23.52	23.069	0.451	64.06
11		8	0.704 gm	24.519	24.110	0.475	67.47
12		10	0.704 gm	24.510	24.010	0.500	71.02

Table No. 6.5

Variation of Pressure with Temperature at Different
heat-treatment duration during mesophase formation
in benzene in Sealed tube.

No. of Observation	Temp. in °C	Duration in hours	Wt. of the sample taken in gm.	Wt. of carbon obtained in gm.	Wt. of HC. in gm.	Pressure developed in the sealed tube
1	540	6	0.704	0.191	0.513	240.415 atm.
2	540	8	0.704	0.220	0.484	233.075 atm.
3	540	10	0.704	0.238	0.466	228.057 atm.
4	550	6	0.704	0.278	0.426	227.77 atm.
5	550	8	0.704	0.303	0.401	220.844 atm.
6	550	10	0.704	0.328	0.376	213.581 atm.
7	560	6	0.704	0.334	0.37	209.31 atm.
8	560	8	0.704	0.384	0.32	194.818 atm.
9	560	10	0.704	0.409	0.295	159.09 atm.
10	570	6	0.704	0.451	0.253	173.99 atm.
12	570	8	0.704	0.475	0.229	156.59 atm.
12	570	10	0.704	0.500	0.204	148.52 atm.

Table 6.6

Particle size data and calculation of mean spherulite size for benzene heat-treated to 540 °C for a duration of 10 hrs.

Size Range in μm .	Mean diameter of size range in μm (d_m)	Number of Spherules observed (n)	Number % N	Relative area/500	Area%	Nd_m	Nd_m^2
0-4.9	2.5	8	8.79	0.0786	0.149	21.975	54.938
5-9.9	7.5	15	16.48	1.3259	2.506	123.60	927.00
10-14.9	12.5	24	26.37	5.8929	11.138	329.625	4120.312
15-19.9	17.5	19	20.87	9.1438	17.282	365.225	6391.438
20-24.9	22.5	15	16.48	11.933	22.554	370.80	8343.00
25-29.9	27.5	3	3.30	3.5652	6.738	90.75	2495.625
35-39.9	37.5	3	3.30	6.6295	12.530	123.75	4640.625
40-44.9	42.5	2	2.20	5.6768	10.729	93.50	3973.75
50-54.9	52.5	2	2.20	8.6625	16.373	115.50	6063.75
		91	100	52.9082	100	1634.725	37010.438

Table 6.7

Particle size data and calculation of mean Spherulite size
for benzene heat-treated to 550 °C for a duration of 10 hrs.

Size Range in μm	Mean diameter of size range in μm (d_m)	No. of Spherules observed (n)	Number% N	Relative area/500	Area%	Nd_m	Nd_m^2
10-14.9	12.5	7	8.046	1.718	0.938	100.575	1257.188
15-19.9	17.5	4	4.598	1.925	1.052	80.465	1408.138
20-24.9	22.5	12	13.793	9.546	5.215	310.342	6982.706
25-29.9	27.5	8	9.195	9.507	5.193	252.863	6953.719
30-34.9	32.5	10	11.494	16.598	9.067	373.555	12140.538
35-39.9	37.5	12	13.793	26.518	14.486	517.238	19396.406
40-44.9	42.5	17	19.540	48.253	26.359	830.450	35294.125
45-49.9	47.5	4	4.598	14.182	17.747	218.405	10374.238
50-54.9	52.5	3	3.448	12.993	7.098	181.020	9503.550
55-59.9	57.5	3	3.448	15.587	8.515	198.260	11399.950
60-64.9	62.5	4	4.598	2.554	1.395	287.375	17570.313
65-69.9	67.5	1	1.149	7.160	3.911	77.558	5235.131
70-74.9	72.5	2	2.299	16.520	9.024	166.678	12084.119
		87	100	183.061	100	3594.784	149600.12

Table 6.8

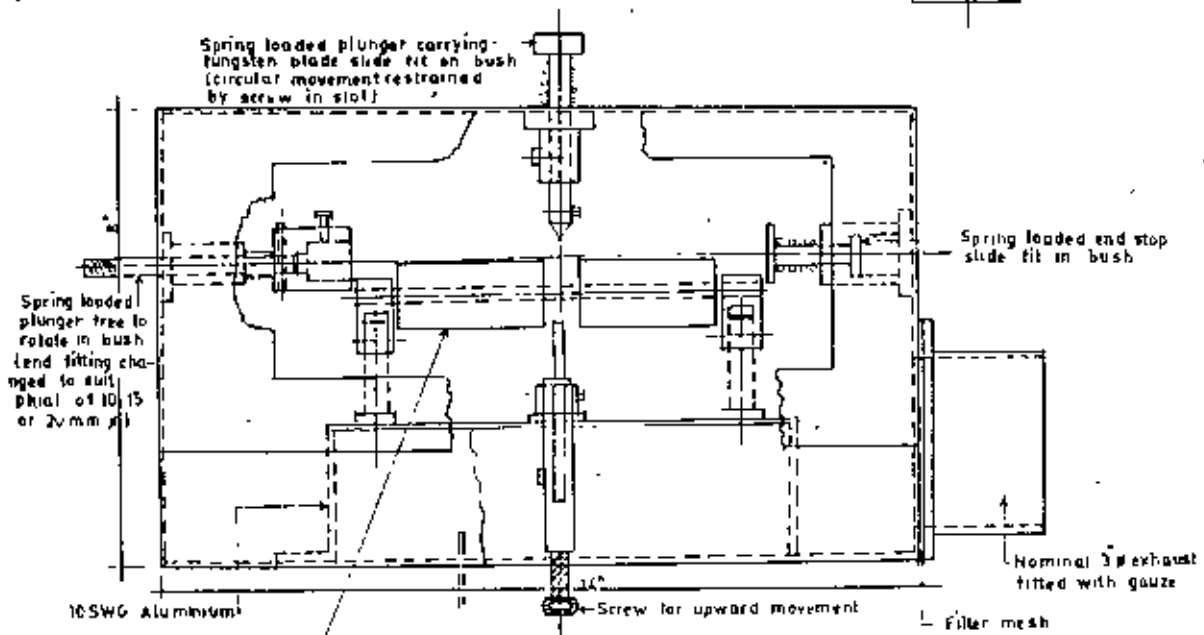
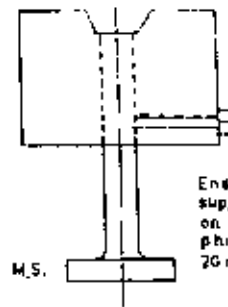
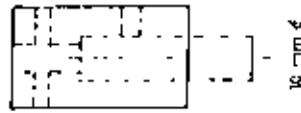
Particle size data and calculation of mean Spherulite size
for benzene heat-treated to 560 °C for a duration of 10 hrs.

Size Range in μm .	Mean diameter of size range in μm (d_m)	Number of spherules observed (n)	Number % N	Relative area/500	Area %	Nd_m	Nd_m^2
15-19.9	17.5	1	1.613	0.481	0.121	28.228	493.981
25-29.9	27.5	1	1.613	1.188	0.299	44.358	1219.831
30-34.9	32.5	1	1.613	1.660	0.418	52.423	1703.731
35-39.9	37.5	4	6.452	8.839	2.223	241.95	9073.125
40-44.9	42.5	11	17.742	31.222	7.853	754.035	32046.488
45-49.9	47.5	5	8.065	7.091	1.783	383.088	18196.656
50-54.9	52.5	4	6.452	17.325	4.357	338.73	17783.325
55-59.9	57.5	5	8.065	25.978	6.534	463.738	26664.906
60-64.9	62.5	9	14.516	55.246	13.895	907.25	56703.125
65-69.9	67.5	2	3.226	14.320	3.602	217.755	14698.463
70-74.9	72.5	5	8.065	41.299	10.387	584.713	42391.656
75-79.9	77.5	2	3.226	18.877	4.748	250.015	19376.163
80-84.9	82.5	2	3.226	21.391	5.380	266.145	21956.963
85-89.9	87.5	3	4.839	36.094	9.078	423.413	37048.594
90-94.9	92.5	2	3.226	26.891	6.763	298.405	27602.463
95-99.9	97.5	1	1.613	14.938	3.763	157.268	15333.581
100-104.9	102.5	2	3.226	33.020	8.305	330.665	33893.163
105-109.9	107.5	1	1.613	18.160	4.567	173.398	18640.231
120-124.9	122.5	1	1.613	23.581	5.931	197.593	24205.081
		62	100	397.601	100	6113.17	419031.526

Table 6.11

Mean arithmetic and area spherulite diameter.

Samples	Heat-treatment temperature ($^{\circ}\text{C}$)	D_d (μm)	D_a (μm)
Benzene C_6H_6	540	16.35	19.24
	550	35.947	38.68
	560	61.132	64.73



16 Teflon rollers press fit onto 3/16" M.S. spindles

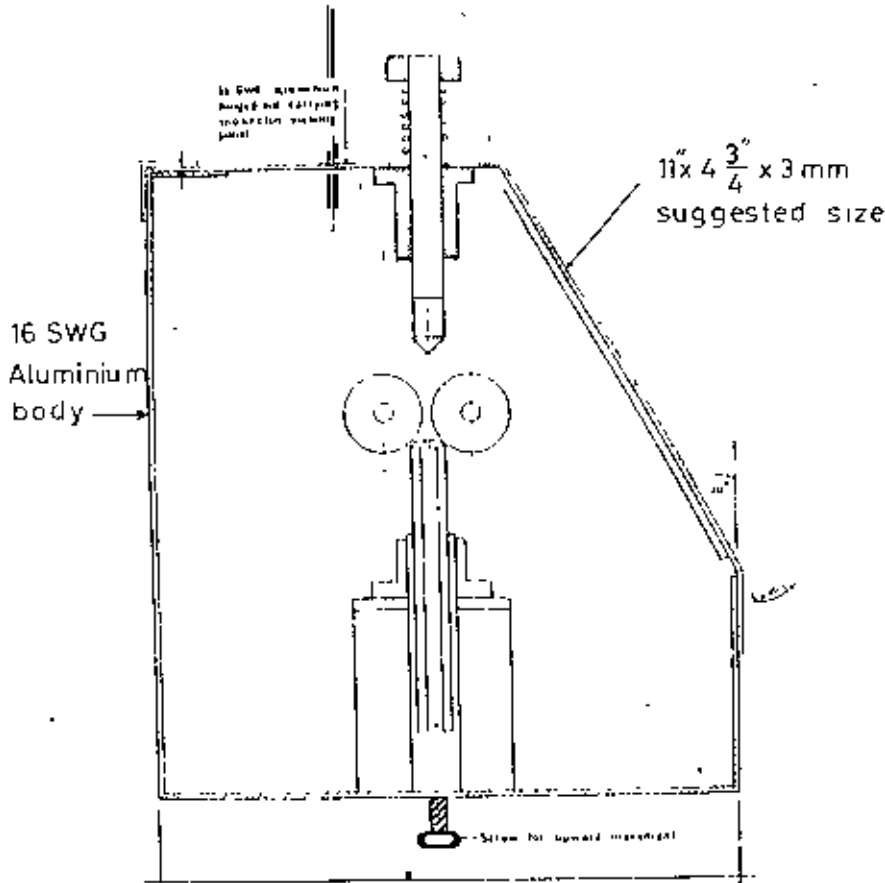


Fig. 6.1 Design plan of the Safety Box.

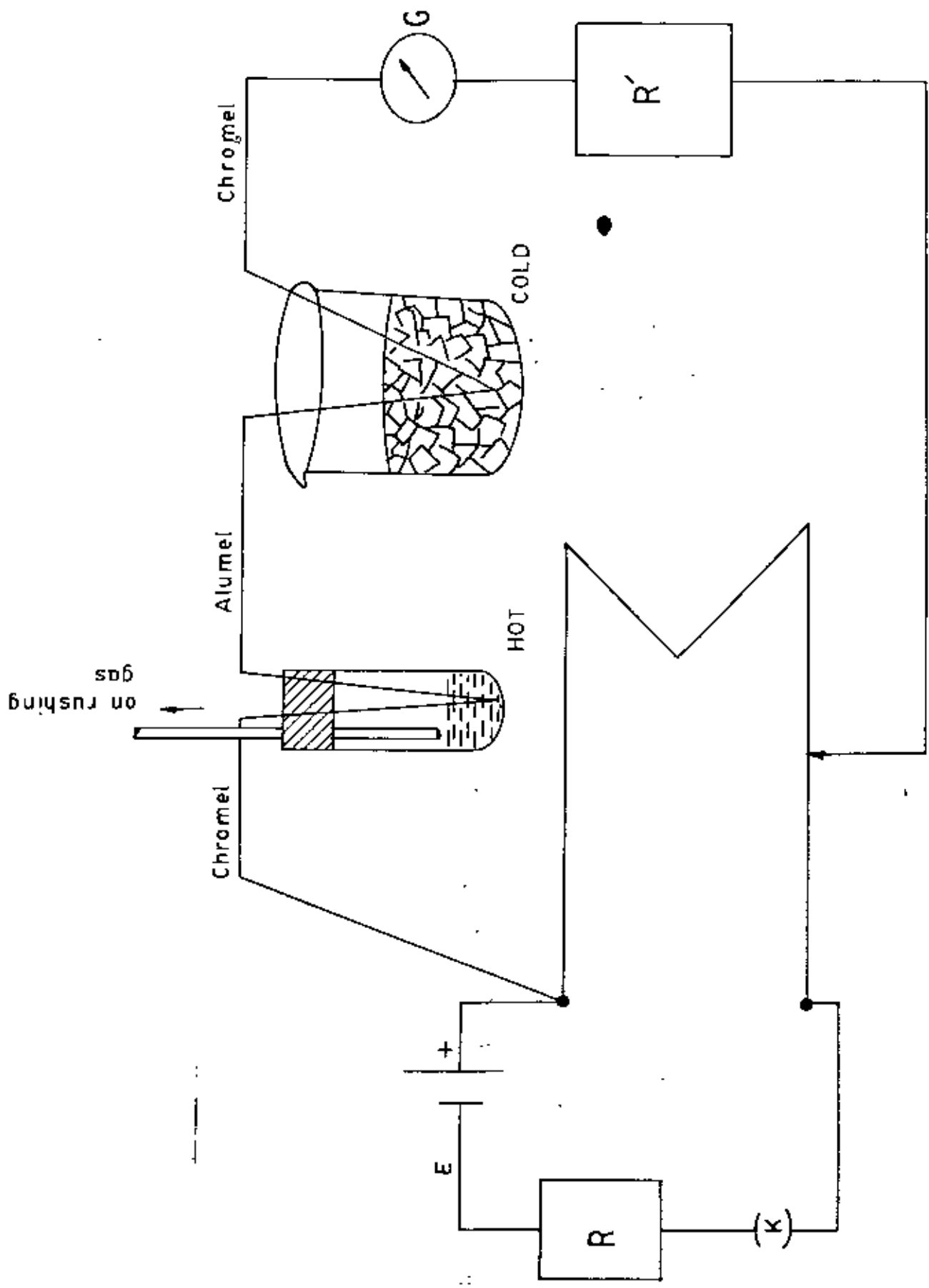


Fig. 6.2 Thermal analysis circuit diagram.

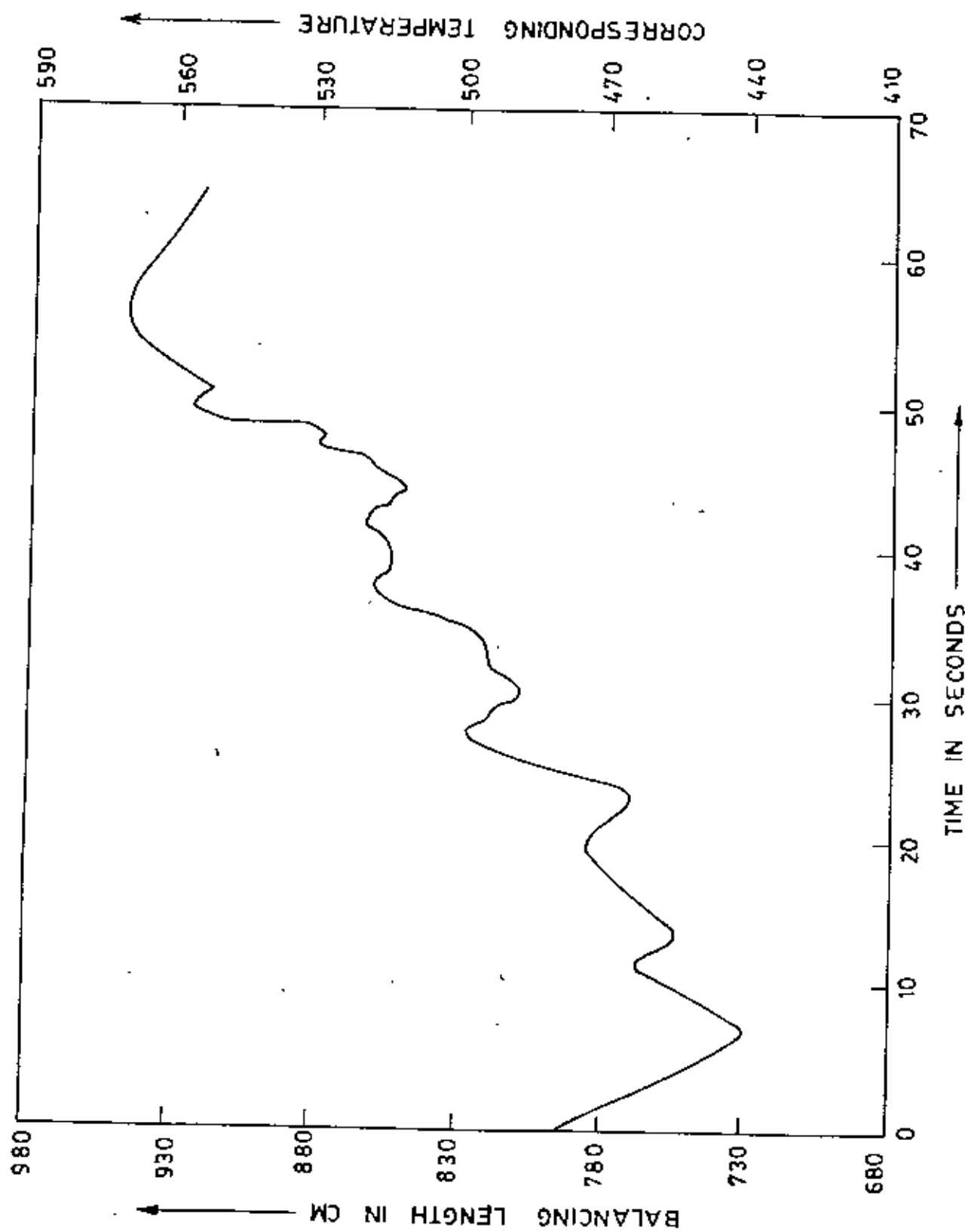


Fig. 6.3 Thermal analysis curve of partially carbonised benzene (C_6H_6) on heat-treatment at $450^\circ C$ for a duration of 8 hours.

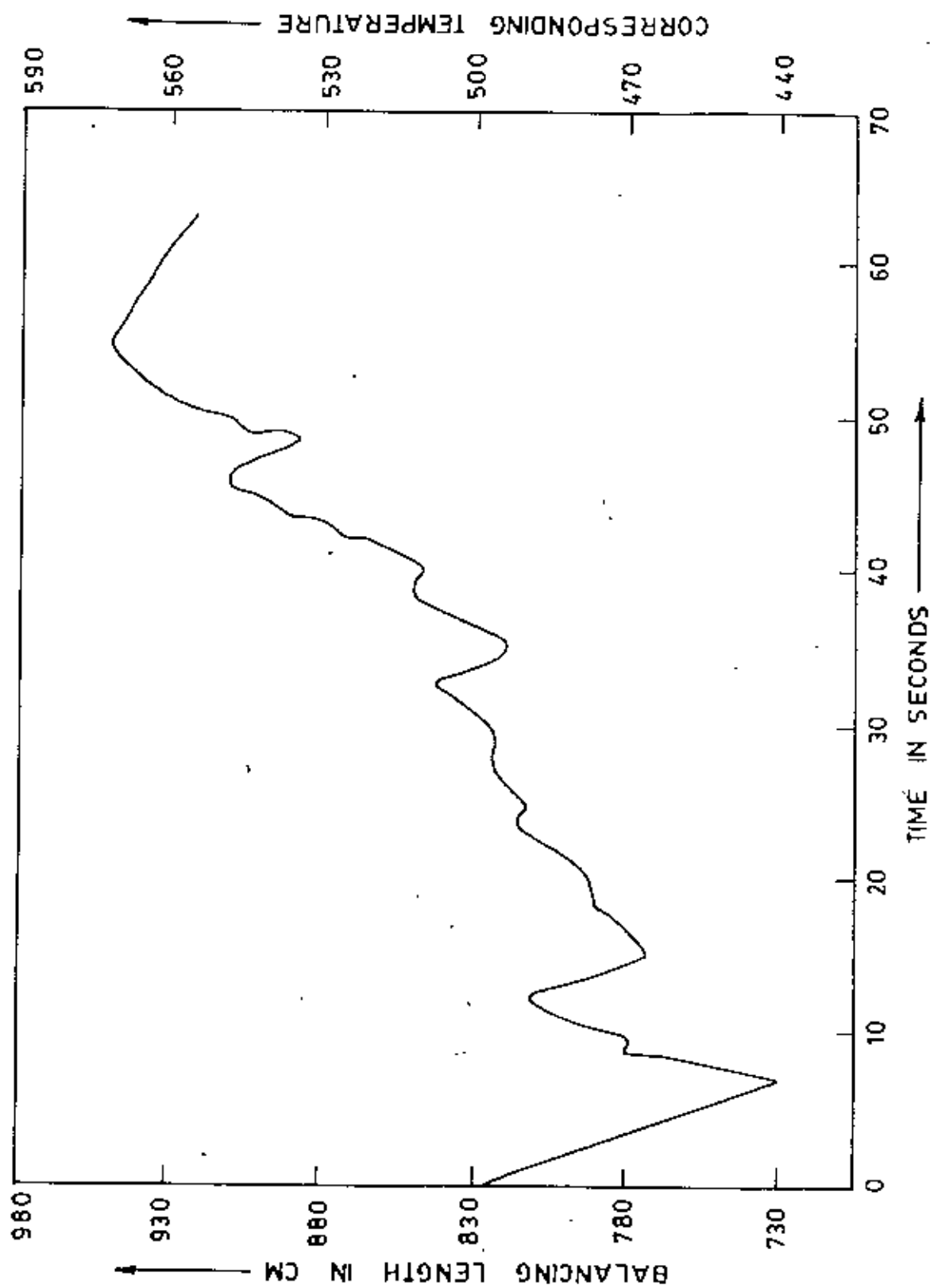


Fig. 6.4 Thermal analysis curve of partially carbonised benzene (C_6H_6) on heat-treatment at $450^\circ C$ for a duration of 12 hours.

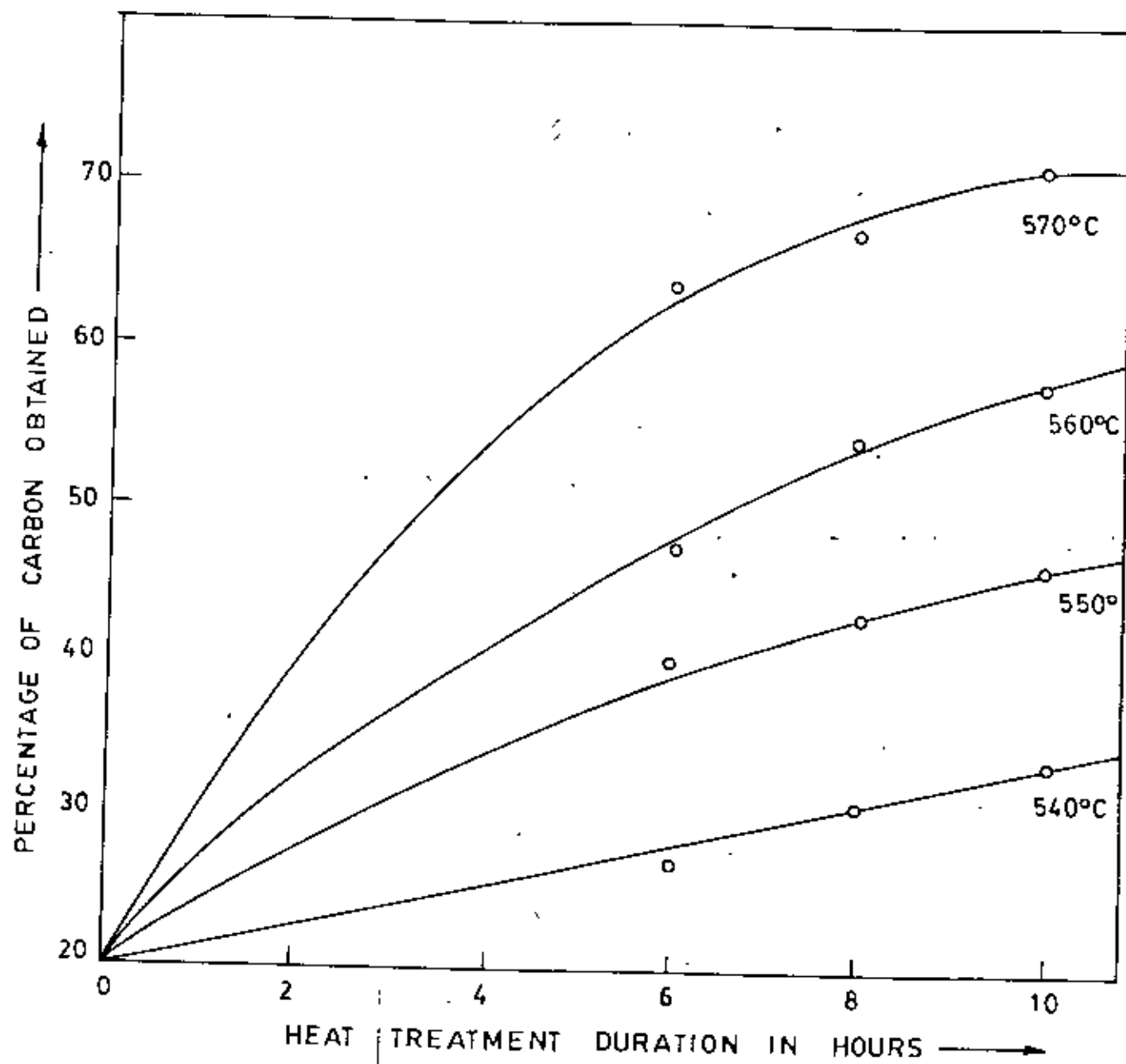


Fig. 6.5 Conversion of Benzene to carbon during mesophase formation.

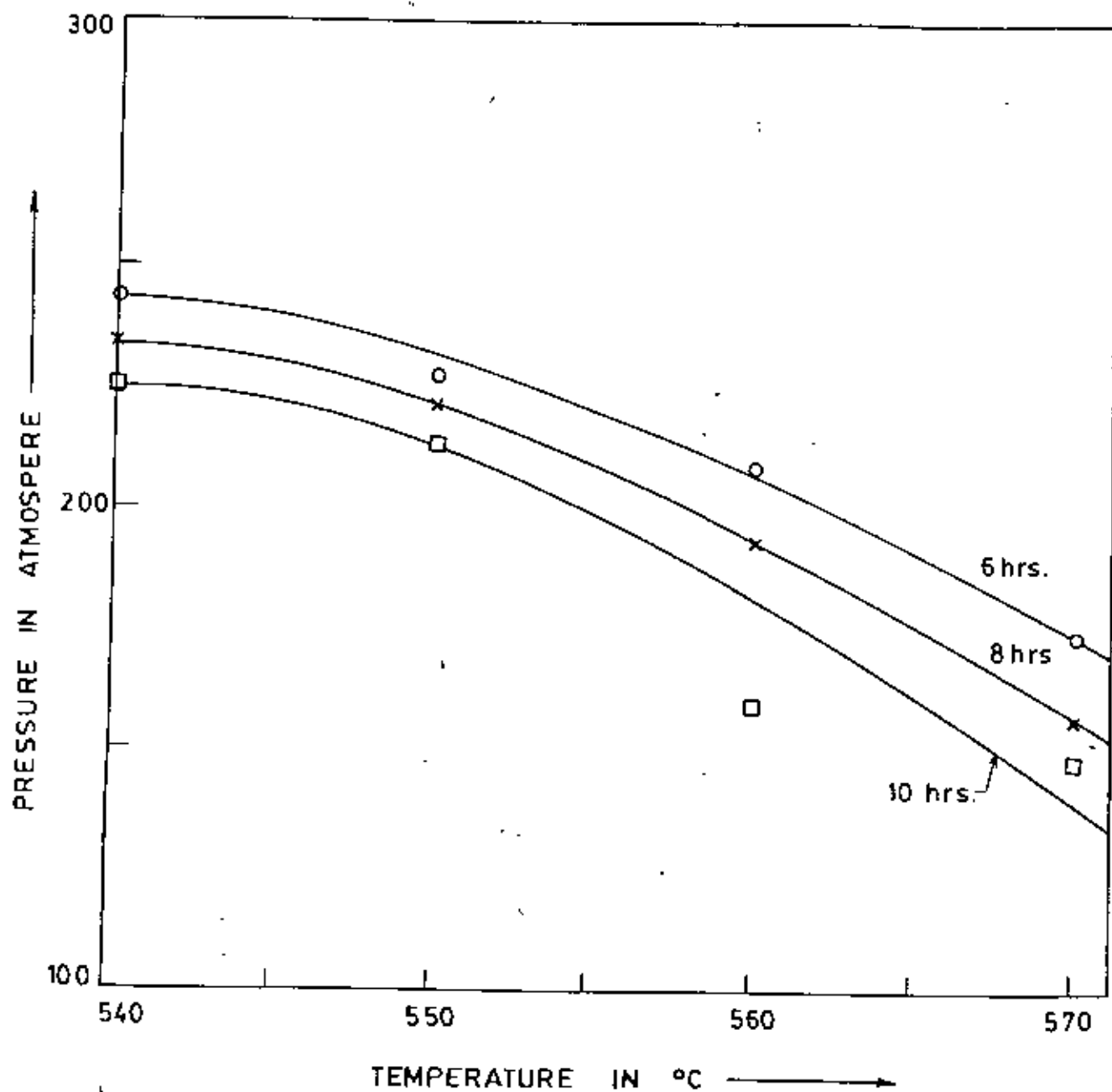


Fig. 6.6 Variation of Pressure with Temperature at different heat-treatment duration during mesophase formation in Benzene.

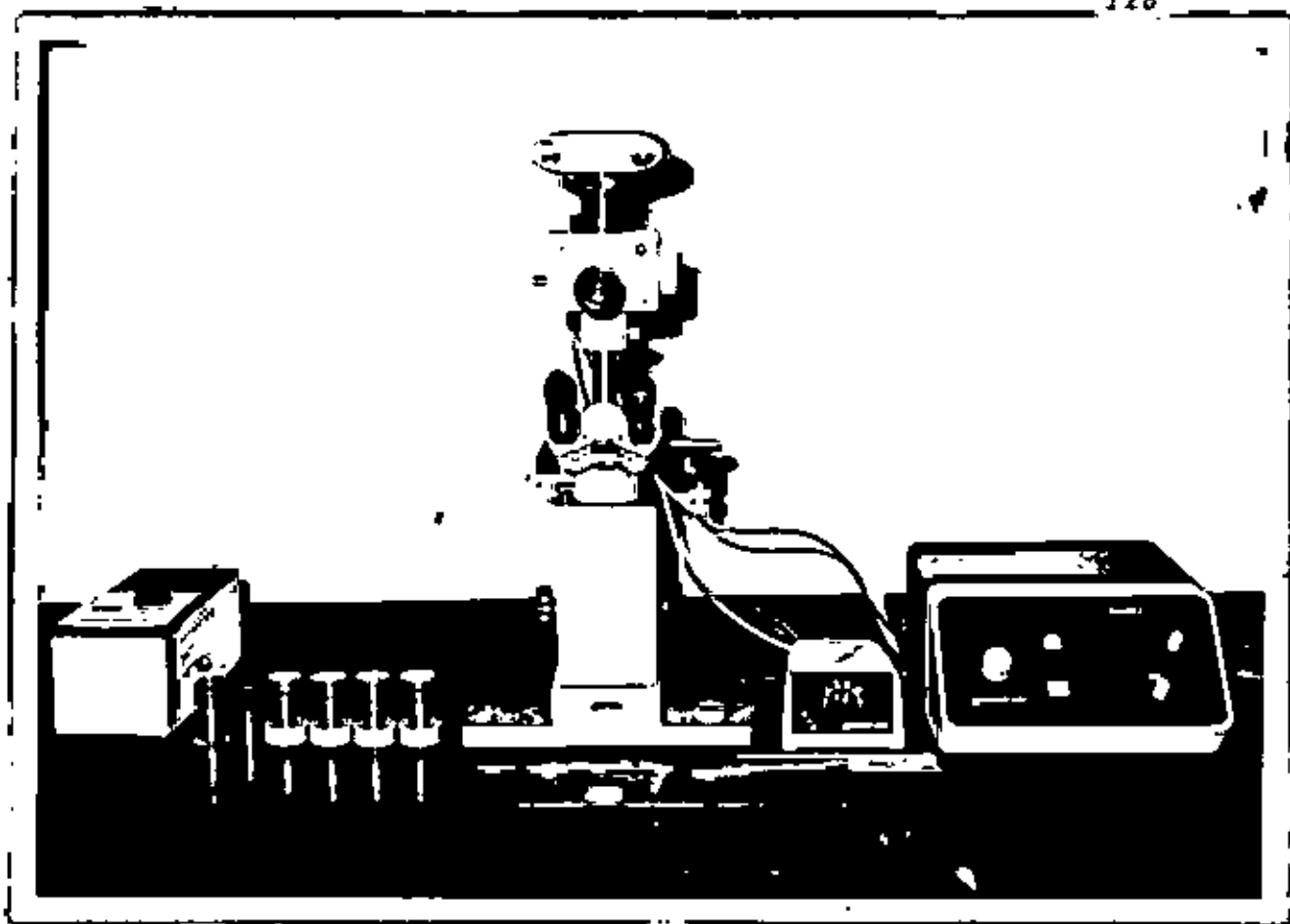


Plate 6.1 REICHERT Motavert Polarizing Microscope equipped with 35 mm kan ES2 Camera.



Plate 6.2 Physically appearing first-type of carbon prepared from benzene.

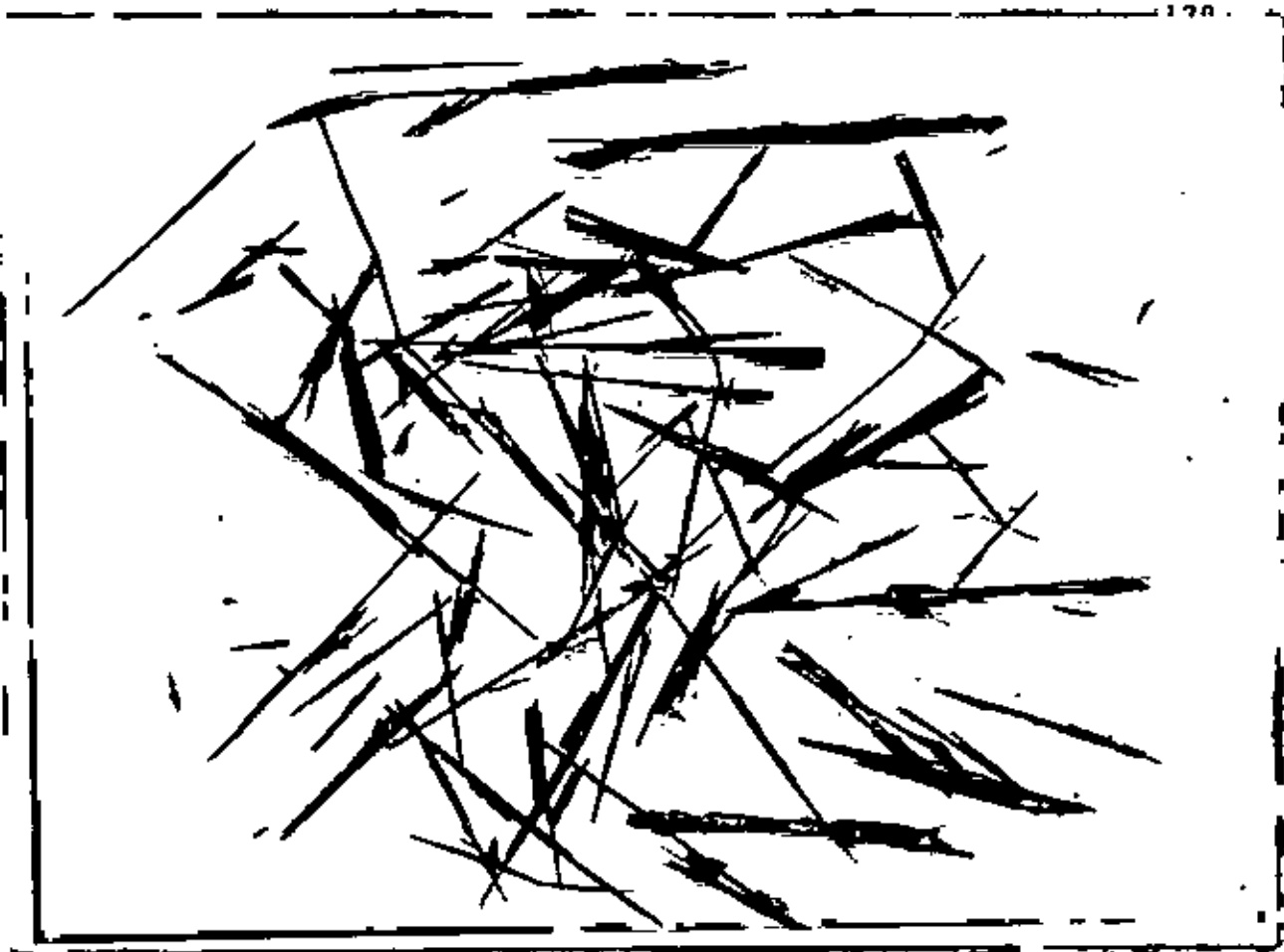


Plate 6.3 Physically appearing second-type of carbon prepared from benzene.

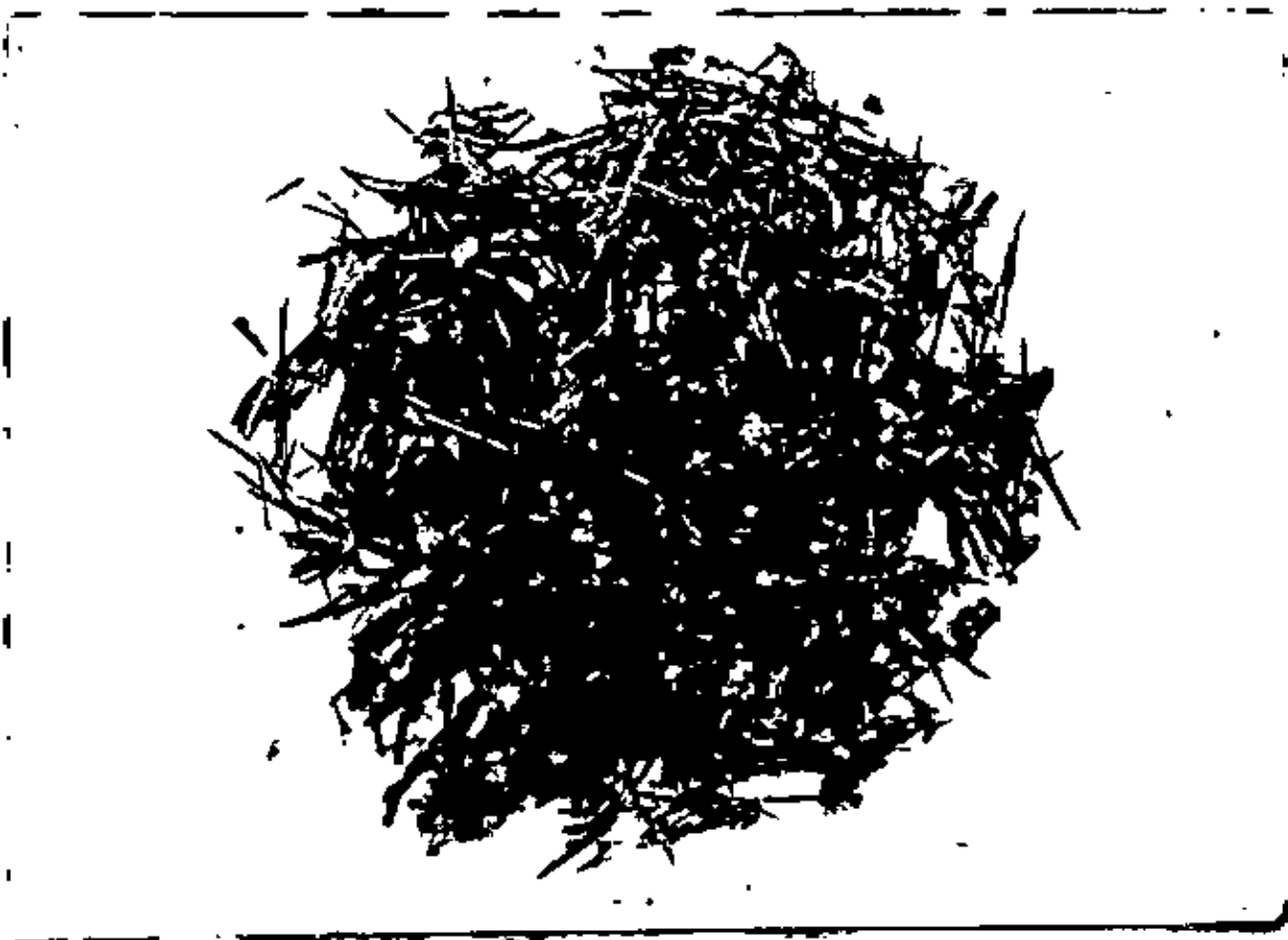


Plate 6.4 Admixture of third and fourth-type of physically appearing carbon prepared from benzene

20 mm

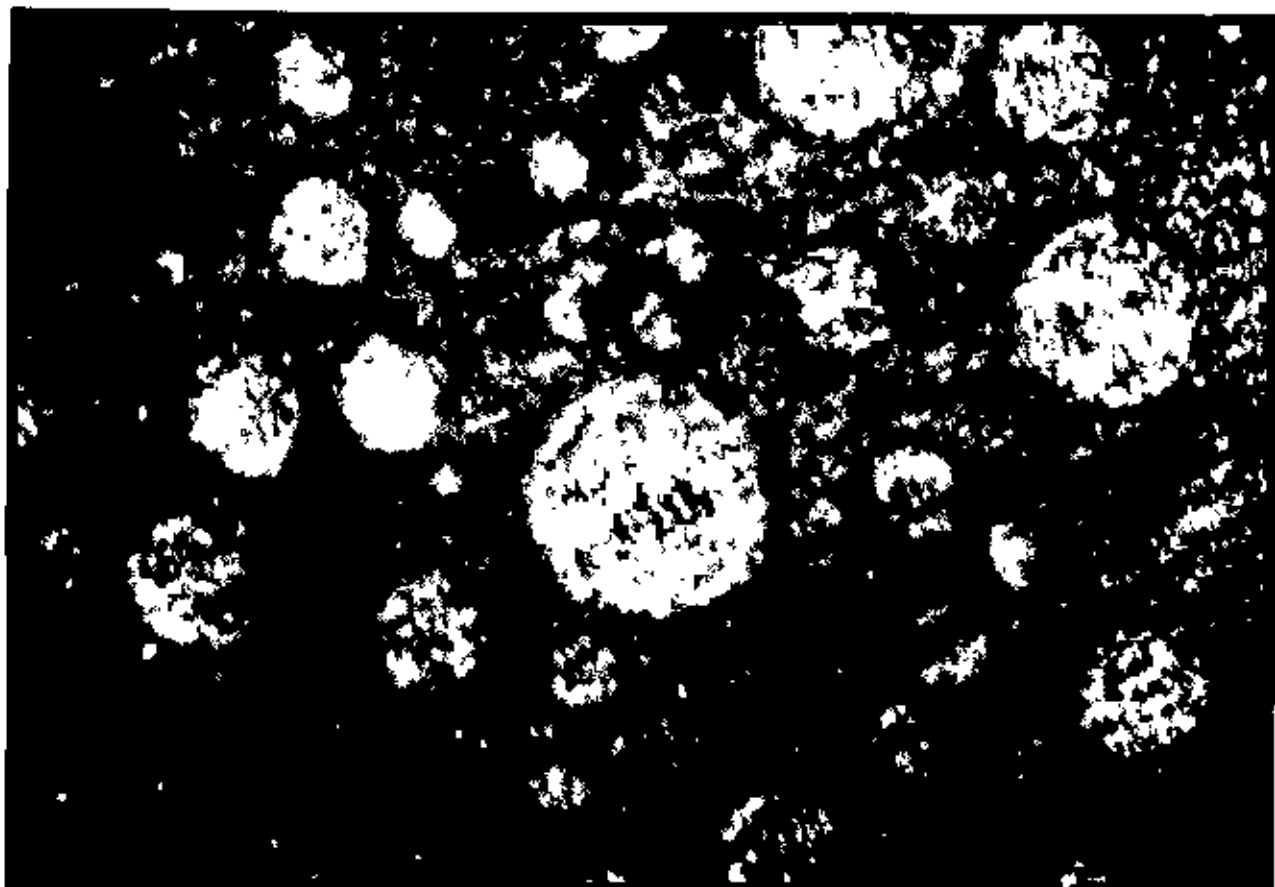


Plate 6.5 Mesophase spherules in benzene heat-treated to 540°C for a duration of 10 hours.

20 mm



Plate 6.6 Mesophase development in benzene heat-treated to 550°C for a duration of 10 hours.

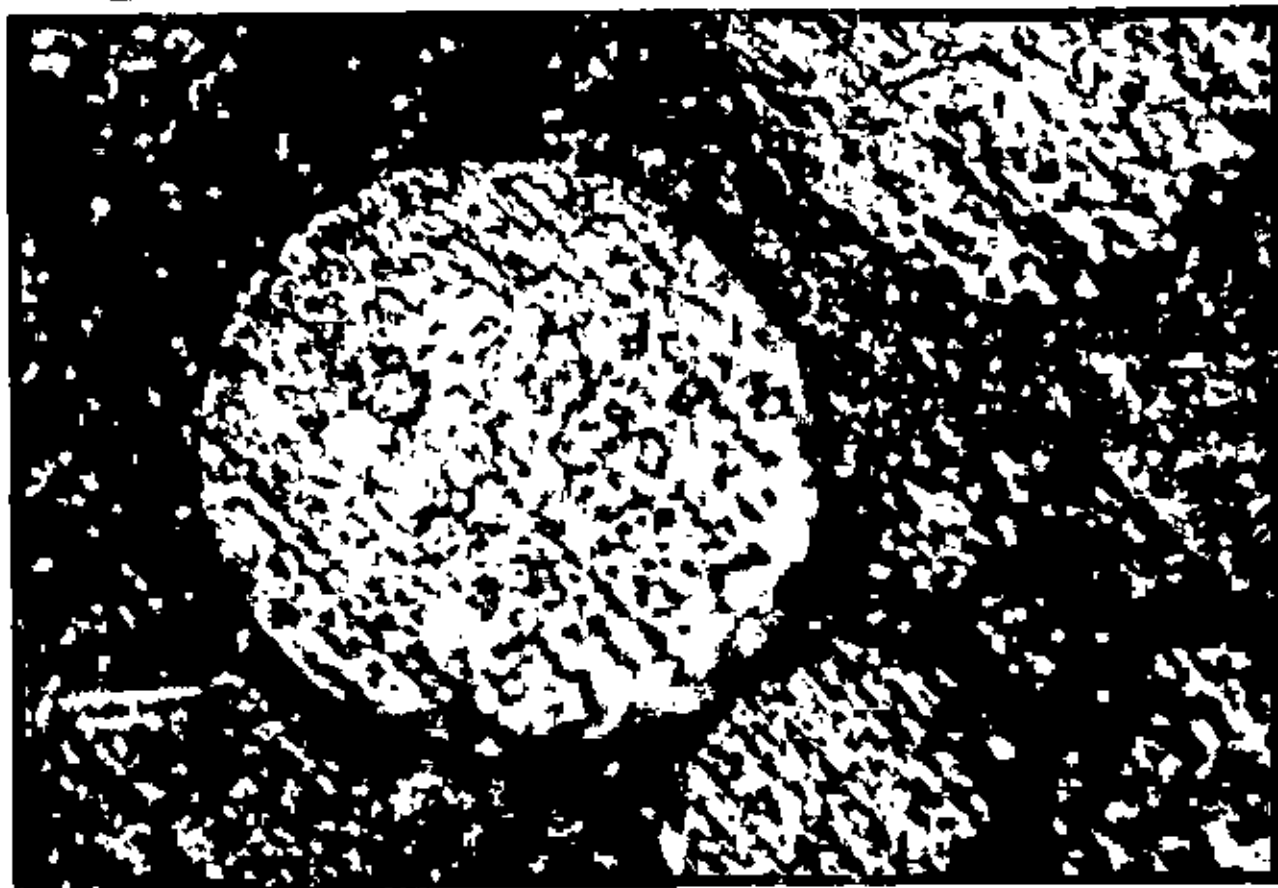
.20 μ m

Plate 6.7. Mesophase development in benzene heat-treated to 560°C for a duration of 10 hours.

20 μ m

Plate 6.8. Mosaic formation in benzene heat-treated 570°C for a duration of 10 hours.

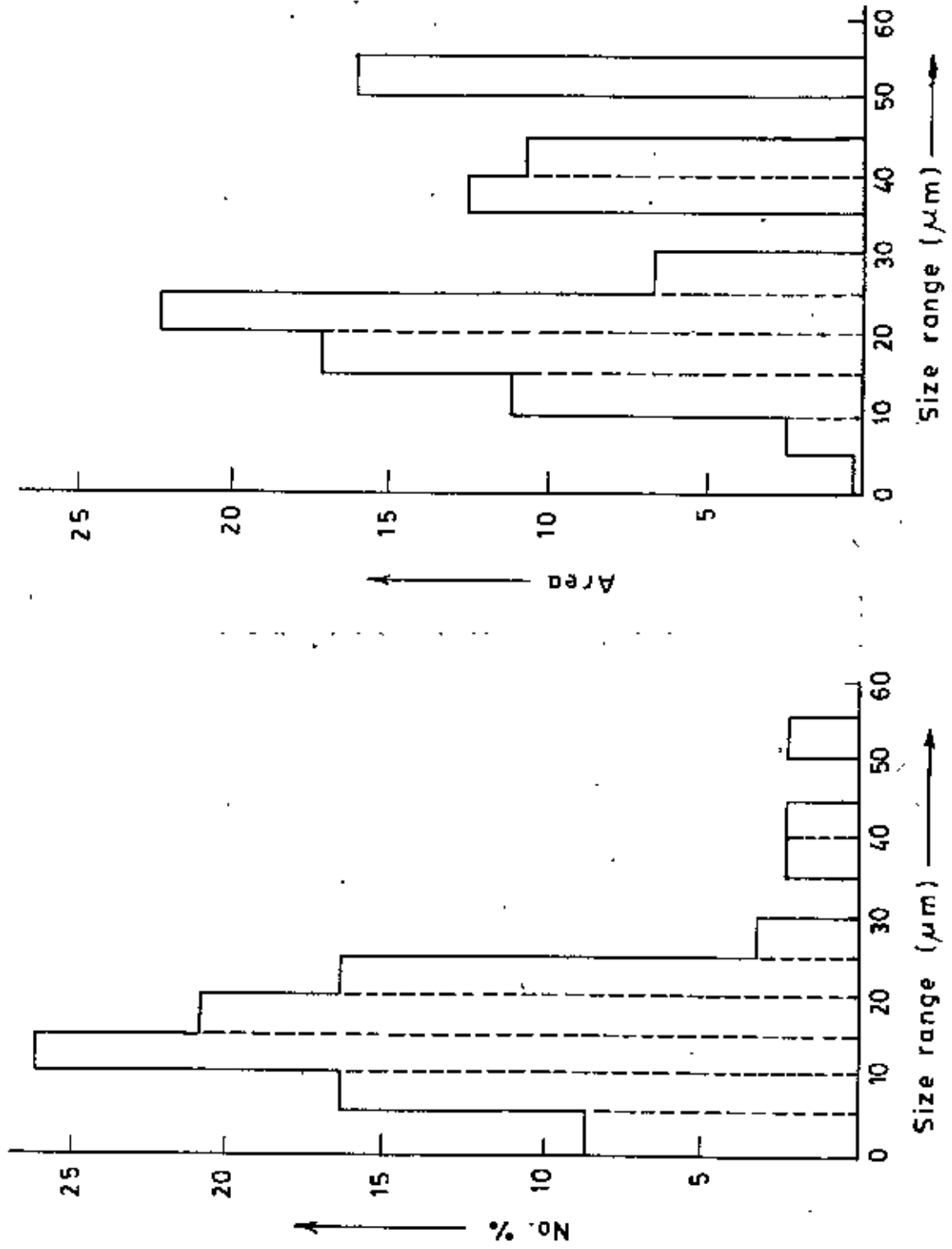


Fig. 6.7 Particle size distribution of benzene heat-treated to 540°C for a duration of 10 hrs.

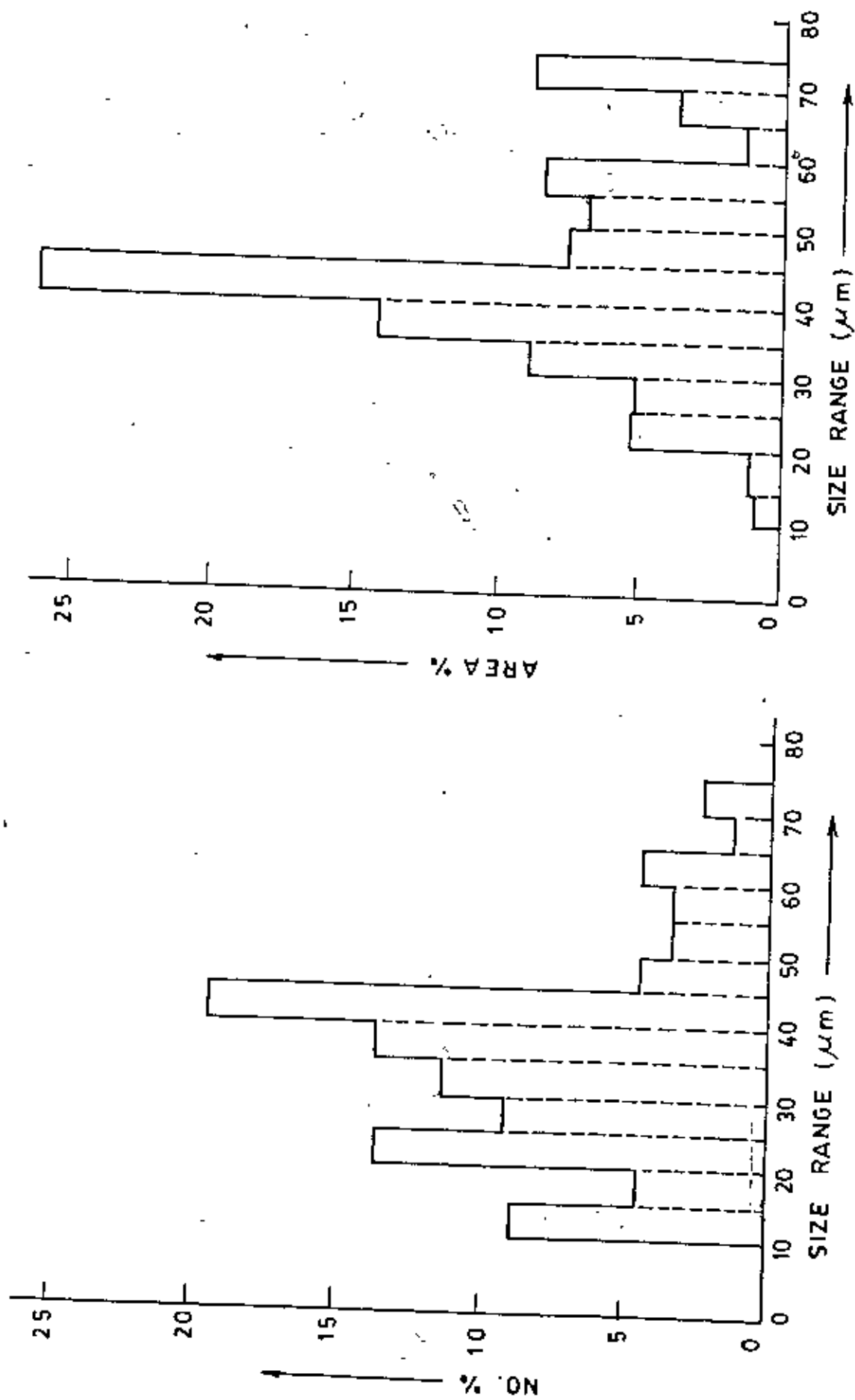


Fig. 6.8 Particle size distribution of benzene heat-treated to 550°C for a duration of 10 hrs.

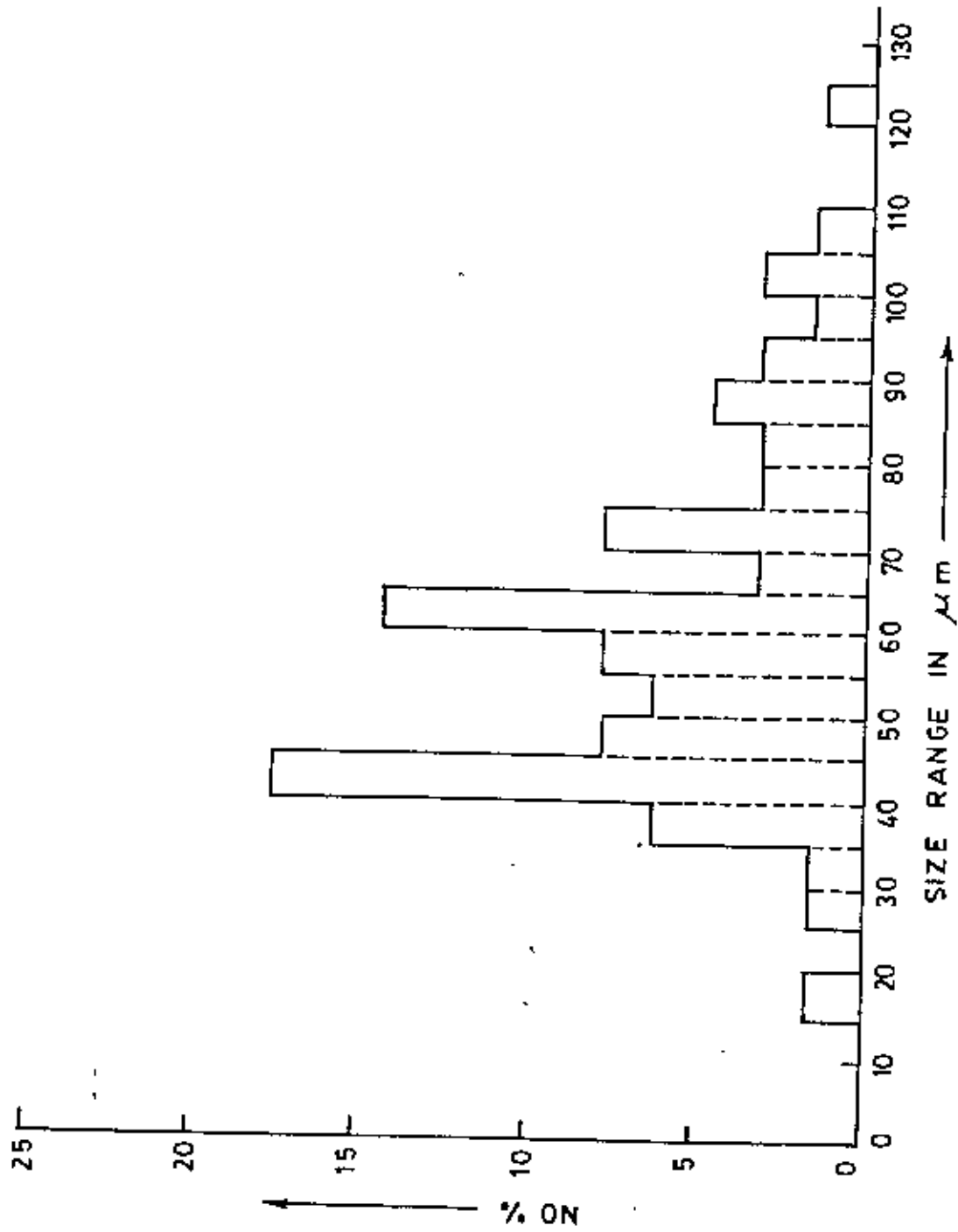


Fig. 6.9 Particle size distribution of benzene heat-treated to 560°C for a duration of 10 hrs. (by No.%)

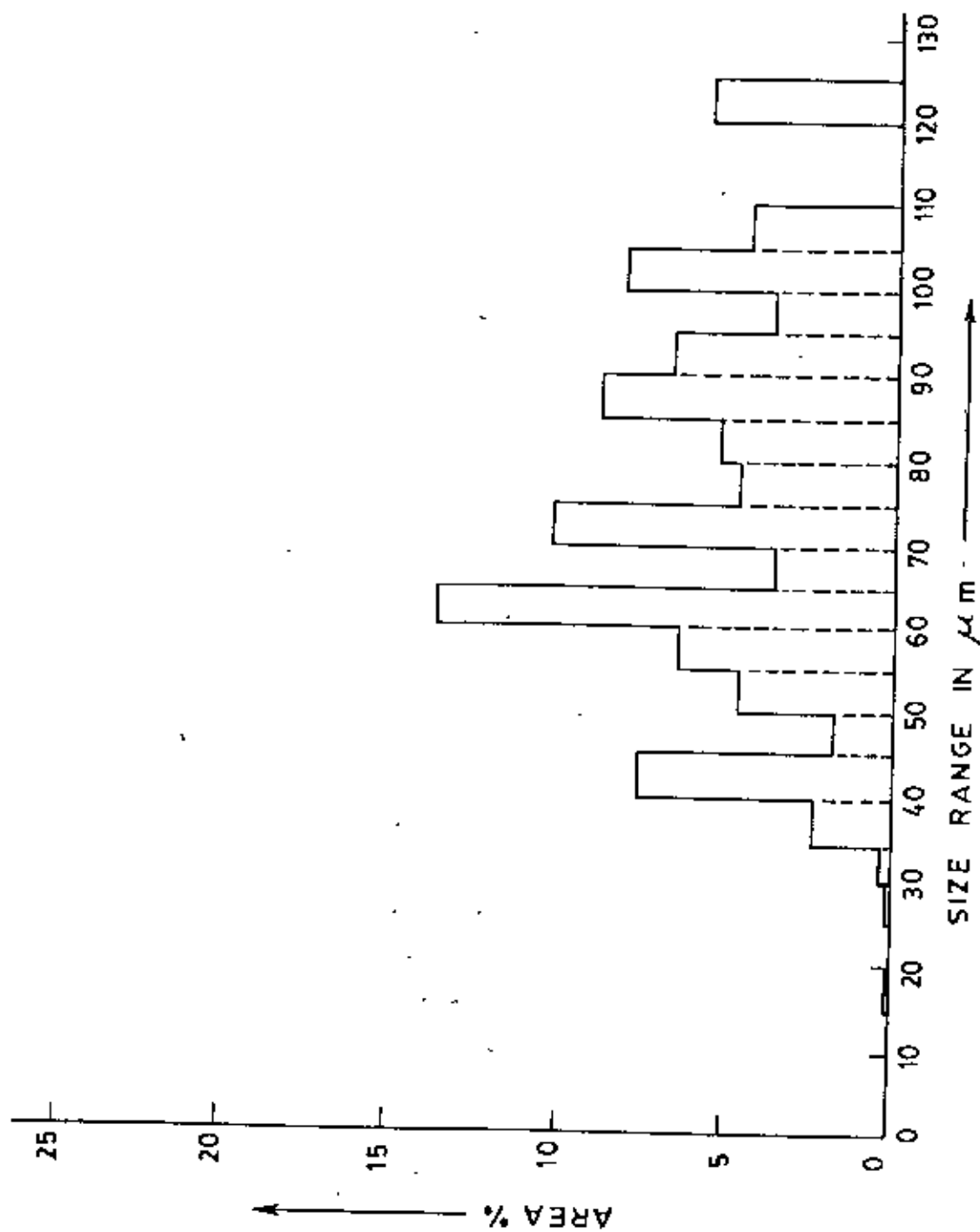


Fig. 6.10 Particle size distribution of benzene heat-treated to 560°C for a duration of 10 hrs. (by Area %.)

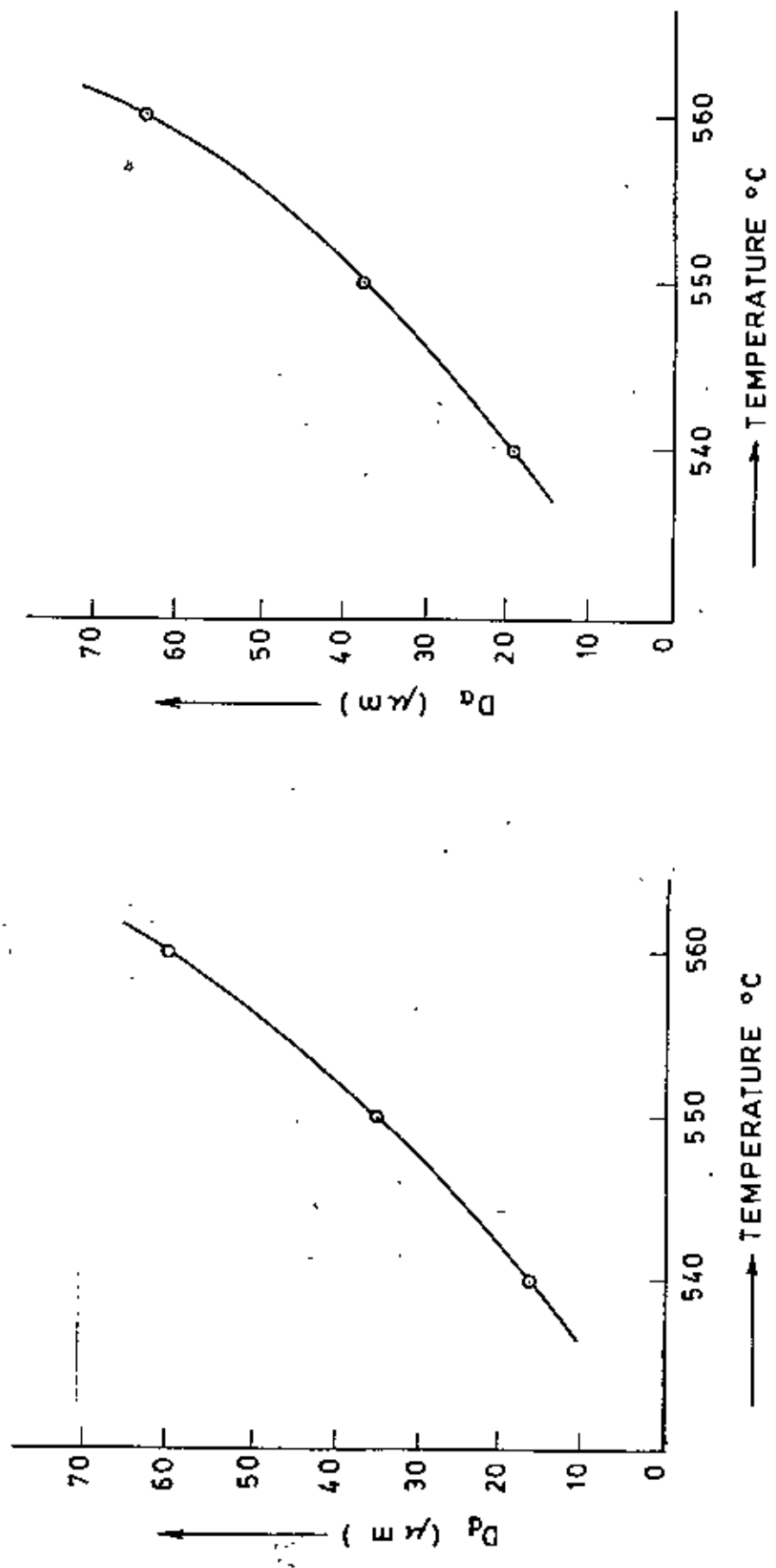


Fig. 6.11 Variation of arithmetic mean spherulite diameter, D_p , and area mean spherulite diameter, D_a , with temperature in the case of benzene.

Reference

- 6.1 Whang, P.W., Dachtler, F. and Walker, P.L.,
J. High Temperatures-High pressures, 1974, 6, 127.
- 6.2 Rüttinger, K.J. and Rosenblatt, U., *Carbon*,
1977, 15, 69.
- 6.3 Honda, H., Kimura, H. and Sanada, Y.,
Carbon, 1971, 9, 695.
- 6.4 Hallimond, A.F., *The polarizing microscope*,
Vickers Instrument, York, 1970.
- 6.5 Hossain, T., Ph.D Thesis, Salford University,
England, 1981, 152
- 6.6 Brooks, B.T., *Ind. Eng. Chem.*, 18, 521, 1926.
- 6.7 Kinney, C.R. and Deibel, E., *Ind. Eng. Chem.*, 46(3),
548, 1954.
- 6.8 Griest, E.M., Webb, W. and Schiessler, R.W.,
J. Chem. Phys., 29, 711, 1958.
- 6.9 Honda, H., Kimura, H., Sanada, Y., Sagawara, S. and
Furuta, T., *Carbon*, 8, 181, 1970.
- 6.10 Gray, G.W., *Molecular Structure and the Properties
of Liquid Crystals*, Academic Press, 1962.
- 6.11 Graham, S.G., Ph.D. Thesis, Salford University
England., 1974, 235.
- 6.12 White, J.L., Guthrie, G.L. and Gardner, J.O.,
Carbon, 1967, 5, 517.
- 6.13 White, J.L., Dubois, J. and Souillart, C., *J.Chim.Phys.*
Special volume, April, 1969, 33; Euratom report
4094e, 1969.

- 6.14 Dubois, J., Agace, C. and White, J.L., Euratom report, 4627e, 1971.
- 6.15 Taylor, G.H., Fuel, 1961, 40, 465.
- 6.16 Schmidt, W.J., Handbuck der Mikroskopie in der Technik, 1:1, 147. Verlag Umshaw (Ed. H. Freund): Frankfurt, 1957.
- 6.17 Brooks, J.D. and Taylor, G.H., Carbon, 1965, 3, 185.
- 6.18 Kovac, C.A. and Lewis, I.C., Carbon, 1978, 16, 433.

